science for a changing world

Field-Trip Guide to Columbia River Flood Basalts, Associated Rhyolites, and Diverse Post-Plume Volcanism in Eastern Oregon

Scientific Investigations Report 2017–5022–O

U.S. Department of the Interior
U.S. Geological Survey

Cover: Photograph looking north at the Leslie Gulch Ash-Flow Tuff exposed in Dago Gulch within the Mahogany Mountain caldera. Photograph by Jason McClaughry. Here the intracaldera tuff is cut by numerous rhyolite dikes marking part of the central vent complex.

Field-Trip Guide to Columbia River Flood Basalts, Associated Rhyolites, and Diverse Post-Plume Volcanism in Eastern Oregon

By Mark L. Ferns, Martin J. Streck, and Jason D. McClaughry

Scientific Investigations Report 2017–5022–O

U.S. Department of the Interior
U.S. Geological Survey

U.S. Department of the Interior
RYAN K. ZINKE, Secretary

U.S. Geological Survey
William H. Werkheiser, Acting Director

U.S. Geological Survey, Reston, Virginia: 2017

For more information on the USGS—the Federal source for science about the Earth, its natural and living resources, natural hazards, and the environment—visit https://www.usgs.gov or call 1–888–ASK–USGS.

For an overview of USGS information products, including maps, imagery, and publications, visit https://store.usgs.gov.

Suggested citation:
Ferns, M.L., Streck, M.J., and McClaughry, J.D., 2017, Field-trip guide to Columbia River flood basalts, associated rhyolites, and diverse post-plume volcanism in eastern Oregon: U.S. Geological Survey Scientific Investigations Report 2017–5022–O, 71 p., https://doi.org/10.3133/sir20175022O.

ISSN 2328-0328 (online)

Preface

The North American Cordillera is home to a greater diversity of volcanic provinces than any comparably sized region in the world. The interplay between changing plate-margin interactions, tectonic complexity, intra-crustal magma differentiation, and mantle melting have resulted in a wealth of volcanic landscapes. Field trips in this series visit many of these landscapes, including (1) active subduction-related arc volcanoes in the Cascade Range; (2) flood basalts of the Columbia Plateau; (3) bimodal volcanism of the Snake River Plain-Yellowstone volcanic system; (4) some of the world's largest known ignimbrites from southern Utah, central Colorado, and northern Nevada; (5) extension-related volcanism in the Rio Grande Rift and Basin and Range Province; and (6) the spectacular eastern Sierra Nevada featuring Long Valley Caldera and the iconic Bishop Tuff. Some of the field trips focus on volcanic eruptive and emplacement processes, calling attention to the fact that the western United States provides opportunities to examine a wide range of volcanological phenomena at many scales.

The 2017 Scientific Assembly of the International Association of Volcanology and Chemistry of the Earth's Interior (IAVCEI) in Portland, Oregon, marks the first time that the U.S. volcanological community has hosted this quadrennial meeting since 1989, when it was held in Santa Fe, New Mexico. The 1989 field-trip guides are still widely used by students and professionals alike. This new set of field guides is similarly a legacy collection that summarizes decades of advances in our understanding of magmatic and tectonic processes of volcanic western North America.

The field of volcanology has flourished since the 1989 IAVCEI meeting, and it has profited from detailed field investigations coupled with emerging new analytical methods. Mapping has been enhanced by plentiful major- and trace-element whole-rock and mineral data, technical advances in radiometric dating and collection of isotopic data, GPS (Global Positioning System) advances, and the availability of lidar (light detection and ranging) imagery. Spectacularly effective microbeam instruments, geodetic and geophysical data collection and processing, paleomagnetic determinations, and modeling capabilities have combined with mapping to provide new information and insights over the past 30 years. The collective works of the international community have made it possible to prepare wholly new guides to areas across the western United States. These comprehensive field guides are available, in large part, because of enormous contributions from many experienced geologists who have devoted entire careers to their field areas. Early career scientists are carrying forward and refining their foundational work with impressive results.

Our hope is that future generations of scientists as well as the general public will use these field guides as introductions to these fascinating areas and will be enticed toward further exploration and field-based research.

Michael Dungan, University of Oregon
Judy Fierstein, U.S. Geological Survey
Cynthia Gardner, U.S. Geological Survey
Dennis Geist, National Science Foundation
Anita Grunder, Oregon State University
John Wolff, Washington State University

Field-trip committee, IAVCEI 2017

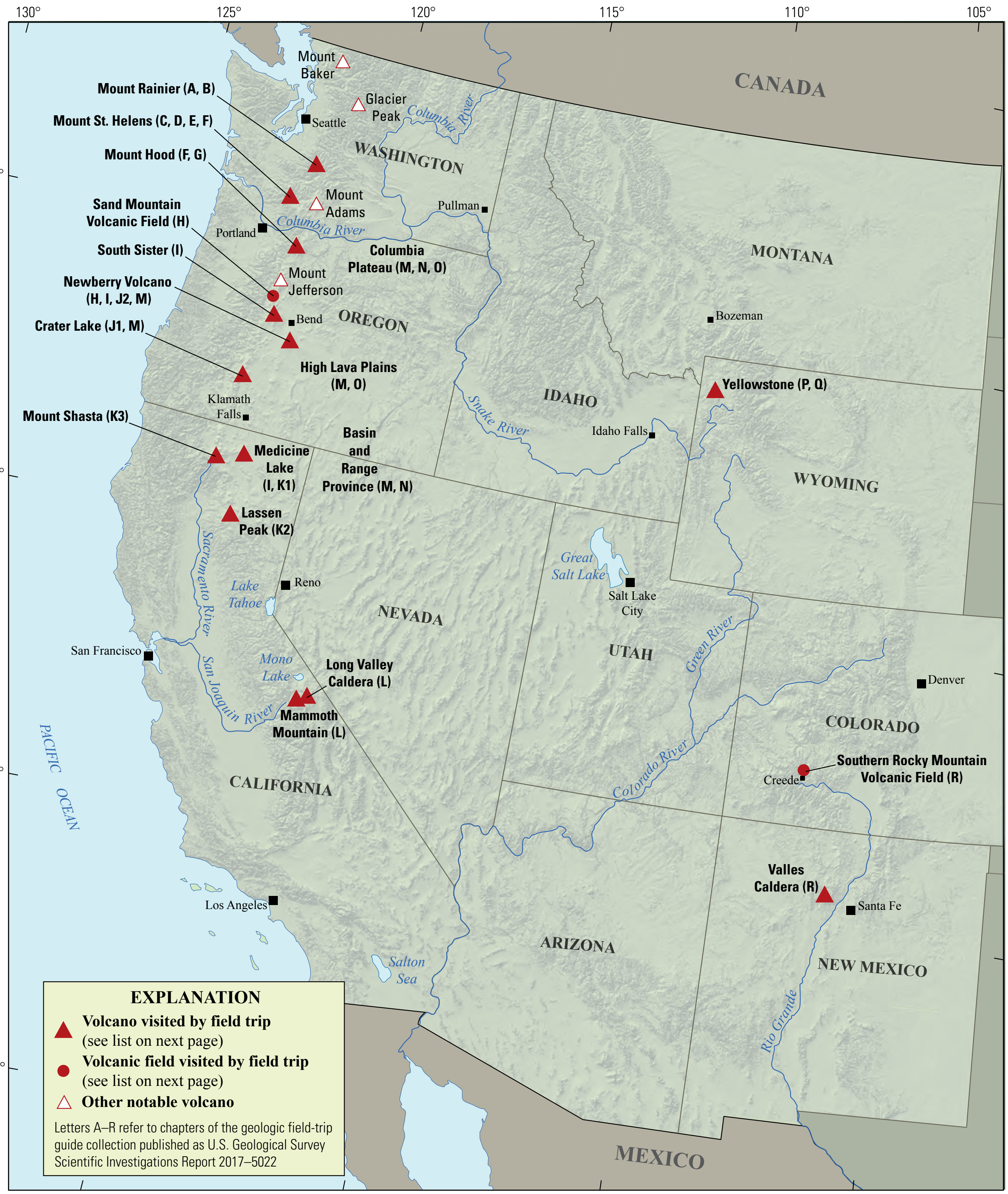

Map of the western United States showing volcanoes and volcanic fields visited by geologic field trips scheduled in conjunction with the 2017 meeting of the International Association of Volcanology and Chemistry of the Earth's Interior (IAVCEI) in Portland, Oregon, and available as chapters in U.S. Geological Survey Scientific Investigations Report 2017–5022. Shaded-relief base from U.S. Geological Survey National Elevation Dataset 30-meter digital elevation model data.

Chapter letter	Title
A	Field-Trip Guide to Volcanism and Its Interaction with Snow and Ice at Mount Rainier, Washington
B	Field-Trip Guide to Subaqueous Volcaniclastic Facies in the Ancestral Cascades Arc in Southern Washington State—The Ohanapecosh Formation and Wildcat Creek Beds
C	Field-Trip Guide for Exploring Pyroclastic Density Current Deposits from the May 18, 1980, Eruption of Mount St. Helens, Washington
D	Field-Trip Guide to Mount St. Helens, Washington—An overview of the Eruptive History and Petrology, Tephra Deposits, 1980 Pyroclastic Density Current Deposits, and the Crater
E	Field-Trip Guide to Mount St. Helens, Washington—Recent and Ancient Volcaniclastic Processes and Deposits
F	Geologic Field-Trip Guide of Volcaniclastic Sediments from Snow- and Ice-Capped Volcanoes—Mount St. Helens, Washington, and Mount Hood, Oregon
G	Field-Trip Guide to Mount Hood, Oregon, Highlighting Eruptive History and Hazards
H	Field-Trip Guide to Mafic Volcanism of the Cascade Range in Central Oregon—A Volcanic, Tectonic, Hydrologic, and Geomorphic Journey
I	Field-Trip Guide to Holocene Silicic Lava Flows and Domes at Newberry Volcano, Oregon, South Sister Volcano, Oregon, and Medicine Lake Volcano, California
J	Overview for Geologic Field-Trip Guides to Mount Mazama, Crater Lake Caldera, and Newberry Volcano, Oregon
J1	Geologic Field-Trip Guide to Mount Mazama and Crater Lake Caldera, Oregon
J2	Field-Trip Guide to the Geologic Highlights of Newberry Volcano, Oregon
K	Overview for Geologic Field-Trip Guides to Volcanoes of the Cascades Arc in northern California
K1	Geologic Field-Trip Guide to Medicine Lake Volcano, northern California, including Lava Beds National Monument
K2	Geologic Field-Trip Guide to the Lassen Segment of the Cascades Arc, northern California
K3	Geologic Field-Trip Guide to Mount Shasta Volcano, northern California
L	Geologic Field-Trip Guide to Long Valley Caldera, California
M	Field-Trip Guide to a Volcanic Transect of the Pacific Northwest
N	Field-Trip Guide to the Vents, Dikes, Stratigraphy, and Structure of the Columbia River Basalt Group, Eastern Oregon and Southeastern Washington
O	Field-Trip Guide to Flood Basalts, Associated Rhyolites, and Diverse Post-Plume Volcanism in Eastern Oregon
P	Field-Trip Guide to the Volcanic and Hydrothermal Landscape of Yellowstone Plateau, Montana and Wyoming
Q	Field-Trip Guide to the Petrology of Quaternary Volcanism on the Yellowstone Plateau, Idaho and Wyoming
R	Field-Trip Guide to Continental Arc to Rift Volcanism of the Southern Rocky Mountains—Southern Rocky Mountain, Taos Plateau, and Jemez Volcanic Fields of Southern Colorado and Northern New Mexico

Contributing Authors

Boise State University
Brittany D. Brand
Nicholas Pollock

Colgate University
Karen Harpp
Alison Koleszar

Durham University
Richard J. Brown

Eastern Oregon University
Mark L. Ferns

ETH Zurich
Olivier Bachmann

Georgia Institute of Technology
Josef Dufek

GNS Science, New Zealand
Natalia I. Deligne

Hamilton College
Richard M. Conrey

Massachusetts Institute of Technology
Timothy Grove

National Science Foundation
Dennis Geist (also with Colgate University and University of Idaho)

New Mexico Bureau of Geology and Mineral Resources
Paul W. Bauer
William C. McIntosh
Matthew J. Zimmerer

New Mexico State University
Emily R. Johnson

Northeastern University
Martin E. Ross

Oregon Department of Geology and Mineral Industries
William J. Burns
Lina Ma
Ian P. Madin
Jason D. McClaughry

Oregon State University
Adam J.R. Kent

Portland State University
Jonathan H. Fink (also with University of British Columbia)
Martin J. Streck
Ashley R. Streig

San Diego State University
Victor E. Camp

Smithsonian Institution
Lee Siebert

Universidad Nacional Autónoma de San Luis Potosi
Damiano Sarocchi

University of California, Davis
Kari M. Cooper

University of Liverpool
Peter B. Kokelaar

University of Northern Colorado
Steven W. Anderson

University of Oregon
Ilya N. Binderman
Michael A. Dungan
Daniele McKay (also with Oregon State University and Oregon State University, Cascades)

University of Portland
Kristin Sweeney

University of Tasmania
Martin Jutzeler
Jocelyn McPhie

University of Utah
Jamie Farrell

U.S. Army Corps of Engineers
Keith I. Kelson

U.S. Forest Service
Gordon E. Grant (also with Oregon State University

U.S. Geological Survey
Charles R. Bacon
Andrew T. Calvert
Christine F. Chan
Robert L. Christiansen
Michael A. Clynne
Michael A. Cosca
Julie M. Donnelly-Nolan
Benjamin J. Drenth
William C. Evans
Judy Fierstein
Cynthia A. Gardner
V.J.S. Grauch
Christopher J. Harpel
Wes Hildreth
Richard P. Hoblitt
Robert A. Jensen
Peter W. Lipman
Jacob B. Lowenstern
Jon J. Major
Seth C. Moran
Lisa A. Morgan
Leah E. Morgan
L.J. Patrick Muffler
James E. O'Connor
John S. Pallister
Thomas C. Pierson
Joel E. Robinson
Juliet Ryan-Davis
Kevin M. Scott
William E. Scott
Wayne (Pat) Shanks
David R. Sherrod
Thomas W. Sisson
Mark Evan Stelten
Weston Thelen
Ren A. Thompson
Kenzie J. Turner
James W. Vallance
Alexa R. Van Eaton
Jorge A. Vazquez
Richard B. Waitt
Heather M. Wright

U.S. Nuclear Regulatory Commission
Stephen Self (also with University of California, Berkeley)

Washington State University
Joseph R. Boro
Owen K. Neill
Stephen P. Reidel
John A. Wolff

Acknowledgments
Juliet Ryan-Davis and Kate Sullivan created the overview map, and Vivian Nguyen created the cover design for this collection of field-trip guide books. The field trip committee is grateful for their contributions.

Contents

Figures

Tables

Conversion Factors

[International System of Units to U.S. customary units]

Multiply	By	To obtain
	Length	
centimeter (cm)	0.3937	inch (in.)
meter (m)	3.281	foot (ft)
kilometer (km)	0.6214	mile (mi)
	Area	
square kilometer (km^2)	0.3861	square mile (mi^2)

[U.S. customary units to International System of Units]

Multiply	By	To obtain
	Length	
foot (ft)	0.3048	meter (m)
mile (mi)	1.609	kilometer (km)
	Area	
square mile (mi^2)	2.590	square kilometer (km^2)

Datum

Horizontal coordinate information is referenced to the World Geodetic System of 1984 (WGS 84) or the North American Datum of 1983 (NAD 83).

Vertical coordinate information is referenced to the North American Vertical Datum of 1988 (NAVD 88).

Abbreviations

An	anorthite
Ab	albite
Ar	argon
asl	above sea level
Ba	barium
BaO	barium oxide
BLM	Bureau of Land Management
bsl	below sea level
cm	centimeters
CRBG	Columbia River Basalt Group
E	excursional polarity
EAR	Division of Earth Sciences
FeO*	iron oxide (expressed as total iron)
fo	forsterite
ft	feet
GPS	global positioning system
HAOT	high alumina olivine tholeiites
ID	Idaho
K	potassium
ka	kilo-annum, or thousands of years before present
km	kilometers
km^2	square kilometers
LOEA	La Grande-Owyhee eruptive axis
m	meters
Ma	mega-annum (million years before present)
MgO	magnesium oxide
mi	miles
mi^2	square miles
N	normal magnetic polarity
NF	National Forest
NV	Nevada
OR	Oregon
Or	orthoclase
ppm	parts per million
R	reverse magnetic polarity
Rb	rubidium
SiO_2	silicon dioxide
Sr	strontium
T	transitional polarity
Ti	titanium
USFS	United States Forest Service
UTM	Universal Transverse Mercator
wt.	weight
WGS84	World Geodetic System of 1984
X_{Fe}	iron composition
XRD	X-ray diffraction
Y	yttrium
Zr	zirconium

Field-Trip Guide to Columbia River Flood Basalts, Associated Rhyolites, and Diverse Post-Plume Volcanism in Eastern Oregon

By Mark L. Ferns,[1] Martin J. Streck,[2] and Jason D. McClaughry[3]

Abstract

The Miocene Columbia River Basalt Group (CRBG) is the youngest and best preserved continental flood basalt province on Earth, linked in space and time with a compositionally diverse succession of volcanic rocks that partially record the apparent emergence and passage of the Yellowstone plume head through eastern Oregon during the late Cenozoic. This compositionally diverse suite of volcanic rocks are considered part of the La Grande-Owyhee eruptive axis (LOEA), an approximately 300-kilometer-long (185 mile), north-northwest-trending, middle Miocene to Pliocene volcanic belt located along the eastern margin of the Columbia River flood basalt province. Volcanic rocks erupted from and preserved within the LOEA form an important regional stratigraphic link between the (1) flood basalt-dominated Columbia Plateau on the north, (2) bimodal basalt-rhyolite vent complexes of the Owyhee Plateau on the south, (3) bimodal basalt-rhyolite and time-transgressive rhyolitic volcanic fields of the Snake River Plain-Yellowstone Plateau, and (4) the High Lava Plains of central Oregon.

This field-trip guide describes a 4-day geologic excursion that will explore the stratigraphic and geochemical relationships among mafic rocks of the Columbia River Basalt Group and coeval and compositionally diverse volcanic rocks associated with the early "Yellowstone track" and High Lava Plains in eastern Oregon. Beginning in Portland, the Day 1 log traverses the Columbia River gorge eastward to Baker City, focusing on prominent outcrops that reveal a distal succession of laterally extensive, large-volume tholeiitic flood lavas of the Grande Ronde, Wanapum, and Saddle Mountains Basalt formations of the CRBG. These "great flows" are typical of the well-studied flood basalt-dominated Columbia Plateau, where interbedded silicic and calc-alkaline lavas are conspicuously absent. The latter part of Day 1 will highlight exposures of middle to late Miocene silicic ash-flow tuffs, rhyolite domes, and calc-alkaline lava flows overlying the CRBG across the northern and central parts of the LOEA. The Day 2 field route migrates to southern parts of the LOEA, where rocks of the CRBG are associated in space and time with lesser known and more complex silicic volcanic stratigraphy associated with middle Miocene, large-volume, bimodal basalt-rhyolite vent complexes. Key stops will provide a broad overview of the structure and stratigraphy of the middle Miocene Mahogany Mountain caldera and middle to late Miocene calc-alkaline lavas of the Owyhee basalt. Stops on Day 3 will progress westward from the eastern margin of the LOEA, examining a transition linking the Columbia River Basalt-Yellowstone province with a northwestward-younging magmatic trend of silicic volcanism that underlies the High Lava Plains of eastern Oregon. Initial field stops on Day 3 will examine key outcrops demonstrating the intercalated nature of middle Miocene tholeiitic CRBG flood basalts, prominent ash-flow tuffs, and "Snake River-type" large-volume rhyolite lava flows exposed along the Malheur River. Subsequent stops on Day 3 will focus upon the volcanic stratigraphy northeast of the town of Burns, which includes regional middle to late Miocene ash-flow tuffs, and lava flows assigned to the Strawberry Volcanics. The return route to Portland on Day 4 traverses across the western axis of the Blue Mountains, highlighting exposures of the widespread, middle Miocene Dinner Creek Tuff and aspects of Picture Gorge Basalt flows and northwest-trending feeder dikes situated in the central part of the CRBG province.

Introduction

This field trip will explore a compositionally diverse late Cenozoic volcanic succession that connects the classical flood basalts of the Columbia River Plateau to middle to late Miocene rhyolites exposed across vast parts of eastern Oregon. We also document the little explored relationships of flood basalts to subsequent volcanism that is compositionally diverse and that lasted nearly continuously for more than 10 million years after the main flood basalt event. A better understanding of the spatial and temporal evolution of the late Cenozoic volcanic rocks of eastern Oregon has led to the recognition that the Columbia River Basalt Group (CRBG) province is strongly bimodal in character, contrary to traditional views (Cummings and others, 2000; Hooper and others, 2002; Camp and others, 2003; Coble and Mahood,

[1]Eastern Oregon University.

[2]Portland State University.

[3]Oregon Department of Geology and Mineral Industries.

2012; Ferns and McClaughry, 2013; and Streck and others, 2015, 2016).

Beginning in Portland, we will travel up the Columbia River and down the La Grande-Owyhee eruptive axis (LOEA) of Ferns and McClaughry (2013) to Lake Owyhee (figs. 1 and 2). We will then head west up the Malheur River, across the flanks of Strawberry Mountain, and make our way back down the John Day River to the Columbia River. Our goals are to give participants an opportunity to explore the geology in the transition zones that link the CRBG to the Yellowstone hot spot. We will look at field relationships that tie tholeiitic flood basalts to large rhyolite lava flows and ash-flow tuffs. We will also explore the progression of volcanism through time from large flood basalt eruptions to small-volume alkalic eruptions. Highlights of the trip include a visit to rhyolite and caldera complexes of the Lake Owyhee volcanic field (LOVF) and a look at a large bimodal vent that generated both late-stage Columbia River Basalt lavas and early Yellowstone-like rhyolite lava flows.

Columbia River Basalt Group

The Miocene Columbia River Basalt Group (CRBG) is the youngest and best preserved continental flood basalt province on

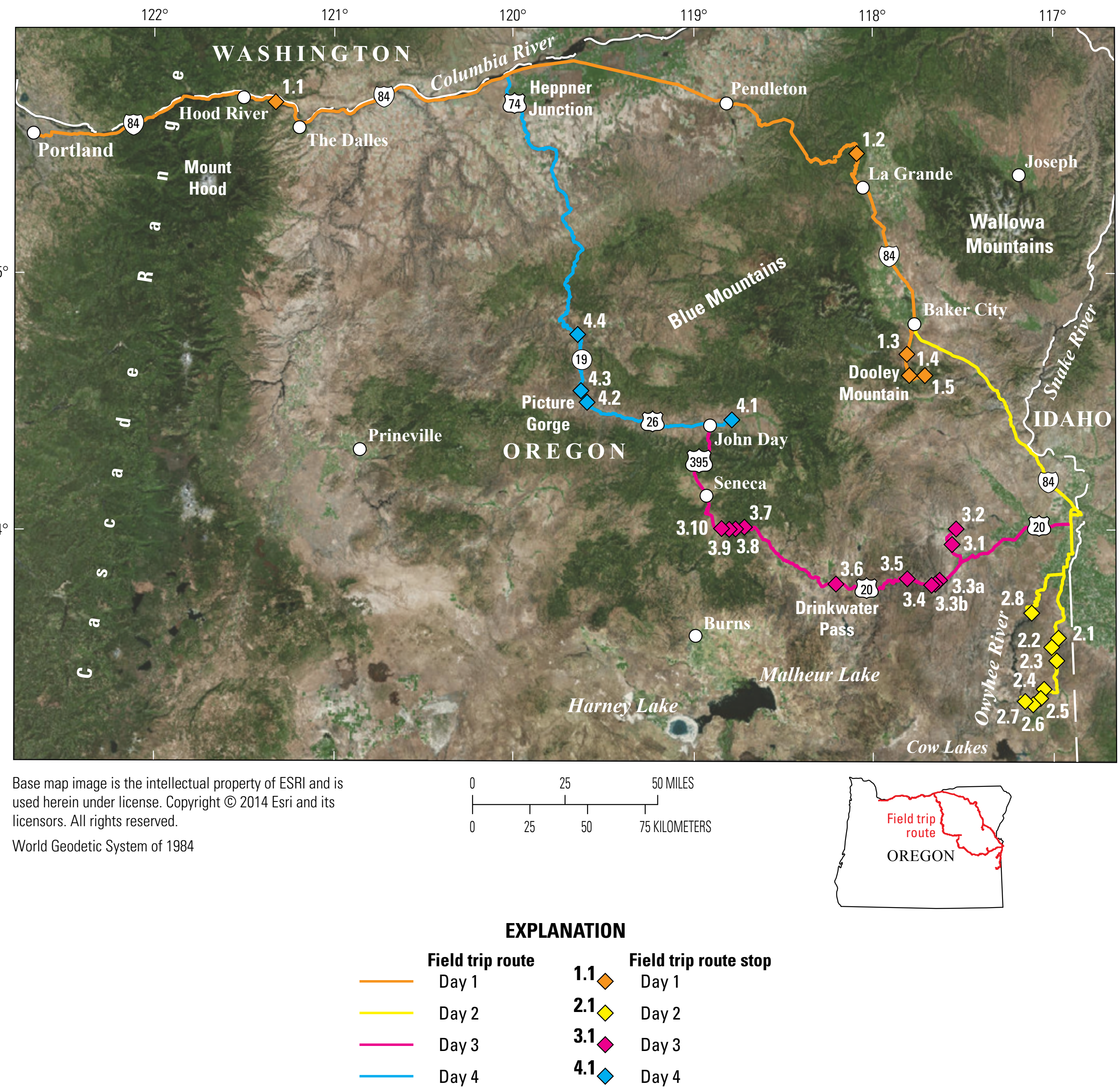

Figure 1. Map showing the field-trip route and the locations of numbered field stops referred to in the text.

Earth (Camp and others, 2013; Reidel and others, 2013a,b). Many researchers, including Duncan (1982), Brandon and Goles (1988, 1995), Draper (1991), Geist and Richards (1993), Hooper and Hawkesworth (1993), Camp (1995, 2013), Dodson and others (1997), Hooper and others (2002, 2007), Camp and others (2003), Camp and Ross (2004), Camp and Hanan (2008), Wolf and others (2008), Wolf and Ramos (2013), and Benson and Mahood (2016), see a link between the CRBG and a Yellowstone hotspot, with both being part of a larger volcanic province. This larger volcanic province includes the voluminous, middle Miocene rhyolite eruptive centers of northern Nevada and southeastern Oregon and the diverging bimodal and time-transgressive rhyolitic volcanic

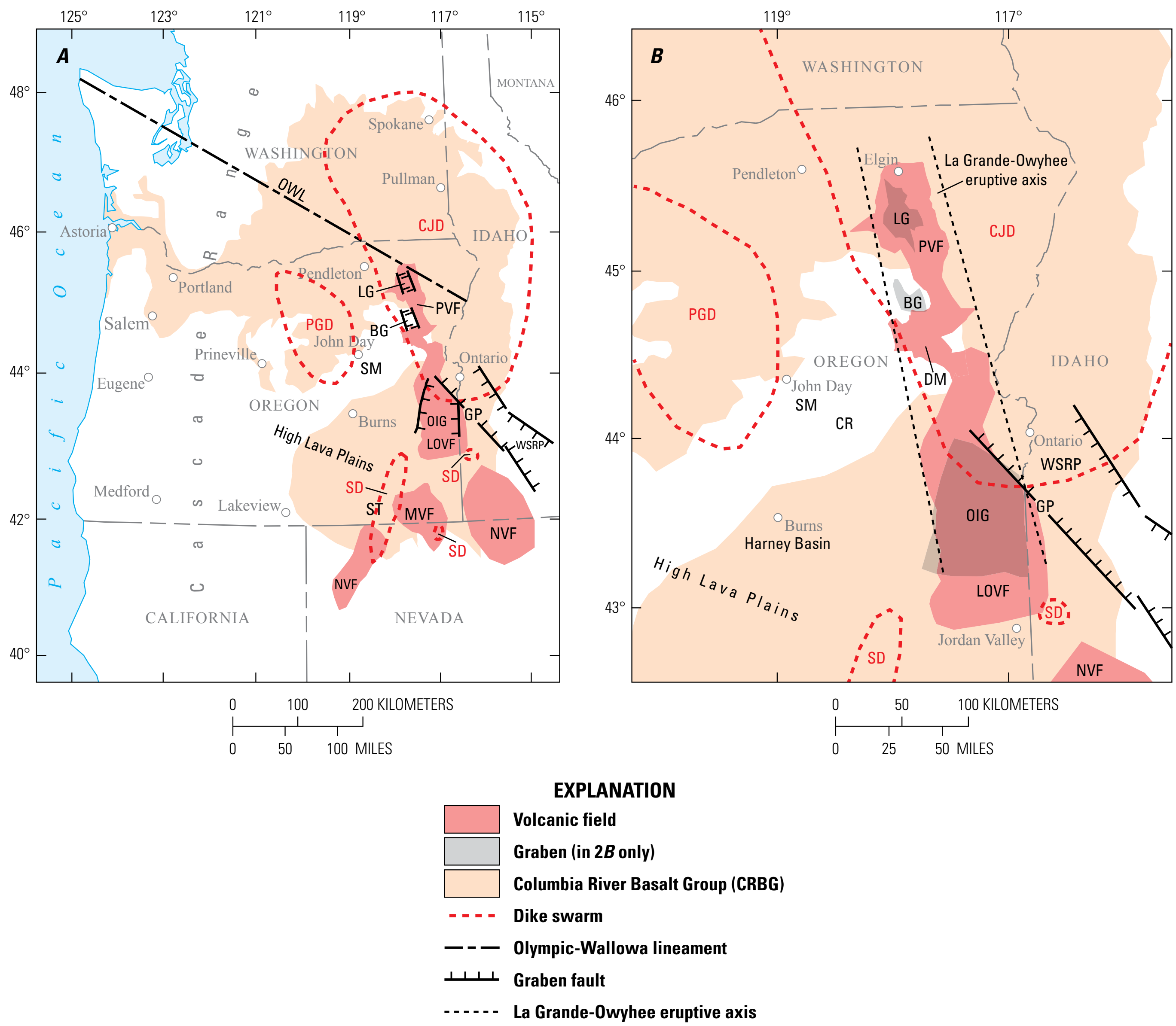

Figure 2. Sketch maps of the Columbia River Basalt Group (CRBG) and the La Grande-Owyhee eruptive axis (LOEA). *A*, Outcrop distribution of the Columbia River Basalt Group (CRBG) in Oregon, Idaho, Nevada, and Washington. Extent of flows includes areas from which the lavas have been eroded in addition to areas where lavas are concealed by younger units. Red-dashed lines indicate the regional distribution of dike swarms related to the CRBG (modified from Reidel and others, 2013a). Distribution of the Picture Gorge dike swarm (PGD) is modified on the basis of our new geologic mapping in the area between John Day and Burns; Prineville dike swarm is not shown as no dikes are known to exist in that area (McClaughry and others, 2009a, b). Regional features are depicted by the following abbreviations: BG, Baker graben; GP, Graveyard Point; LG, La Grande graben; LOVF, Lake Owyhee volcanic field; MVF, McDermitt volcanic field; NVF, northern Nevada volcanic fields; OIG, Oregon-Idaho graben; OWL, Olympic-Wallowa lineament; PVF, Powder River volcanic field; SM, Strawberry Mountain; ST, Steens Mountain; WSRP, western Snake River Plain. *B*, Eastern Oregon (part of A) showing the location of the La Grande-Owyhee eruptive axis (LOEA). Abbreviations are the same as in A. Additional abbreviations: CJD, Chief Joseph dike swarm; CR, Castle Rock; DM, Dooley Mountain; SD, Steens Mountain dike swarm. Note that the Picture Gorge dike swarm (PGD) is synonymous with the Monument dike swarm, and Strawberry Mountain (SM) is the location of the Strawberry Volcanics.

fields of the Snake River Plain-Yellowstone Plateau of Idaho and Wyoming and the High Lava Plains of central Oregon.

The name "Columbia River lava" was first used by Russell (1901) to describe lava flows of post John Day and pre-Mascall age (Merriam, 1901). Smith (1901) used "Yakima basalt" to describe lava flows high in the section in Washington. "Steens Basalt" was first used by Fuller (1931) for lavas at Steens Mountain in southeast Oregon. Waters (1961) first used the name "Picture Gorge Basalt" to describe lavas believed to lie beneath the Yakima basalt in Oregon. Brown and Thayer (1967) defined the Columbia River Group to include the Picture Gorge Basalt, the Yakima basalt, the Mascall Formation, and a "rhyolitic marginal facies" that bordered the Strawberry Volcanics of Thayer (1957).

All rocks other than mafic lava flows were excluded from the CRBG by Swanson and others (1979a) when the CRBG was defined to include the Imnaha Basalt, Grande Ronde Basalt, Picture Gorge Basalt, Wanapum Basalt, and Saddle Mountains Basalt as formal formations (fig. 3). The CRBG has since been

Series	Group	Formation	Member	Age (Ma)	Magnetic Polarity
Miocene, upper	Columbia River Basalt Group	Saddle Mountains Basalt	Lower Monumental Member	6	N
			Ice Harbor Member	8.5	
			Basalt of Goose Island		N
			Basalt of Martindale		R
			Basalt of Basin City		N
			Buford Member		R
			Elephant Mountain Member	10.5	R, T
middle			Craigmont Member		T
			Swamp Creek Member		T
			Feary Creek member		T
			Pomona Member	12	R
			Esquatzel Member		N
			Grangeville Member		
			Basalt of Eden		R
			Weissenfels Ridge Member		
			Basalt of Slippery Rock		N
			Basalt of Tenmile Creek		N
			Basalt of Lewiston Orchards		N
			Basalt of Cloverland		N
			Asotin Member	13	
			Basalt of Huntzinger		N
			Basalt of Lapwai		N
			Wilbur Creek Member		
			Basalt of Wahluke		N
			Umatilla Member	13.5	
			Basalt of Sillusi		N
			Basalt of Umatilla Member		N
		Wanapum Basalt	Priest Rapids Member		
			Basalt of Lolo	14.5	R
			Basalt of Rosalia		R
			Roza Member		T, R
			Shumaker Creek Member		N
			Frenchman Springs Member		
			Basalt of Sentinel Gap		N
			Basalt of Sand Hollow	15.2	N
			Basalt of Silver Falls		N, E
			Basalt of Ginkgo		E
			Basalt of Palouse Falls		E
			Lookingglass member		N
			Eckler Mountain Member		
			Basalt of Dodge		N
			Basalt of Robinette Mountain		N
			Vantage horizon		
		Grande Ronde Basalt (Prineville basalt)	Sentinel Bluffs Member	15.6	N_2
			Winter Water member		
			Fields Spring member		
			Indian Ridge member		
			Ortley member		
			Armstrong Canyon member		
			Buttermilk Canyon member		
			Slack Canyon member		
lower			Meyer Ridge member		R_2
			Grouse Creek member		
			Wapshilla Ridge member		
			Mount Horrible member		
		(Picture Gorge Basalt)	Cold Spring Ridge member		N_1
			Hoskin Gulch member		
			China Creek member		
			Frye Point member		
			Downey Gulch member		
			Brady Gulch member		?
			Kendrick Grade member		R1
			Center Creek member		
			Skeleton Creek member		
			Rogersburg member		
			Teepee Butte Member		
			Birch Creek member		
			Buckhorn Springs member		
		Imnaha Basalt		17.5	R1
					T
					N0
					R0

Figure 3. Chart showing stratigraphy and nomenclature for the Columbia River Basalt Group (CRBG). Figure modified from Reidel and others (2002), with updated stratigraphy from Reidel and others (2013a) and Reidel and Tolan (2013). Magnetic polarities combined with numerals within the Grande Ronde and Imnaha Basalts identify mapped magnetostratigraphic units as defined by Reidel and others (2013a). Abbreviations: E, excursional polarity; Ma, mega-annum (million years before present); N, normal polarity; R, reverse polarity; T, transitional polarity; ?, polarity uncertain.

expanded to include the Prineville basalt, basalt of Malheur gorge, and Steens Basalt (Hooper and others, 2002, 2007; Camp and others, 2003, 2013; Camp and Ross, 2004; Reidel and others, 2013b). With recognition of contemporaneous rhyolitic and mafic volcanism across eastern Oregon (Coble and Mahood, 2012; Streck and others, 2015, 2016), the "rhyolitic marginal facies" of Brown and Thayer (1967) has become more important to the concept of a larger Columbia River Basalt-Yellowstone province.

Workers in the southern and central parts of the province (Hooper and Swanson, 1990; Hooper and others, 2002; Camp and others, 2003; Ferns and McClaughry, 2013; Steiner and Streck, 2013a) document a general pattern in which magmatism progresses from voluminous tholeiitic flood basalts through large silicic eruptions to succeeding eruptions of smaller volume of calc-alkaline lavas and finally to much smaller volume of alkaline lavas. This general age progression and change in composition has been the basis for six stages of volcanism defined by Ferns and McClaughry (2013) along the LOEA in the eastern part of the CRBG province. These six stages are presented in this report as a framework to place local eruptive units into a bigger, province-wide context.

La Grande-Owyhee Eruptive Axis

The La Grande-Owyhee eruptive axis (LOEA) in eastern Oregon is an approximately (~) 300-kilometer (km)-long (185 mile (mi)), north-northwest-trending, middle Miocene to Pliocene volcanic belt located along the eastern margin of the Columbia River basalt province (Ferns and McClaughry, 2013) (figs. 2*A*, 2*B*). The eruptive axis extends from the town of Elgin on the north to the town of Jordan Valley on the south and lies between the Chief Joseph dike swarm on the east and the Monument dike swarm and the middle Miocene Strawberry Volcanics on the west (fig. 2*B*). It is defined by numerous volcanic vents contained within or directly adjacent to the La Grande (LG), Baker (BG), and Oregon-Idaho (OIG) grabens from which a progressive assemblage of mafic to intermediate tholeiitic, calc-alkaline, and alkalic lavas (fig. 4) and rhyolites erupted. These volcanic rocks, erupted from and preserved within the eruptive axis, form a stratigraphic link between the flood-basalt-dominated Columbia Plateau on the north and bimodal basalt-rhyolite vent complexes of the Owyhee Plateau on the south.

Volcanism along the La Grande-Owyhee eruptive axis progressed through six stages beginning in the middle Miocene and continuing through the Pliocene (figs. 4, 5, and 6). Stage 1 volcanism was characterized by 16.7 to 15.9 Ma (mega-annum) fissure eruptions that produced the Imnaha and Grande Ronde Basalt. Stage 2 was characterized by ~16 to 15.5 Ma fissure eruptions of highly evolved, tholeiitic lavas (icelandites). Stage 3

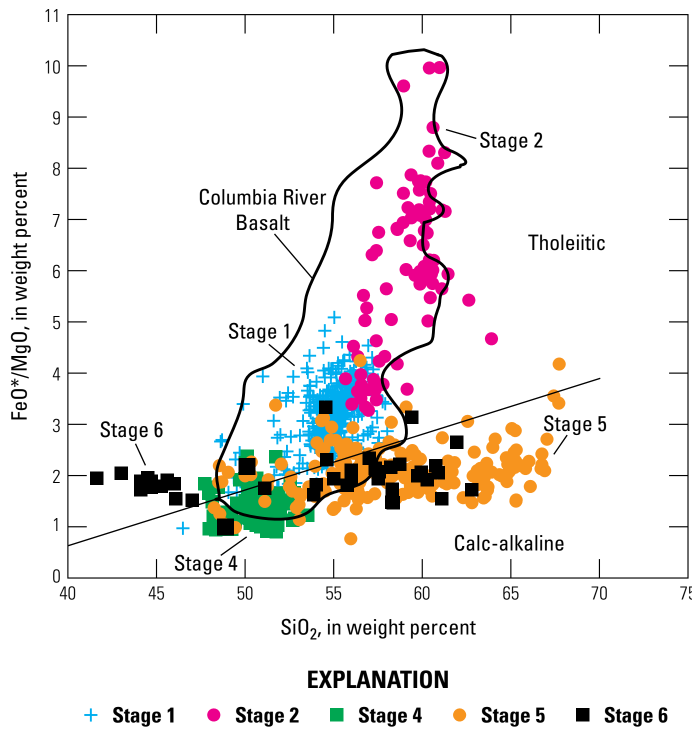

Figure 4. FeO*/MgO vs. SiO_2 variation diagram for volcanic rocks within the La Grande-Owyhee eruptive axis. Blue crosses are stage 1 tholeiitic flood basalts; pink circles are stage 2 icelandites; green squares are stage 4 olivine basalts; orange circles are stage 5 calc-alkaline volcanics; black squares are stage 6 alkalic volcanics. The sketched field displays the range of chemical compositions for the entire Columbia River Basalt Group (Ferns and others, 2010). Analyses are from Lees (1994), Binger (1997), and Ferns and McConnell (2005). Tholeiitic and calc-alkaline fields are from Miyashiro (1974). FeO* is total iron.

Figure 5. Sketch maps (*A*–*H*) showing the volcanic evolution of the La Grande-Owyhee eruptive axis. *A*, Mapped outcrop distribution of the Columbia River Basalt Group (CRBG) in Oregon—stage 1 flood basalts (CRBG lavas) in eastern Oregon. Note that the distribution in adjacent Idaho and Washington is not shown. *B*, Mapped outcrop distribution of stage 2 icelandites along the La Grande-Owyhee eruptive axis. *C*, Mapped outcrop distribution of the stage 3 Dinner Creek Tuff. The location labeled "CR" (Castle Rock) is the inferred eruptive center for this tuff. *D*, Mapped outcrop distribution of the stage 3 rhyolite and ash-flow tuff of the Lake Owyhee volcanic field (LOVF). Dooley Mountain is shown as "DM." Note that the Littlefield Rhyolite, Cottonwood Mountain rhyolite, and Leslie Gulch Ash-Flow Tuff are all included in the stage 3 rhyolite and ash-flow tuff shown. *E*, Mapped outcrop distribution of stage 4 olivine basalts along the La Grande-Owyhee eruptive axis. Olivine basalt abbreviations: LC, basalt of Little Catherine Creek; TP, Timms Peak Basalt. *F*, Mapped outcrop distribution of stage 5 andesite and dacite calc-alkaline volcanics along the La Grande-Owyhee eruptive axis. Calc-alkaline volcanics abbreviations: KS, Keeney Sequence; PRV, Powder River volcanics; SMV, Strawberry Volcanics. *G*, Mapped outcrop distribution of stage 6 alkalic volcanics along the La Grande-Owyhee eruptive axis. *H*, Mapped distribution of stages 1 to 6 volcanic vents along and adjacent to the La Grande-Owyhee eruptive axis. Regional features in *A*–*H* are depicted by the following symbols: BG, Baker graben; CJD, Chief Joseph dike swarm; CR, Castle Rock; LG, La Grande graben; NVF, northern Nevada volcanic fields; OIG, Oregon-Idaho graben; PGD, Picture Gorge dike swarm; SD, Steens Mountain dike swarm; SM, Strawberry Mountain; WSRP, western Snake River Plain.

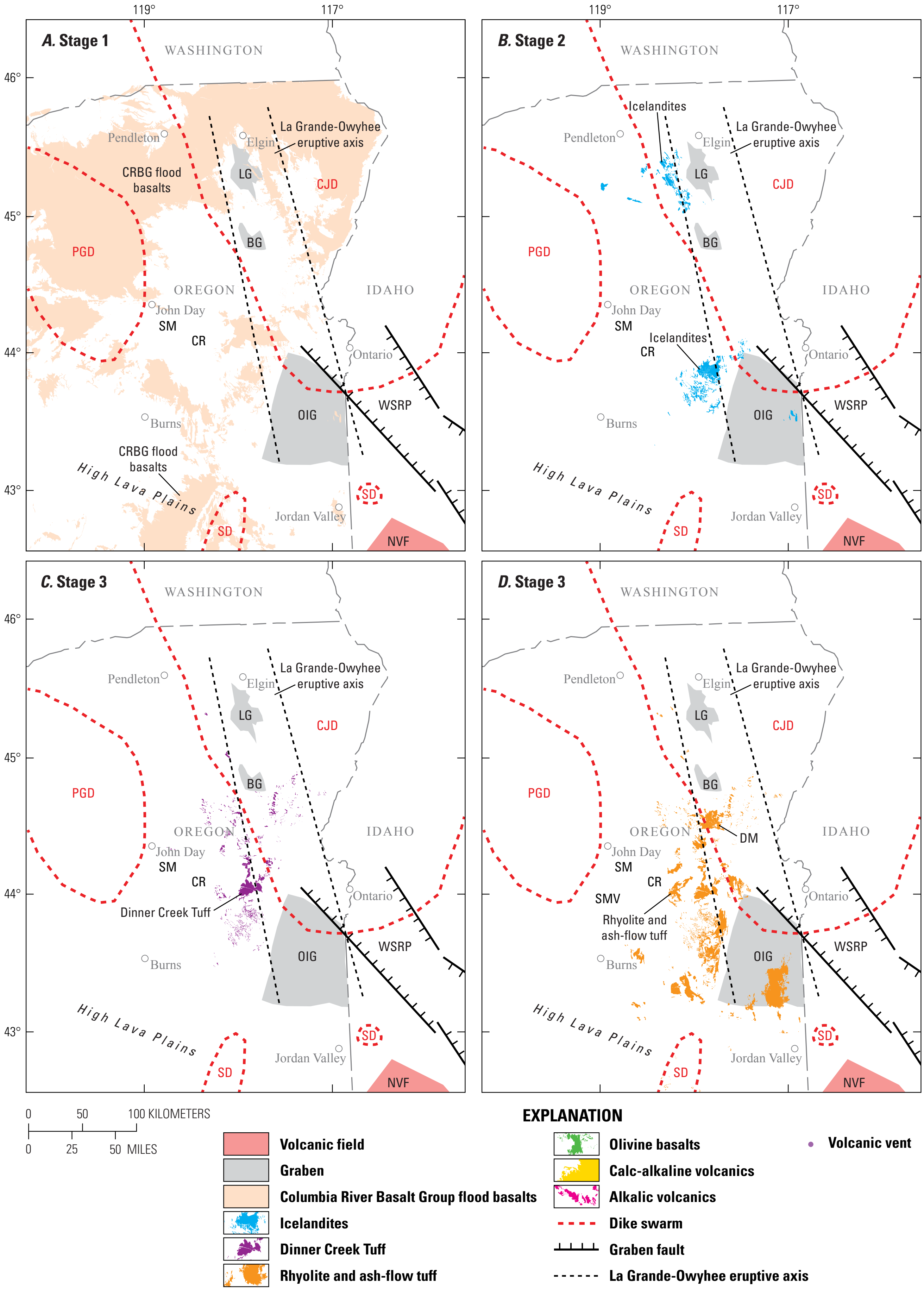
A. Stage 1
B. Stage 2
C. Stage 3
D. Stage 3
119°
117°
46°
45°
44°
43°
WASHINGTON
OREGON
IDAHO
Pendleton
Elgin
John Day
Ontario
Burns
Jordan Valley
La Grande-Owyhee eruptive axis
CRBG flood basalts
Icelandites
Dinner Creek Tuff
Rhyolite and ash-flow tuff
LG
BG
CJD
PGD
SM
CR
SMV
DM
OIG
WSRP
SD
NVF
High Lava Plains
0 50 100 KILOMETERS
0 25 50 MILES
EXPLANATION
Volcanic field
Graben
Columbia River Basalt Group flood basalts
Icelandites
Dinner Creek Tuff
Rhyolite and ash-flow tuff
Olivine basalts
Calc-alkaline volcanics
Alkalic volcanics
Dike swarm
Graben fault
La Grande-Owyhee eruptive axis
Volcanic vent

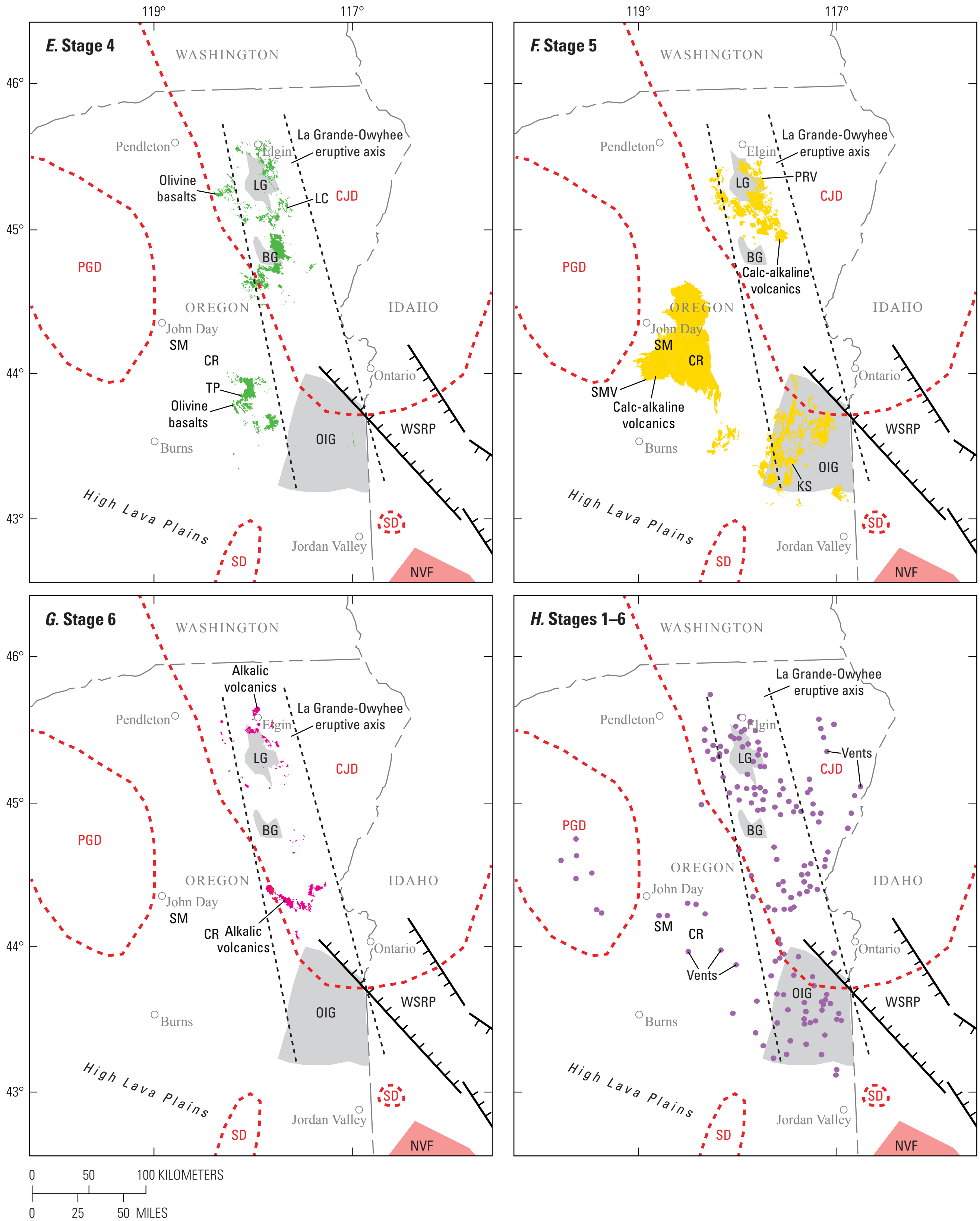
E. Stage 4
F. Stage 5
G. Stage 6
H. Stages 1–6
119°
117°
46°
45°
44°
43°
WASHINGTON
OREGON
IDAHO
Pendleton
Elgin
John Day
Burns
Ontario
Jordan Valley
La Grande-Owyhee eruptive axis
Olivine basalts
LC
TP
PRV
KS
SMV
Calc-alkaline volcanics
Alkalic volcanics
Vents
LG
BG
SM
CR
OIG
CJD
PGD
SD
NVF
WSRP
High Lava Plains
0 50 100 KILOMETERS
0 25 50 MILES

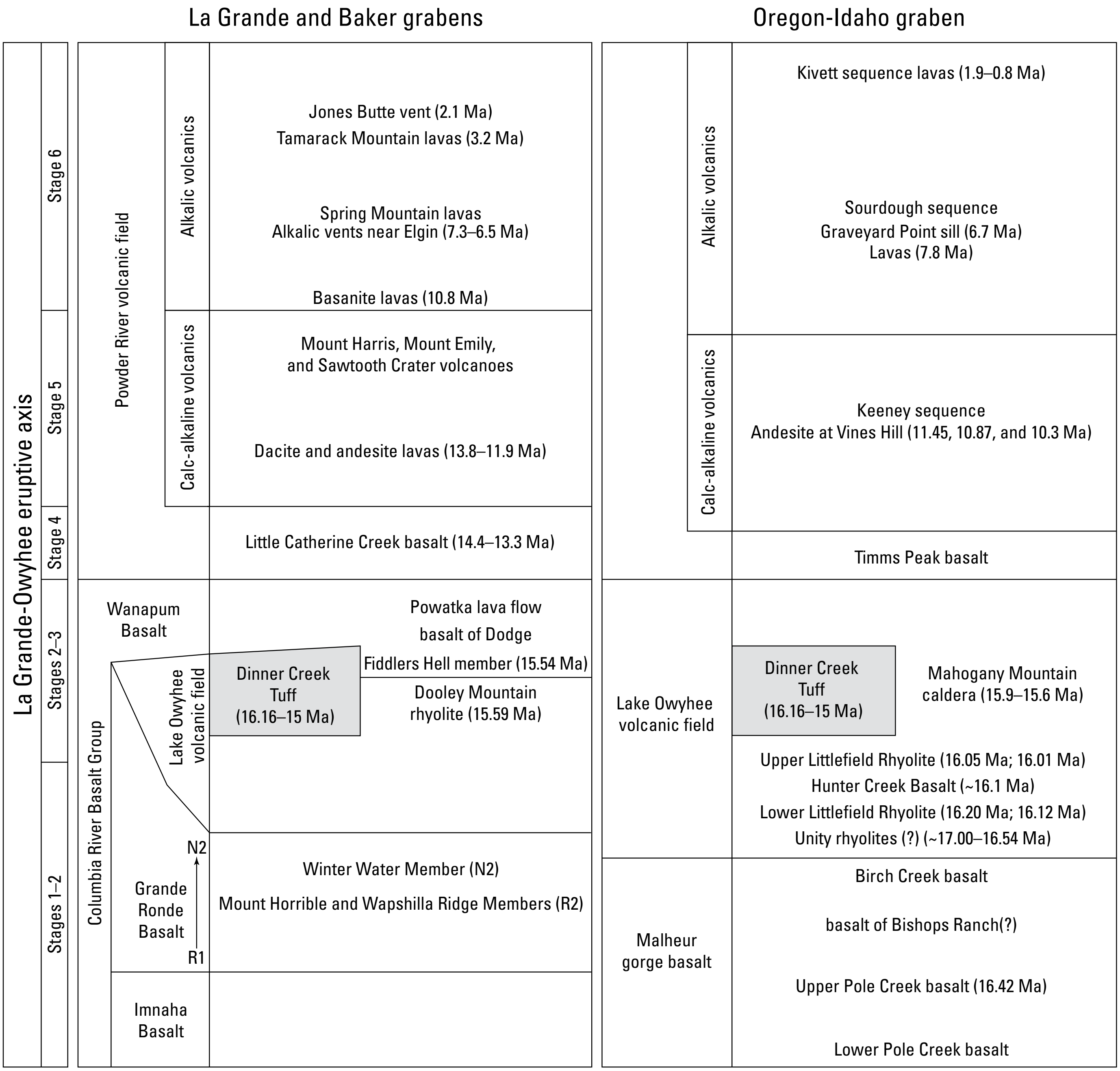

Figure 6. Correlation diagram showing the general stratigraphic relationships among units mapped along the La Grande-Owyhee eruptive axis. The Dinner Creek Tuff, shown with gray shade, is an extensive ash-fall unit exposed over a wide geographic area from north to south along the eruptive axis. Magnetic polarities (normal [N], reverse [R]) combined with numerals within the Grande Ronde Basalt identify mapped magnetostratigraphic units as defined by Reidel and others (2013a). Abbreviations: Ma, mega-annum (million years before present); "(?)," stratigraphic position uncertain.

was distinguished by ~16.5 to 14.7 Ma caldera-forming eruptions of ash-flow tuffs and rhyolite lava flows and domes. Stage 4 was marked by 14.7 to 13.7 Ma fissure eruptions that produced olivine basalts. Stage 5 was characterized by the eruption of 13.5 to 10.0 Ma calc-alkaline basaltic andesite, andesite, and dacite lavas (for the Strawberry Volcanics west of the LOEA, the age range is 15.5 to 12.5 Ma). Stage 6 was characterized by 7 to 1 Ma small-volume alkalic eruptions.

Pre-Tertiary Basement Rocks

The La Grande-Owyhee eruptive axis cuts across a basement collage of accreted terranes that now lie a short distance outboard of the cratonic and Late Cretaceous intrusive basement rocks (Idaho Batholith) of western Idaho (fig. 7). Between the La Grande Graben and Ontario, the CRBG and a wide variety of middle Miocene and younger volcanic rocks lie directly atop pre-Tertiary basement rocks. Tertiary volcanic and sedimentary rocks older than the CRBG are for the most part conspicuously absent in the area. Accreted terrane basement rocks encountered along the field-trip route are a composite mass of 3 late Paleozoic to early Mesozoic allochthonous terranes that have been stitched together by Late Jurassic and Early Cretaceous intrusions.

The northernmost Wallowa terrane is a block of Permian and Triassic oceanic island-arc volcanic rocks and successor Late Triassic to Early Jurassic basinal sedimentary rocks (fig. 7). The island-arc volcanic sequence includes a complexly deformed mass of lavas, domes, mudflow breccias and tuffs that are locally cut by coeval Triassic subvolcanic intrusions (Kurz and others, 2008). Successor basinal deposits include reef-facies limestones and fine-grained argillite. Zircon populations indicate that the fine-grained sediments were deposited in basin(s) isolated from the continental margin (LeMaskin and others, 2008).

The central Baker terrane is a tectonic collage of ocean-floor sedimentary rocks, ocean-floor and island-arc volcanic rocks, and serpentinite matrix-dominated mélange (fig. 7). Kays and others (1987) describes three components in the Baker terrane as (1) the northernmost and largely oceanic crust of the Bourne subterrane, consisting of Pennsylvanian, Permian, and Triassic chert-argillite broken formation and island-arc basement rocks (Ferns and Brooks, 1995; Schwartz and others, 2010); (2) the westernmost, serpentinite matrix-dominated mélange of the Greenhorn subterrane (Ferns and Brooks, 1995); and (3) the southernmost

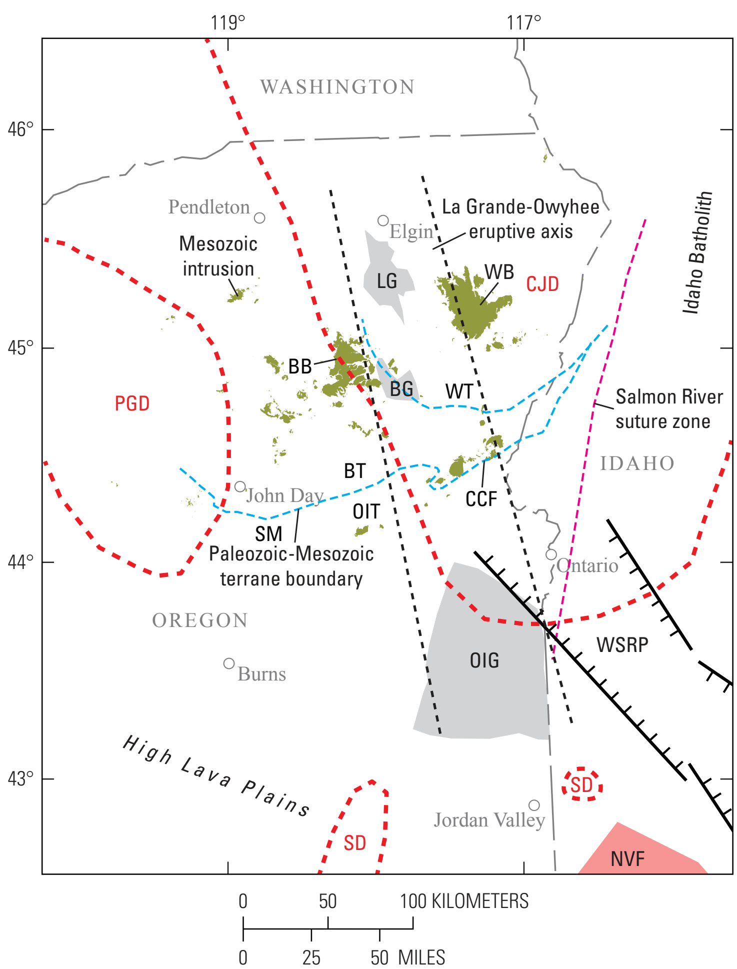

Figure 7. Sketch map showing the major Paleozoic-Mesozoic terrane boundaries in eastern Oregon and western Idaho. Major Mesozoic (Late Jurassic and Early Cretaceous) intrusions in northeast Oregon are shown in green shade. Regional features are depicted by the following abbreviations: BB, Bald Mountain Batholith; BG, Baker graben; BT, Baker terrane; CCF, Connor Creek Fault; CJD, Chief Joseph dike swarm; LG, La Grande graben; NVF, northern Nevada volcanic fields; OIG, Oregon-Idaho graben; OIT, Olds Ferry-Izee terrane; PGD, Picture Gorge dike swarm; SD, Steens Mountain dike swarm; SM, Strawberry Mountain; WB, Wallowa Batholith; WSRP, western Snake River Plain; WT, Wallowa terrane.;

and more highly metamorphosed Burnt River Schist (Gilluly, 1937; Kays and others, 1987).

The southernmost Olds Ferry-Izee terrane as used herein, includes the Olds Ferry and Izee terranes of Silberling and others (1984) (fig. 7). The Olds Ferry-Izee terrane includes an underlying sequence of partially eroded Permian and Late Triassic volcanic and volcaniclastic rocks (Huntington Formation of Brooks, 1979) and a overlying sequence of Late Triassic and Early Jurassic basinal sedimentary rocks. The basinal sedimentary sequence includes conglomerates containing clasts weathered from the underlying Huntington Formation, limestone, and local evaporate gypsum deposits, and fines upward into deeper-water turbidite facies made up of argillite and fine-grained sandstones. The exposure belt widens westward to near Izee where additional middle Mesozoic sedimentary units are exposed. Precambrian detrital zircons indicate that the Olds Ferry-Izee terrane formed a volcanic arc marginal to the North American Craton (LeMaskin and others, 2008).

Terrane boundaries have been intruded by a series of Mesozoic (Late Jurassic and Early Cretaceous) granitoid intrusions that are thought to stitch the terranes together (fig. 7). Johnson and Schwartz 2009) and Schwartz and others (2014) document three pulses of granitoid magmatism, commencing at 159 Ma and culminating at 118 Ma.

Graben Structures

The volcanic rocks that define the LOEA coincide with three north-trending, late Cenozoic grabens. These include from north to south the La Grande, Baker, and Oregon-Idaho grabens (fig. 2). The La Grande and Baker grabens occur along major Mesozoic terrane boundaries (fig. 7). Both grabens are considered to be right-lateral extensional duplexes or pull-apart structures (Hooper and others, 2007) within the transfer zone that links the Olympic-Wallowa lineament and the Western Snake River Plain (Mann and Meyers, 1993) (fig. 2). The Baker graben forms the boundary between the Wallowa and Baker terranes, while Wallowa terrane rocks cannot be traced west of the La Grande graben (figs. 2 and 7). The Baker graben is a smaller, asymmetric half-graben marked by large- to moderate-displacement, northeast-side down faults on its southern and western flanks. Graben-bounding faults along the front of Elkhorn Ridge on the west side of the graben may still be considered active. These structures have accommodated at least 3,280 feet (ft) (1,000 meters (m)) of displacement since the late Miocene. Both grabens are bounded by late Quaternary faults; most of the offset along the graben-bounding faults post-dates stage 5 calc-alkaline volcanism that occurred at about 13.5 Ma and 10.0 Ma. The La Grande graben is flanked on both the west and northeast flanks by large, Quaternary displacement faults, still considered active (Mann and Meyers, 1993; Ferns and others, 2010). Cumulative displacement along the western graben faults is in excess of 3,608 ft (1,100 m) (Ferns and others, 2010). The central part of the La Grande graben contains as much as 2,624 ft (800 m) of mostly fine-grained, semi-consolidated Neogene sedimentary rocks (Hampton and Brown, 1964; Van Tassel and others, 2001, 2002; Ferns and others, 2010).

The Oregon Oregon-Idaho Idaho graben, located south of Ontario, is a 30-mi-wide (50 km), north-south trending, fault-bounded depression that formed in the middle and late Miocene (Ferns and others, 1993a,b; Cummings and others, 2000) (fig. 2). Initiation of graben subsidence began between 15.5 and 15.3 Ma, following the largest eruptions of the CRBG, and coincident with the eruption of large-volume rhyolite lavas and caldera-related ash-flow tuffs from vents located both within and along the margins of the graben. Following initial subsidence and regional silicic eruptions (stage 3 volcanism), the Oregon-Idaho graben developed through three stages. The initial stage (15.3–14.3 Ma) included the deposition of fluvial and lacustrine sediment across the graben. The second stage (14.3–12.6 Ma) marked the onset of calc-alkaline volcanism in the area. Intragraben fault zones also developed during this time creating smaller distinct subbasins that served as catchments for a complexly intertonguing and fault-bounded succession of lavas, deposits from maar complexes, and coeval arkosic and tuffaceous sedimentary rocks. During the third stage (12.6–10.5 Ma) subbasins were filled by graben-wide fluviatile and lacustrine sedimentary rocks. Subsidence within the Oregon-Idaho graben ceased sometime during the late Miocene. The graben is truncated on the south by the younger east-west trending Antelope Valley graben (Ferns and others, 1993b) and Quaternary basalts of the Jordan Craters volcanic field. The northern end of the Oregon-Idaho graben is truncated by the Adrian fault zone, which is the western extension of the southern bounding faults to the Western Snake River Plain (Ferns and others, 1993a; Hooper and others, 2007).

Northern Part of the La Grande-Owyhee Eruptive Axis

The northern part of the LOEA extends from Elgin on the north to Dooley Mountain on the south and includes both the La Grande and Baker grabens (figs. 2 and 5). The following section describes the characteristics of the volcanic succession in the northern part of the LOEA and discusses key stratigraphic relationships amongst the 6 described stages.

Stage 1 in the northern part of the LOEA corresponds to the main phase of CRBG volcanism, marked by the fissure eruptions that formed the Imnaha Basalt and Grande Ronde Basalt on the north (figs. 2, 3, and 6; tables 1 and 2). A greater than (>) 1,640-ft (500-m)-thick section of stage 1 Grande Ronde Basalt flows is exposed beneath Indian Rock (Stop 1.2) on the western escarpment of the La Grande graben. The top of the stage 1 sequence at Indian Rock is marked by an ~330-ft (100-m)-thick section of normal (N) polarity lava flows (uppermost Grand Ronde N2 magnetostratigraphic unit) that resemble the Winter Water member. The N2 unit thins to the south, where upper R2 (R=reverse polarity) Grand Ronde lava flows beneath Mount Emily are overlain by stage

2 Fiddlers Hell member lava flows (tables 2 and 3). The base of the >1,310 ft (400 m) section of Grande Ronde Basalt flows below Mount Emily is marked flows correlative to the Center Creek member in the lower R1 Grand Ronde Basalt magnetostratigraphic unit. The Sentinel Bluffs Member, that typically marks the top of the Grand Ronde Basalt on the Columbia Plateau, is not present in the section beneath Mount Emily (fig. 3).

Table 1. Major and trace element analyses, sample location, isotopic age, and stage for Columbia River Basalt located north of Elgin.

[Major elements have been normalized to a 100 percent total on a volatile-free basis and recalculated as oxides, with total iron expressed as FeO*. The reported isotopic age was determined by the $^{40}Ar/^{39}Ar$ method. All analyses are from Ferns and McConnell (2005). Abbreviations: ID, identification number; Ma, mega-annum (million years before present); na, not applicable; nd, no data or not analyzed; WSU, Washington State University]

Formation	Grande Ronde Basalt	Wanapum Basalt				Saddle Mountains Basalt	
Member or unit	Sentinel Bluffs Member	Basalt of Dodge	Powatka lava flow	Frenchman Springs Member	Dinner Creek Tuff, cooling unit 2	Basalt of Umatilla Member	Basalt of Eden
Stage	1	1	1	1	3	na	na
Isotopic age (Ma)	nd	nd	nd	nd	nd	13.64±0.17	nd
Field sample ID	01-LG-19	01-LG-47A	00-LG-88	01-LG-22	01-LG-01B	01-LG-95	01-LG-25
Latitude (north)	45.726	45.667	45.588	45.728	45.736	45.739	45.732
Longitude (west)	117.811	117.886	117.859	117.808	117.866	117.905	117.805
Major elements as oxides, in weight percent							
SiO_2	53.36	51.77	54.96	50.91	75.38	54.70	52.32
Al_2O_3	13.69	15.55	13.43	13.32	13.01	13.51	13.12
TiO_2	2.084	1.338	2.770	3.141	0.203	2.863	2.817
FeO*	13.08	10.56	12.97	15.06	2.56	12.74	13.76
MnO	0.226	0.167	0.282	0.240	0.065	0.191	0.232
CaO	8.51	11.00	6.82	8.38	0.95	6.28	7.48
MgO	4.37	6.08	2.54	4.15	nd	2.80	3.67
K_2O	1.14	0.36	1.85	1.35	5.50	2.57	2.05
Na_2O	3.14	2.88	3.13	2.79	2.32	3.44	3.06
P_2O_5	0.399	0.295	1.240	0.655	0.011	0.902	1.485
Trace elements, in parts per million							
Ni	14	39	16.00	13	4	2	12
Cr	39	182	11	40	nd	5	45
Sc	41	41	36	42	3	30	31
V	370	307	176	439	nd	203	157
Ba	569	307	1,258	594	1632	3130	1,860
Rb	20	6	44	32	98	45	37
Sr	345	398	341	312	78	265	250
Zr	150	106	250	192	404	481	486
Y	35	30	63	47	73	47	65
Nb	13.2	8.9	19.6	16.5	22.7	21.9	35.8
Ga	19	18	19	21	22	21	23
Cu	27	75	20	3	nd	3	12
Zn	117	88	164	134	132	125	145
Pb	9	3	10	12	13	15	9
La	15	14	37	14	38	43	54
Ce	47	41	94	73	79	69	121
Th	6	2	5	5	3	8	7
Laboratory	WSU	WSU	WSU	WSU	WSU	WSU	WSU

Table 2. Major and trace element analyses, sample location, isotopic age, and stage for lava flows from the La Grande area.

[Major elements have been normalized to a 100 percent total on a volatile-free basis and recalculated as oxides, with total iron expressed as FeO*. Reported isotopic ages for samples 3, 6, and 7 determined by the $^{40}Ar/^{39}Ar$ method; sample 8 isotopic age determined by the K/Ar method. All analyses are from Ferns and McConnell (2005). Abbreviations: FRAN, Franklin and Marshall College; ID, identification number; Ma, mega-annum (million years before present); na, not applicable; nd, no data or not analyzed; WSU, Washington State University]

Formation or location	Grande Ronde Basalt			Dinner Creek Tuff	Powder River volcanic field			
Member, unit, or location	Unit N2	Fiddlers Hell member		na	Basalt of Little Catherine Creek	Mount Emily	Horseshoe basin	Sugarloaf Mountain
Stage	1	2	2	3	4	5	6	6
Age (Ma)	nd	nd	15.54 ± 0.10	nd	nd	13.4 ± 0.2	10.80 ± 0.18	7.26 ± 0.11
Sample number	1	2	3	4	5	6	7	8
Field sample ID	LG-153	SV-49C	TF-145C	03-B-60	00-LG-75	SV-12	99-LCC-115	02-LG-26
Latitude (north)	45.4633	45.4396	45.1029	44.6735	45.5783	45.3957	45.3047	45.4550
Longitude (west)	118.0927	118.0835	118.0520	117.6232	117.7650	118.1050	117.6587	118.217
Major elements as oxides, in weight percent								
SiO_2	54.45	56.48	59.50	73.48	50.82	65.19	44.67	55.17
Al_2O_3	13.73	13.51	13.17	13.29	16.31	16.49	14.87	17.75
TiO_2	2.27	2.33	1.93	0.260	1.54	0.66	2.82	1.58
FeO*	12.66	11.55	10.91	3.79	9.20	3.83	14.46	7.05
MnO	0.22	0.23	0.22	0.070	0.17	0.06	0.19	0.12
CaO	7.67	6.73	5.28	1.15	9.87	5.14	8.98	7.7
MgO	3.70	3.05	1.84	0.42	8.09	2.49	7.58	3.47
K_2O	1.66	2.09	2.50	4.43	0.68	1.66	1.24	2.09
Na_2O	3.25	3.40	3.86	3.08	2.84	4.18	4.64	4.16
P_2O_5	0.39	0.63	0.49	0.03	0.49	0.30	0.79	0.91
Trace elements, in parts per million								
Ni	2	nd	nd	3	199	30	86	15
Cr	23	12	nd	5	369	44	117	20
Sc	30	30	21	5	30	9	27	13
V	419	227	69	15	244	89	341	154
Ba	655	873	962	1600	386	533	342	1032
Rb	36	45	63	77	5	23	4	11
Sr	315	321	307	112	455	607	1250	2148
Zr	172	202	243	398	97	158	79	159
Y	38	46	55	69.7	25	16	18	15
Nb	15.7	19.7	21.1	23.9	7.1	9	7	8.6
Ga	24	20	23	21	15	21	21	26
Cu	23	4	nd	nd	72	16	122	55
Zn	131	143	143	141	90	74	134	119
Pb	9	6	10	16	4	8	nd	14
La	22	43	46	46	11	22	15	43
Ce	43	62	75	100	31	78	54	97
Th	4	10	7	6.7	nd	6	nd	1
Laboratory	WSU	WSU	WSU	FRAN	WSU	WSU	WSU	WSU

Table 3. Major and trace element analyses and sample location for stage 2 lavas.

[Major elements have been normalized to a 100 percent total on a volatile-free basis and recalculated as oxides, with total iron expressed as FeO*. Analyses are from Ferns and McConnell (2005),[1] Edwards (2013),[2] and Webb and others (2015).[3] Abbreviations: FRAN, Franklin and Marshall College; ID, identification number; nd, no data or not analyzed; WSU, Washington State University]

Formation or member	Fiddlers Hell member				Hunter Creek Basalt		
Stage	2	2	2	2	2	2	2
Field sample ID	98-LG-162[1]	SVC49D[1]	SV49C[1]	TF-117[1]	CNHS-02[2]	CNHS-07[2]	BW-13-09[3]
Latitude (north)	45.4138	45.4395	45.4396	45.0852	44.0440	44.0182	nd
Longitude (west)	118.1522	118.0830	118.0835	118.1020	117.4644	117.4563	nd
Major elements as oxides, in weight percent							
SiO_2	60.19	59.96	56.48	60.55	60.42	56.03	55.40
Al_2O_3	13.35	13.43	13.51	13.37	12.89	13.61	13.46
TiO_2	1.98	1.97	2.320	1.96	1.48	2.32	2.34
FeO*	10.81	10.70	11.55	10.14	12.06	11.65	13.04
MnO	0.18	0.22	0.230	0.18	0.28	0.22	0.21
CaO	4.81	5.22	6.73	4.96	5.11	6.60	7.04
MgO	1.60	1.64	3.05	1.63	1.26	3.03	3.35
K_2O	2.31	2.30	2.09	2.29	2.8	1.91	1.98
Na_2O	3.98	3.77	3.40	4.12	3.21	3.14	2.71
P_2O_5	0.80	0.80	0.63	0.80	0.47	0.50	0.472
Trace elements, in parts per million							
Ni	nd	nd	nd	nd	16	14	5
Cr	3	nd	12	6	5	13	7
Sc	23	27	30	26	12	29	31
V	76	76	227	72	39	298	361
Ba	926	978	873	967	2,229	755	724
Rb	63	55	45	61	174	62	49
Sr	316	309	321	312	267	333	309
Zr	246	238	202	239	293	231	217
Y	64	56	46	54	40	38	42
Nb	18.9	21.9	19.7	20.9	18.7	16.3	15.2
Ga	27	22	20	22	18.6	19.7	21.0
Cu	3	nd	4	2	3	20	12
Zn	151	149	143	145	82	130	142
Pb	8	8	6	12	20	nd	8
La	44	33	43	56	51	20	30
Ce	80	67	62	85	121	48	61
Th	12	10	10	10	19	8	6
Laboratory	WSU	WSU	WSU	WSU	FRAN	FRAN	WSU

Grande Ronde Basalt flows in the western escarpment of the La Grande graben are believed to be underlain by Imnaha Basalt. Farther east, the deep Minam River canyon cuts through Grande Ronde Basalt and into underlying Imnaha Basalt, exposing an ~492-ft (150-m)-thick section of N1 Grande Ronde and an ~1,640-ft (500-m)-thick section of Imnaha Basalt. It should be noted however, that the Imnaha Basalt fills into an irregular surface of pre-Tertiary rocks that may extend beneath the La Grande graben.

The stage 2 sequence is defined by tholeiitic andesites (icelandites), characterized by high FeO*/MgO ratios, that erupted near the end of the main phase of Grande Ronde Basalt volcanism (fig. 4, table 3). These are evolved flows that typically contain 55 to 61 weight (wt.) percent SiO_2 with MgO less than (<) 3.50 wt. percent, as compared to 53 to 56 wt. percent SiO_2 in typical Grande Ronde Basalt. The stage 2 Fiddlers Hell member defines the top of the Grande Ronde Basalt near La Grande (Ferns and Madin, 1999), and resembles the Powatka and Lookingglass lava flows that mark the base of the Wanapum Basalt to the north. P.R. Hooper (oral commun., 1999) suggested that perhaps the Fiddlers Hell member should be considered to be part of the younger Wanapum Basalt. Madin (1998) reported an $^{40}Ar/^{39}Ar$ isotopic age of 15.54 ± 0.10 Ma for the Fiddlers Hell member.

Fiddlers Hell member flows can be traced south of Mount Emily, where they overlie R2 Grande Ronde Basalt; on the northwest side of the Baker Valley, the Fiddlers Hell member flows overlie N1 Grande Ronde Basalt flows (Madin, 1998). Analyzed cuttings from deep water wells in the Grande Ronde Valley provide additional stratigraphic control on the Fiddlers Hell member. The basalt of Dodge, a high-aluminum olivine basalt, that marks the base of the Wanapum Basalt (Hooper and others, 2011), is found between the Fiddlers Hell member and a sequence overlying Grande Ronde-like flows that erupted from north-trending linear ridges composed of welded spatter.

Stage 3 is marked by large rhyolite ash-flow tuffs and rhyolite lavas that erupted from rhyolite eruptive centers and caldera complexes along the central and southern parts of LOEA (figs. 2, 5*D*, and 6). The Dinner Creek Tuff (Haddock, 1967) is the most extensive stage 3 unit, extending over an area in excess of 7,722 square miles (mi^2) (20,000 square kilometers (km^2)) (Streck and others, 2015) (fig. 5*C*). Source caldera(s) for the four discrete ignimbrites that make up the Dinner Creek are believed to lie in the Castle Rock-Ironside Mountain area northeast of the town of Burns (Rytuba and Vander Meulen, 1991; Streck and others, 2015), on the west margin of the Lake Owyhee volcanic field. New radiometric ages indicate that the stage 3 rhyolite ignimbrites, lava flows, and domes erupted between >16.5 to 15 Ma (Streck and others, 2016) and are contemporaneous with late stage 1 and stage 2 mafic magmatism (fig. 6).

The stage 3 sequence in the northern part of the LOEA is limited to distal air-fall tuffs and limited exposures of non-welded lithic tuff. Feldspar compositions ($An_{19.4}Ab_{75.4}Or_{5.2}$, and 0.25 wt. percent BaO) from an air-fall tuff that overlies a Frenchman Springs flow to the north at Lookingglass match Dinner Creek unit 2 feldspars ($An_{19.6}Ab_{75.4}Or_{5.1}$, and 0.26 wt. percent BaO) (Streck and others, 2015). The stage 3 section is thin and poorly exposed, generally marked by landslides and spring lines where overlain by Saddle Mountains Basalt or olivine basalt flows. Streck and others (2015) report $^{40}Ar/^{39}Ar$ ages for the Dinner Creek unit 2 of 15.45 ± 0.15 Ma, 15.48 ± 0.13 Ma, and 15.53 ± 0.15 Ma.

Stages 4, 5, and 6 on the north end of the LOEA together form the Powder River volcanic field of Bailey (1990) and Hooper and Swanson (1990). The base of the Powder River volcanic field is marked by an extensive sequence of olivine basalt flows that defines stage 4 volcanism (figs. 5*E* and 6). Stage 5 is defined by the sequence of thick andesite and dacite calc-alkaline lavas that form the larger vents in the Powder River volcanic field (figs. 5*F*). Most of the vents are monogenetic and defined by flows as thick as 330 ft (100 m) that cover more than 11.6 mi^2 (30 km^2). Mount Harris, at the north end of the East Grande Ronde Valley fault zone, is a small composite vent intruded by a summit dacite plug that has yielded an $^{40}Ar/^{39}Ar$ age of 11.8 ± 0.12 Ma (Ferns and others, 2010). Reported $^{40}Ar/^{39}Ar$ ages range from 13.38 ± 0.24 Ma and 13.4 ± 0.2 Ma for Mount Emily (Ferns and others, 2010) to 13.1 ± 0.1 Ma at Sawtooth Crater (Bailey, 1990).

Powder River volcanic field andesite and dacite flows are aphyric or microphyric with very small (<2 millimeters) phenocrysts of pyroxene and plagioclase. Many flows are high-silica andesite and dacite that fall along a calc-alkaline trend, with overall compositions ranging from basaltic andesite (53.45 wt. percent SiO_2) to high silica dacite (68.96 wt. percent SiO_2). Flows are generally characterized by low Niobium (Nb) contents and are considered to be crustal partial-melts derived from old island arc and oceanic crust (Bailey, 1990; Hooper and Swanson, 1990). Andesite compositions resemble that suggested for adakites with high SiO_2 (>56 wt. percent), Al_2O_3 (>15 wt. percent), and Sr (>400 parts per million); and low MgO (<3.0 wt. percent) and Sr/Y (>20).

Stage 6 flows in the northern part of the La Grande-Owyhee eruptive axis, transition from the basanite flows of Horseshoe Basin (Ferns and others, 2010), which have yielded $^{40}Ar/^{39}Ar$ plateau ages of 10.85 ± 0.18 and 11.6 ± 0.4 Ma, through small mugearite and benmoreite flows, to very small high-silica andesite domes at Jones Butte and Tamarack Mountain. Ferns and others (2010) report an $^{40}Ar/^{39}Ar$ whole-rock isochron age of 5.79 ± 0.9 Ma for a trachyandesite north of Elgin. A K/Ar age for Jones Butte of 2.0 ± 0.8 Ma is reported by Bunker and others (1982). Madin (1998) reports a $^{40}Ar/^{39}Ar$ age of 3.18 ± 0.15 Ma for Tamarack Mountain high-silica andesite. Many stage 6 lavas are highly phyric, with plagioclase and hornblende phenocrysts. Mugearite lavas near Elgin contain a pleochroic brown amphibole. They are sodium-rich alkaline rocks that are uniformly characterized by high Sr contents and high Sr/Y ratios. The youngest stage 6 vents include a high silica hornblende andesite vent at Jones Butte near Elgin and a high silica andesite flow located between the La Grande and Baker grabens at Tamarack Mountain.

Southern Part of the La Grande-Owyhee Eruptive Axis

The southern part of the LOEA extends from Dooley Mountain on the north through Jordan Valley on the south and includes the Lake Owyhee volcanic field and the Oregon-Idaho graben (figs. 2 and 5). The following section describes the characteristics of the volcanic succession in the southern part of the LOEA and discusses key stratigraphic relationships among the six described stages of volcanism.

Stage 1 CRBG flow stratigraphy in the south has not been established, with individual flows appearing to be less extensive than the "great" flows of the Columbia Plateau. Large rhyolite lava flows and caldera complexes cover critical areas between Columbia River Basalt flows exposed at Steens Mountain, on the Malheur River gorge and in the Silver City area of western Idaho.

The eastern margin of the Oregon-Idaho graben (Cummings and others, 2000) is defined by north-trending fault blocks of mafic lavas known as the basalt of Bishops Ranch (Kittleman and others, 1965, 1967). Ferns and others (1993a,b) consider these flows to be part of an early tholeiitic sequence equivalent to the CRBG (fig. 5*A*). The basalt of Bishops Ranch includes trachybasaltic andesite, trachyandesite lava flows, and autoclastic breccias that are cut by hornblende dacite plugs (Ferns, 1989a). Similar flows underlie a palagonite vent complex farther south near the Oregon-Idaho border (MacLeod, 1990a). Stratigraphic position of the Bishops Ranch within the CRBG is unclear. The Bishops Ranch lava flows resemble basaltic trachyandesite flows described by Camp and others (2013) in the upper Steens Basalt. Edwards (2013) shows that drill holes at Neal Hot Springs penetrated a sequence of subalkaline basaltic andesite and andesite lavas beneath the Birch Creek basalt unit and above the lower Pole Creek unit of Lees (1994) that resemble the uppermost CRBG flows at Silver City (Hasten, 2012) (fig. 6). Aseto (2012) reports an $^{40}Ar/^{39}Ar$ age on plagioclase of 16.18 ± 0.18 Ma from the mafic lavas at Silver City. Hooper and others (2002) and Camp and others (2003) consider the Birch Creek basalt to be equivalent to the Grande Ronde Basalt and the lower Pole Creek to be equivalent to the Steens Basalt. These all are part of the stage 1 lavas of Ferns and McClaughry (2013) (fig. 6).

Stage 2 is defined in the southern LOEA by basaltic andesitic and icelandite lavas of the Hunter Creek Basalt (figs. 5B and 6). The Hunter Creek is interbedded with large stage 3 rhyolite lava flows of the Littlefield Rhyolite (Kittleman and others, 1967) and overlies cooling unit 1 of the Dinner Creek Tuff as defined by Streck and others (2015) (figs. 5*B*, 5*C*, and 5*D*). The Littlefield Rhyolite is made up of at least three large-volume rhyolite lava flow packages that extend over an area of 463 mi^2 (1,200 km^2). Stage 2 Hunter Creek icelandite flows and stage 3 Littlefield Rhyolite lava flows appear to have erupted from a series of north-trending dikes along the western margin of Oregon-Idaho graben (fig. 5*B*). On the Malheur River, Hunter Creek flows overlie an older Littlefield Rhyolite lava flow (Edwards, 2013; Webb and others, 2015, 2016) that may be equivalent to the Cottonwood Mountain rhyolite of Evans and Binger (1999). Stages 2 and 3 magmatism in the Malheur gorge appear to have been very closely linked (Webb and others, 2016).

The Leslie Gulch Ash-Flow Tuff Member of Sucker Creek Formation (Kittleman and others, 1967) and Spring Creek tuff (Vander Meulen and others, 1987a,b) are areal-restricted stage 3 rhyolite ash-flow tuffs that erupted from the rhyolite caldera complex at Mahogany Mountain (Rytuba and others, 1985; Marcy and others, 2013).

The most extensive of stage 4 olivine basalt flows crop out on the west flank of the Oregon-Idaho graben (fig. 5*E*). Flows equivalent to the Timms Peak basalt extend from the Malheur gorge to the uplands east of Burns (Camp and others, 2003; Johnson and others, 1998). Large mafic sills exposed low in the Oregon-Idaho graben (Ferns and others, 1993a) and areas to the west (Johnson and others, 1998) also appear to be linked to stage 4 magmatism.

The transition from stage 4 olivine basalt flows to more evolved stage 5 calc-alkaline flows is more subtle in the south. Early stage 5 lavas are represented by calc-alkaline basalt and basaltic andesite flows at the base of the Owyhee basalt (Ferns and Cummings, 1992) that are intercalated with mafic hyaloclastite deposits and calc-alkaline rhyolite lava flows (fig. 5*F*). Edwards (2013) reported 40Ar/39Ar ages from flows equivalent to the upper calc-alkaline map units of Ferns and others (1993a,b) that range from 8.81 ± 0.05 Ma to 12.29 ± 0.09 Ma.

Early stage 6 lavas (fig. 5G) in the south are correlative with the Sourdough sequence of Lees (1994) and include the small volcano at Malheur Butte . Olivine basalt flows at the base of the late Miocene Lake Idaho sequence more closely resemble the olivine tholeiites of the Snake River Plain (Leeman, 1982).

Volcanism West of the LOEA: Strawberry Volcanics—High Lava Plains

The area north of Burns lies between the High Lava Plains and the Picture Gorge Basalt member of the CRBG and lies immediately west of the presumed source caldera(s) for the Dinner Creek Tuff, near Castle Rock. Work by Steiner and Streck (2013a) farther north reveals a compositionally diverse suite of volcanic rocks centered on Strawberry Mountain 18.6 mi (30 km) east-southeast of the town of John Day that provides a link between the CRBG Picture Gorge dike swarm of central Oregon and the large rhyolite centers of the Lake Owyhee volcanic field (fig. 2). Work to date (Steiner and Streck, 2013a,b) suggests a volcanic progression from flood basalts and large-scale silicic volcanism to later calc-alkaline magmatism somewhat similar to, yet markedly different than the six-stage magmatic progression evident in the LOEA (fig. 6). The marked difference lies in the large Devine Canyon and Rattlesnake ash-flow tuffs that erupted in this region following eruption of the Strawberry Volcanics. The silicic eruptions mark the onset of a western sweep of silicic magmatism from ~12 to 0.01 Ma (MacLeod and others, 1976; Jordan and others, 2004; Ford and others, 2013) through the High Lava Plains of central Oregon that makes a mirror image of the northeastward age progression of silicic volcanism of the Snake River Plain and Yellowstone Plateau (Christiansen and Yeats 1992; Christiansen and others, 2002; Pierce and Morgan, 2009).

Strawberry Volcanics

The name “Strawberry Volcanics” (Thayer, 1957; Brown and Thayer, 1967) was given to the diverse group of volcanic rocks that overlie Paleogene and pre-Tertiary basement rocks over an area of 3,600 km^2 along the south and eastern margins of the John Day Valley (Thayer, 1957). Robyn (1979) determined that the Strawberry Volcanics were generally younger than the main phase of the Columbia River Basalt, and calc-alkaline in character. Robyn (1979) also highlighted the occurrence of calc-alkaline andesite in this intra-continental setting far from subduction. Recent work by Streck and Steiner (2013a) and Steiner (2015) show that rocks mapped as Strawberry Volcanics include a predominantly calc-alkaline suite and a smaller volume mildly tholeiitic suite (fig. 8). The Strawberry Volcanics also include rhyolite and minor dacite. Other than for FeO*, the calc-alkaline and tholeiitic basalts and basaltic andesites (<55 wt. percent SiO_2) are essentially indistinguishable. Rare basalts resemble lavas of the Steens Basalt.

The Strawberry Volcanics was defined on the north by a basal sequence of olivine basalt flows that strongly resemble the stage 4 olivine basalts of the LOEA that are intercalated with basalt flows similar to those of the Picture Gorge Basalt. The Strawberry Volcanics are in part correlative with the “Tba” basalt and andesite unit of Greene and others (1972) north of Burns.

The occurrence of volcanic rocks more silicic than andesite was mentioned to occur in the “marginal facies of the Columbia River Group” of Brown and Thayer (1967), north of the John Day River near John Day, which is now recognized as Dinner Creek unit 2, and by Robyn (1979) for a small patch of rhyolitic rocks southwest of Strawberry Mountain.

Work to date indicates that the early eruptions of rhyolites in the southern part of the Strawberry Volcanics are coeval with CRBG magmatism of the Grande Ronde Basalt (figs. 3 and 5*F*). Steiner and Streck (2013a) report $^{40}Ar/^{39}Ar$ radiometric ages from critical outcrops that suggest volcanism in the southern part of the Strawberry volcanic field began with rhyolite volcanism at ~16.16 ± 0.17 Ma and lasted until about ~12 Ma, roughly overlapping with the main pulse of the Grande Ronde Basalt, and coincident with Wanapum Basalt and early eruptions of the Saddle Mountains Basalt. Currently, the oldest reported age in the Strawberry Volcanics on a calc-alkaline andesite (57.6 wt. percent SiO_2) is 15.57 ± 0.16 Ma by Steiner (2015).

Steiner and Streck (2013a) present trace element data from the Strawberry Volcanics that indicate an open-system process in which assimilation and magma-mixing of partial melts allows for the evolution of calc-alkaline, “arc-like” andesite magmas from a tholeiitic parent. The transition from tholeiitic flood basalts to calc-alkaline magmas in the Strawberry volcanic field in the middle Miocene corresponds with similar transitions seen southeast of Burns (Camp and others, 2003) in the Oregon-Idaho graben (Lees, 1994; Ferns and McClaughry, 2013) and in the Powder River volcanic field (Bailey, 1990; Hooper and Swanson, 1990; Ferns and McClaughry, 2013). Such a transition has also been reported for the late Miocene from the Harney basin west of Burns (Streck and Grunder, 2012). The most mafic magmas of the Strawberry Volcanics (≤54 wt. percent SiO_2) share geochemical signatures with lavas of the CRBG; therefore, strongly suggesting that the CRBG lavas and Strawberry Volcanics have a similar petrogenetic origin (Steiner, 2015).

Regionally Widespread Late Miocene Ash-Flow Tuffs of the High Lava Plains

The High Lava Plains stretch from the western end of the central CRBG province to the volcanic arc of the Cascade Mountains. Late Miocene to Quaternary volcanism of the High Lava Plains is strongly bimodal with rhyolite forming dome complexes and ignimbrites and bimodal with basalt and basaltic andesite erupted as widespread lavas typically a few meters to 10 m thick (MacLeod and others, 1976; Jordan and others, 2004; Streck and Grunder, 2008; Ford and others, 2013). The High Lava Plains defines a northwestward-younging magmatic trend of silicic volcanism that is a mirror image of the northeastward age progression of silicic volcanism of the Snake River Plain and Yellowstone Plateau (Christiansen and Yeats, 1992; Christiansen and others, 2002; Pierce and Morgan, 2009). Based on estimates of aerial extents and thicknesses, mafic rocks and rhyolites are subequal in volume on the High Lava Plains. Intermediate compositions are scarce and, where they occur, are mainly simple mixtures of mafic and rhyolitic magmas (Linneman and Myers, 1990; Streck and Grunder, 1999; Johnson and Grunder, 2000). Among several ignimbrites that erupted from vents along the High Lava Plains the 9.7 Ma Devine Canyon Tuff and the 7.1 Ma Rattlesnake Tuff stand out by their extreme distribution area; each covering an area in excess of 20,000 km^2 (Green and others, 1973; Streck and Grunder, 1995; Wacaster and others, 2011) representing about 300 cubic kilometers (km^3) of mostly high-silica, rhyolitic, metaluminous to peralkaline magma (Greene, 1973; Streck and Grunder, 1995, 1997; Wacaster and others, 2011). Both tuffs are believed to have erupted from the Harney basin from now-concealed calderas near the town of Burns (fig. 2). Both the Devine Canyon and Rattlesnake tuffs formed single cooling units commonly between 8 to 20 m thick (Green and others, 1973, Streck and Grunder, 1995). Erosional remnants of both tuffs can be found within a radius of ~62 to 93 mi (100 to 150 km) around their source area.

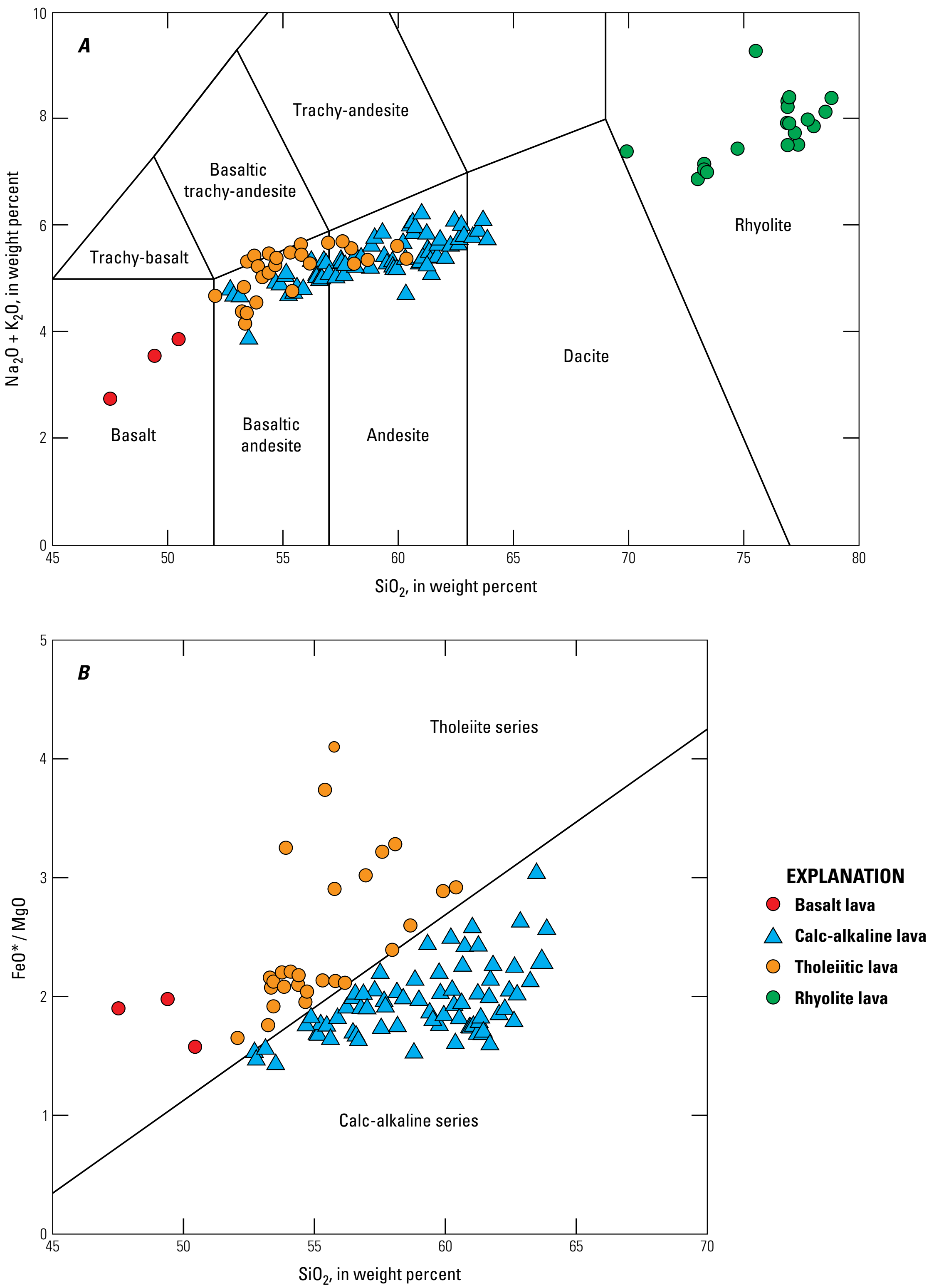

Figure 8. Geochemistry classification diagrams showing results from rocks of the Strawberry Volcanics. *A,* Total alkalis ($Na_2O + K_2O$) vs. SiO_2 of whole-rock X-ray fluorescence (XRF) analyses (normalized to 100 percent anhydrous). Fields are from Le Bas and others (1986) and Le Maitre and others (1989). *B,* FeO*/MgO vs. SiO_2. Fields of tholeiitic and calc-alkaline series are from Miyashiro (1974). Analyses shown in both *A* and *B* are from Steiner and Streck (2013). FeO* is total iron.

Icelandites

Iron-rich andesitic magmas (icelandites) are a common magma type to both the LOEA and the Burns area (fig. 5*B*). In the northern part of the LOEA (Day 1), the Fiddler's Hell member icelandites are present at the top of the Grande Ronde Basalt section. In the southern part of the LOEA (Day 2), evolved tholeiites make up the basalt of Bishops Ranch, and are possibly associated with the Mahogany Mountain caldera. Outcrops on Day 3 visit icelandite vent complexes associated with the large rhyolite lava flows of the Littlefield Rhyolite, and icelandites exposed north of Burns.

The icelandites appear to be process, rather than time related. Stratigraphic relationships determined from wells in the Grande Ronde Valley (northern LOEA) place the Fiddlers Hell eruptions prior to the first Wanapum Basalt eruptions. Madin (1998) reports a radiometric age of 15.54 Ma for a Fiddlers Hell flow to the south. Hunter Creek Basalt eruptions at Namorf (southern LOEA; Stops 3.3a and 3.3b) are tightly constrained by radiometric ages of underlying and overlying rhyolite lava flows that constrain the iron-rich basaltic andesitic lava age between 16.15 and 16.05 Ma. Icelandites at Stop 3.9 have a maximum age of 15.5 Ma, as they overlie cooling unit 2 of the Dinner Creek Tuff at Stop 3.10 and may be close in age to the youngest cooling unit of the Dinner Creek, the ~15 Ma cooling unit 4.

Wolff and others (2008) suggests that the main CRBG units of the Steens Basalt, Imnaha Basalt, and Grande Ronde Basalt were stored in a common centralized storage system centered about 40 km west of the town of Ontario and extending in either direction for ~37 to 62 mi (60 to 100 km) (fig. 5*A*). From there, mafic magmas traveled in dikes to their respective eruption sites (Wolff and others, 2008). The area of this hypothetical storage system encloses most rhyolitic centers of the Lake Owyhee volcanic field (figs. 5*C*, 5*D*). Streck and others (2015, 2016) present petrological evidence that mafic magmas, similar to upper Grande Ronde Basalt, must have been present below upper crustal rhyolite centers that likely imposed some control on where mafic magmas could erupt. The significance for the discussion here is that the timing and composition of icelandites suggest that they are the last pulse of the main CRBG, and the local venting of icelandites further suggests that CRBG reservoirs existed within the proposed area of Wolff and others (2008).

Field-Trip Stop Descriptions and Road Log

The field trip leaves from the Oregon Convention Center in Portland. While a majority of this field trip travels over major paved highway and secondary roads, sections of the route traverse over unpaved Bureau of Land Management (BLM) or United States Forest Service (USFS) roads at higher elevations that may be impassable in the late fall, winter, and early spring. Please check with the BLM or USFS for current road conditions on federally managed land before embarking on the trip. Independent readers of this guide are encouraged to carry a detailed Oregon road atlas to aid in navigation along the field-trip route. Map coordinates (latitude and longitude) are provided for field-trip stops in order to allow the interested reader to visit these sites in the field or to remotely visualize the area using Google Earth™. Coordinates are provided in two systems including (1) Geographic (datum in World Geodetic System 1984 (WGS84); units in decimal degree); and (2) Universal Transverse Mercator (UTM) Zone 10 (datum in WGS84; units in meters). Decimal degree coordinates can be entered into the "Fly to" box (for example, 45.6613°, -121.4712°) in the search toolbar, and Google Earth will automatically locate and "fly" to the specified site. UTM coordinates are provided for the reader who would like to more precisely locate and visit sites in the field using a handheld GPS unit. As of this writing, Google Earth is not yet configured to understand UTM coordinates entered into the "Fly to" box.

Day 1. Columbia River Basalt Group and Northern Part of the La Grande-Owyhee Eruptive Axis

Day 1 traverses the Columbia River gorge eastward to Baker City, focusing on prominent outcrops that reveal a distal succession of laterally extensive, large-volume tholeiitic flood lavas of the Grande Ronde, Wanapum, and Saddle Mountains Basalt formations of the CRBG. These "great flows" are typical of the well-studied, flood-basalt-dominated Columbia Plateau, where interbedded silicic and calc-alkaline lavas are conspicuously absent. The latter part of Day 1 will highlight exposures of middle to late Miocene silicic ash-flow tuffs, rhyolite domes, and calc-alkaline lava flows overlying the CRBG across the northern and central parts of the LOEA.

The road log begins at the Oregon Convention Center in Portland, Oreg. Numbers to the left on the road log is the cumulative mileage from the Oregon Convention Center starting point, with kilometers provided in parenthesis. Field-trip Stops 1.1 to 4.4 are shown in figure 1.

Road Log
Cumulative Mileage
mi (km)

0.0 (0.0) Leave the Oregon Convention Center and go south on NE Martin Luther King Jr. Blvd/OR 99E toward NE Irving Street. Cross I–84.

0.2 (0.3) Turn left onto NE Everett Street.

0.3 (0.5) Merge onto I–84 E towards the Portland Airport/The Dalles. Drive east to Exit 69 (Mosier).

8.0 (12.9) Rocky Butte is the isolated, high-standing hill visible just west of the interstate. The butte is the eroded intrusive core to a 285 ± 16 ka (kilo-annum) olivine-phyric, calc-alkaline basaltic andesite vent within the late Pliocene and Pleistocene Boring volcanic field (Evarts and others, 2009).

17.0 (27.4) Sandy River crossing.

31.0 (49.8) Multnomah Falls is visible to the right (south).

44.0 (70.8) Town of Cascade Locks. The flow-on-flow sequence of early to middle Miocene Columbia River Basalt exposed along the interstate route is tilted to the south, exposing more poorly consolidated volcaniclastic rocks of the underlying early Miocene Eagle Creek Formation. These rocks are also prominently exposed in large landslide headscarps forming the skyline north of the Columbia River. Repeated failures along the south-dipping contact between flows of the CRBG and Eagle Creek Formation have generated large landslide complexes that previously blocked the Columbia River, forming the Bridge of the Gods. The latest landslide occurred around 1450 A.D. (O'Connor and Burns, 2009).

60.0 (96.6) 3.5 Ma pillow delta, with well-developed, west-dipping foreset beds exposed on both sides of the highway between aphyric to sparsely olivine-phyric basaltic lavas of the basalt of Ruthton Point (McClaughry and others, 2012).

63.0 (101.4) Hood River. The city of Hood River resides in the Hood River Valley, located along the axis of the Quaternary to Pliocene High Cascades volcanic arc in northern Oregon. From Three Sisters (central Oregon) north to Mount Adams (Washington State), the young High Cascades occupy an ~18.6-mi (30-km)-wide, discontinuous and structurally segmented graben formed as a result of a northward propagating rift (Conrey and others, 2002). Between Mount Hood and Mount Adams, the structural depression occupied by the High Cascades coincides with the Hood River graben, a half-graben that forms the Hood River Valley (McClaughry and others, 2012). The eastern margin of this graben is defined by the north-northwest striking Hood River fault zone an en-echelon succession of normal faults which began forming during the late Pliocene or early Pleistocene (McClaughry and others, 2012). A number of Pleistocene shield volcanoes and cinder cones, including Underwood Mountain visible north of the Columbia River, lie within the Hood River graben.

64.0 (103.0) The interstate crosses several strands of the late Pliocene and Quaternary Hood River fault zone, just east of the city of Hood River. Strands here displace a sequence of CRBG lava flows and younger late Pliocene lava flows with a down-on-the-west sense of displacement.

69.0 (111.0) Mosier. **Exit right off of I–84 at Mosier, Exit 69.** Turn right and proceed 0.2 mi (0.3 km) miles south, toward Mosier. The road crosses the rail line and makes a sharp turn to the left (east) towards Mosier. Just after the left bend in the road, turn left (north) on Rock Creek Road. Proceed 0.8 mi (1.2 km) on Rock Creek Road to the parking area and trailhead for the Mark O. Hatfield Trail. Leave the vehicle and return by foot 0.1 mi (0.16 km) northeast to the trailhead. **Stop 1.1** is a short traverse (0.8 mi (1.3 km) roundtrip) west on the paved Mark O. Hatfield Trail to a primitive viewpoint that showcases a broadly folded, flow-on-flow succession of CRBG lavas incised by the Columbia River. The parking area has restroom facilities; handicapped accessible parking is available at the trailhead.

Stop 1.1. Mark O. Hatfield Trail—Overview of Columbia River Basalt Group "Great Flows" (lat 45.6856° N., long 121.4116° W.)

Views to the north and east from Stop 1.1 reveal both the sequence of tholeiitic CRBG "great flows," and the fold-belt structure that has been imposed on the section of flows, both during and after their emplacement (fig. 9). The eastern Columbia River gorge is underlain by an extensive succession of chemically distinct CRBG flows that are correlative with regionally widespread lavas exposed eastward across the Columbia Plateau. Members of the CRBG exposed in the eastern Columbia River gorge include the Pomona Member of the Saddle Mountains Basalt; the Priest Rapids and Frenchman Springs Member of the Wanapum Basalt; the Sentinel Bluffs Member, Winter Water member, and Ortley members of the N2 magnetostratigraphic unit of the Grande Ronde Basalt; lavas forming the Grouse Creek and Wapshilla Ridge members of the R2 magnetostratigraphic unit; and the Downey Gulch member of the N1 magnetostratigraphic unit (figs. 3 and 9; Wells and others, 2009; McClaughry and others, 2012). CRBG formations not exposed in the Columbia gorge include the older Steens Basalt and Imnaha Basalt, and coeval Picture Gorge Basalt and Prineville basalt (fig. 3). Interbedded silicic units are, for the most part, conspicuously absent in the Columbia River gorge (see Brown and Thayer, 1967, for discussion). Individual CRBG units can be difficult to identify with certainty in the field, but can be distinguished on the basis of a multiple criteria mapping approach using stratigraphic position and thickness, geochemistry, magnetic polarity, paleomagnetic analysis of oriented core samples, and petrography following the work of Swanson and others (1979a,b), Reidel and others (1989, 2013), Beeson and others (1985, 1989), Wells and others (1989, 2009), and Hooper (2000). The primary uncertainties in accurately mapping these flows arise from (1) poor exposure and recognition of flow contacts; (2) intra-flow chemical variation; and (3) the

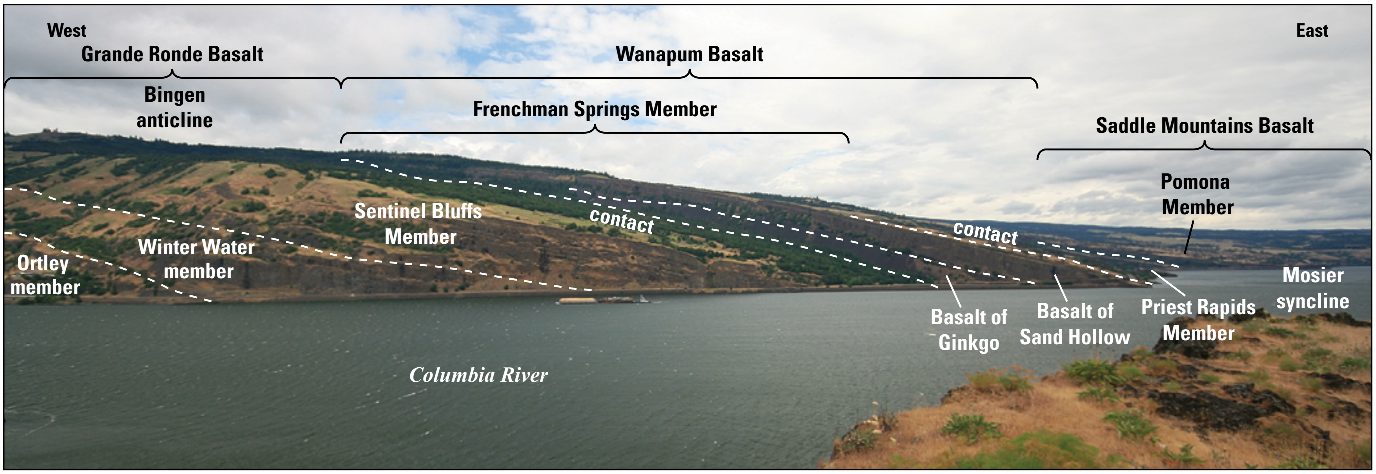

Figure 9. Photograph from Stop 1.1 looking north and east across the Columbia River from the Mark O. Hatfield Trail into the paired Bingen anticline and Mosier syncline. The area is underlain by an extensive, distal succession of Columbia River Basalt Group (CRBG) lavas that are part of the Grande Ronde, Wanapum, and Saddle Mountains Basalt formations. Photograph by Jason McClaughry.

effect of weathering on chemical composition (Wells and others, 2009).

CRBG lavas present in the eastern Columbia River gorge were erupted from north-northwest-trending linear fissure systems in the eastern part of the Columbia Plateau largely between ~17 and 14 Ma. Sources for the older Grande Ronde Basalt flows are marked by the Chief Joseph dike swarm (Taubeneck, 1970), while Frenchman Springs dikes lie west of the Chief Joseph dike swarm (Martin and others, 2013), near the northern terminus of the LOEA. Younger Pomona and Priest Rapids source dikes are exposed farther east in Idaho (Tolan and others, 2009). Eastern Columbia Plateau-derived flows traversed down an ancestral paleoslope westward through the Columbia Trans-Arc Lowland toward the low-relief topography of western Oregon (Tolan and Beeson, 1984; Beeson and others, 1985, 1989; Tolan and others, 1989; Wells and others, 1989, 2009; McClaughry and others, 2012) (fig. 2). The Columbia Trans-Arc Lowland was a generally southwest-northeast-directed, ~37-mi-wide (60 km) topographic low that extended across the ancestral Cascade Range during the middle Miocene (Beeson and others, 1989; Beeson and Tolan, 1990).

CRBG flows and to a lesser extent younger strata in the eastern Columbia River gorge are broadly folded into a series of east-northeast-trending folds, segmented by a number of northwest-trending strike-slip faults and localized thrust faults. Stop 1.1 places us along the eastward-dipping transitional limb linking the paired Bingen anticline and Mosier syncline (fig. 9). Fold structures in the eastern Columbia River gorge are part of the regionally extensive Yakima Fold Belt, a regional set of asymmetric, typically southeast-verging, locally overturned and faulted anticlinal ridges separated by broad synclinal valleys (Swanson and others, 1979a, 1981; Anderson, 1987; Watters, 1989; Reidel and Campbell, 1989; Tolan and Reidel, 1989, Anderson and others, 2013). The Yakima Fold Belt covers much of the western and west-central Columbia Plateau (Tolan and others, 2009) and extends westward beneath the Cascade Range. East-west-directed folds across the Columbia Plateau are inferred by other workers to have formed in response to a north-northwest to south-southeast compressional stress regime (Reidel and Campbell, 1989; Beeson and Tolan, 1990; Anderson and others, 2013). Deformation in the Yakima Fold Belt has persisted since at least the middle Miocene, with a majority of the present structural relief developing since ~10.5 Ma (Reidel and Campbell, 1989; Tolan and others, 2009). Structural warping in the western part of the Yakima Fold Belt during the middle Miocene is inferred to have increasingly restricted the distribution of the younger parts of the Grande Ronde, Wanapum, and Saddle Mountains Basalts to structural lows in the Columbia River gorge and Willamette Valley (Vogt, 1981; Beeson and others, 1985; Anderson and Tolan, 1986). Successively younger lavas, most notably flows in the Priest Rapids and Pomona Members, were partially or wholly confined to paleocanyons. The thickness and distribution of these CRBG units through the Columbia River gorge locally show evidence of restricted distribution and thinning across anticlines, although these ancient channel remnants do not precisely correspond to present-day structural highs and lows (Anderson, 1987; Anderson and Vogt, 1987; Beeson and Tolan, 1990). Folds continued to develop in post-CRBG time, as large accumulations of volcaniclastic and sedimentary detritus shed from the late Miocene Cascades (locally the Dalles Formation) preferentially accumulated in basins along synclinal troughs. Post-Pliocene fold deformation is evidenced by lavas as young as 3.05 Ma, that are broadly folded and are structurally dismembered by fold-associated, northwest-trending strike-slip or oblique slip faults in the Hood River Valley (McClaughry and others, 2012). Additional evidence for Pliocene and younger fold deformation and faulting in the Yakima Fold Belt is presented by Anderson and others (2013), who report that Pliocene flows in the Simcoe Mountains volcanic field (eastern Washington State) have been faulted and folded to varying degrees.

Return to vehicle and drive 1.0 mi back to interchange for I–84. Turn right and merge onto I–84 E. Proceed east toward The Dalles.

Cumulative Mileage
mi (km)

85.0 (136.8) City of The Dalles.

106.0 (170.6) Biggs Junction.

139.0 (223.7) Town of Arlington. I–84 E begins to climb away from the Columbia River.

166 (267.2) City of Boardman. Coarse gravels here were left by the westward passage of catastrophic Ice-Age Missoula floods generated by the repeated collapse of ice-dams on upper tributaries to the Columbia River located in western Montana.

190 (305.8) Umatilla River crossing at town of Stanfield. The higher peaks on the south (right) are part of the Blue Mountains uplift, which is cored by a variety of older Tertiary sedimentary and volcanic rocks, Cretaceous marine sediments, and older pre-Tertiary metamorphic and intrusive basement rocks. The uplift separates the main exposure belt of the Picture Gorge Basalt to the south from the classical Saddle Mountains-Wanapum-Grande Ronde Basalt stratigraphy exposed across the Columbia Plateau and westward through the Columbia River gorge.

211 (339.5) City of Pendleton.

218 (350.8) Town of Mission and Wildhorse Casino.

245 (394.3) Summit Road/Mt Emily. **Exit right off of I–84, Exit 243.** Turn left onto U.S. Forest Service Road 31 (Summit/Mt Emily Road). Proceed northeast toward Indian Rock. The road crosses the N2 Winter Water Member of the CRBG (fig. 3).

248.3 (399.6) Fiddlers Hell icelandite flow.

255.0 (410.4) Stage 6 vents are exposed on the south (Sugarloaf Mountain) and north (Spring Mountain).

263.7 (424.4) Turn right onto U.S. Forest Service Road 3120 (Skyline Road). Proceed south along the ridge top. The canyons on the west are incised into a westward-dipping slope of Grande Ronde Basalt flows. The abrupt chasm on the east marks the east face of the West Grande Ronde Valley fault zone (Ferns and others, 2010).

266.3 (428.6) **Stop 1.2.** An improved parking area and overlook structure capping Indian Rock marks the site for Stop 1.2. A short walk from the parking area takes the field trip to the overlook structure and then onward to spectacular rock exposures forming Indian Rock. The parking area has restroom facilities and 2 picnic sites.

Stop 1.2. Indian Rock-La Grande Graben Overlook (lat 45.4653° N., long 118.0970° W.)

Indian Rock Overlook is a magnificent viewpoint providing a panoramic perspective of the La Grande graben (Grande Ronde Valley). The overlook is located near a major route traditionally used by Native Americans while transiting the Blue Mountains into the Grande Ronde Valley. It was built through the cooperative efforts of the U.S. Forest Service and Army National Guard 1249th Engineering Battalion.

Indian Rock provides an ideal geologic overlook, revealing the transition zone between the classical CRBG stratigraphy of the Columbia Plateau exposed in the canyons north of Elgin and the more chemically varied lavas exposed southward in the LOEA (figs. 2*B*, 5, and 10). Indian Rock itself is a ~200-m-wide (diameter) cylindrical plug of mafic palagonitic breccia, first interpreted as a diatreme by Taubeneck (1980). Ferns and McClaughry (2013) recognize Indian Rock as vent source for a series of distinct mafic flows capping the nearby ridgetop. Mafic, ridge-capping flows are highly evolved tholeiite lavas that are part of the Fiddlers Hell member of the Grande Ronde Basalt (Ferns and Madin, 1999; Ferns and others, 2010). These evolved tholeiites contain as much as 61 wt. percent SiO_2 and display a strong FeO* enrichment-MgO depletion trend (table 2). We herein refer to such rocks as "icelandites" to distinguish them from andesites that lie on a calc-alkaline trend. Madin (1998) reports a $^{40}Ar/^{39}Ar$ age of 15.54 ± 0.01 Ma for Fiddlers Hell lavas.

The fault-bounded depression viewed on the east is the ~25-mi (40 km)-long La Grande graben (Grande Ronde Valley), the northernmost of three north-trending, late Cenozoic grabens that coincide with the LOEA (fig. 2). These include from north to south the La Grande, Baker, and Oregon-Idaho grabens (fig. 2). The La Grande graben is flanked on both the west and northeast flanks by large, Quaternary displacement faults, still considered active (Mann and Meyers, 1993; Ferns and others, 2010). Cumulative displacement along the western graben faults is in excess of 3,608 ft (1,100 m) (Ferns and others, 2010). The central part of the La Grande graben contains as much as 2,624 ft (800 m) of mostly fine-grained, semi-consolidated Neogene and younger sedimentary rocks lying above a faulted section of rocks forming part of the CRBG and Powder River volcanics (Hampton and Brown, 1964; Van Tassel and others, 2001, 2002; Ferns and others, 2010).

Deep wells drilled in search of groundwater resources in the Grande Ronde Valley have provided a wealth of data regarding the subsurface geology of the area, and have permitted key

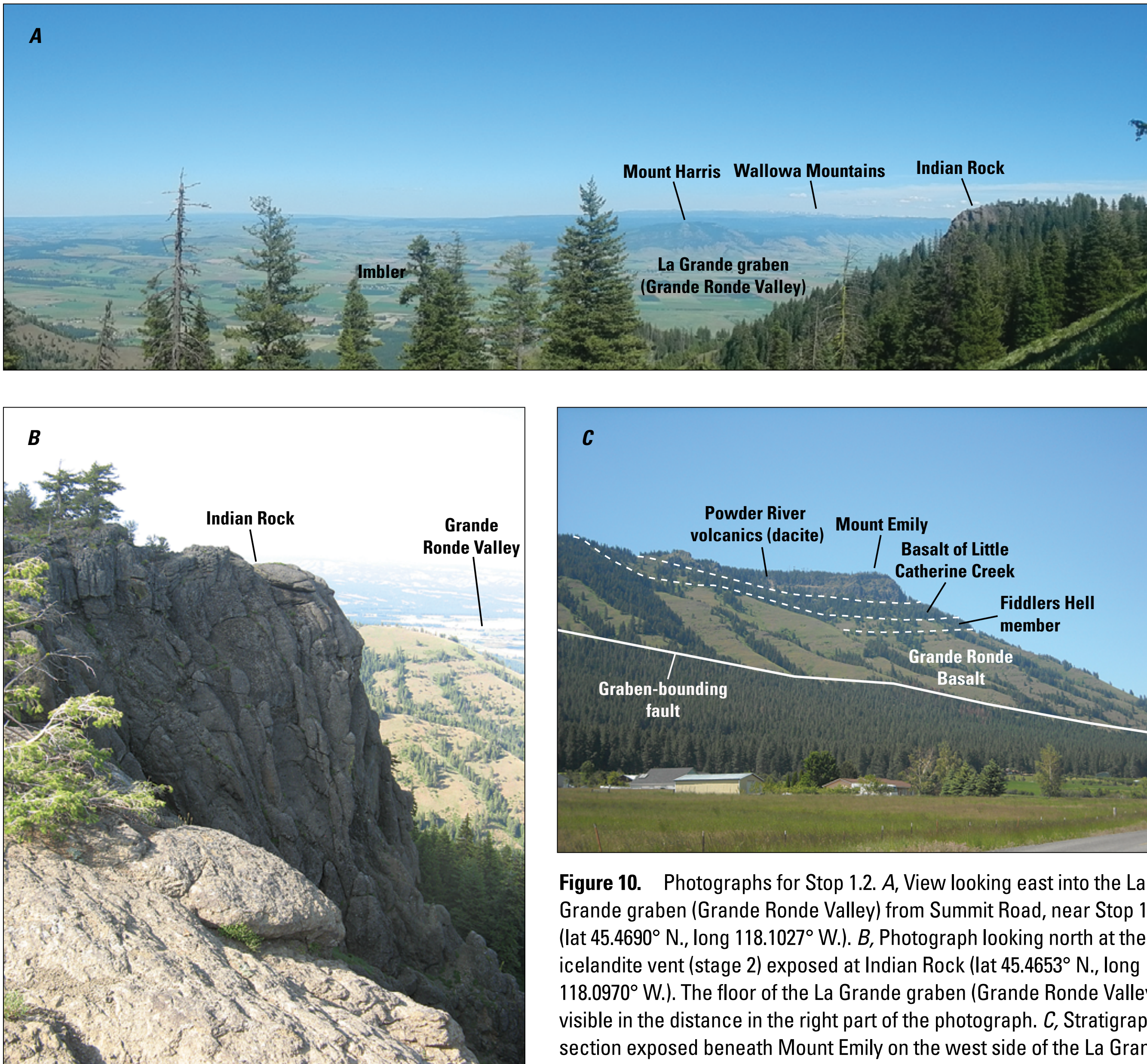

Figure 10. Photographs for Stop 1.2. *A*, View looking east into the La Grande graben (Grande Ronde Valley) from Summit Road, near Stop 1.2. (lat 45.4690° N., long 118.1027° W.). *B,* Photograph looking north at the icelandite vent (stage 2) exposed at Indian Rock (lat 45.4653° N., long 118.0970° W.). The floor of the La Grande graben (Grande Ronde Valley) is visible in the distance in the right part of the photograph. *C,* Stratigraphic section exposed beneath Mount Emily on the west side of the La Grande graben. The photograph is looking northwest from Orchard Road (lat 45.4144° N., long 118.0609° W.). Photographs by Jason McClaughry.

correlations with equivalent strata exposed in adjacent upland areas (fig. 11). A number of deep wells, exceeding 2000 ft (610 m) in total depth, have been drilled in central parts of the valley since the middle to late 1990s. Cuttings obtained from regular intervals (~10 ft) in these wells have allowed us to create subsurface lithologic and geochemical stratigraphic sections that are comparable with detailed geologic mapping and geochemical reference sections collected at the surface (Ferns and others, 2010). Detailed regional geologic mapping combined with well-constrained subsurface sections have provided valuable insight into the stratigraphic interrelationships between CRBG lavas, compositionally diverse lavas of the Powder River volcanic field, and silicic tuff units. These sections have also revealed important information regarding the structural evolution of the La Grande graben and cumulative offset across the structure from the middle Miocene to present.

Laterally extensive CRBG units, such as the Fiddlers Hell member (stages 1 and 2), and Powder River volcanic field units, such as the basalt of Little Catherine Creek (stage 4) are readily identifiable through geochemical analyses of well cuttings. Less

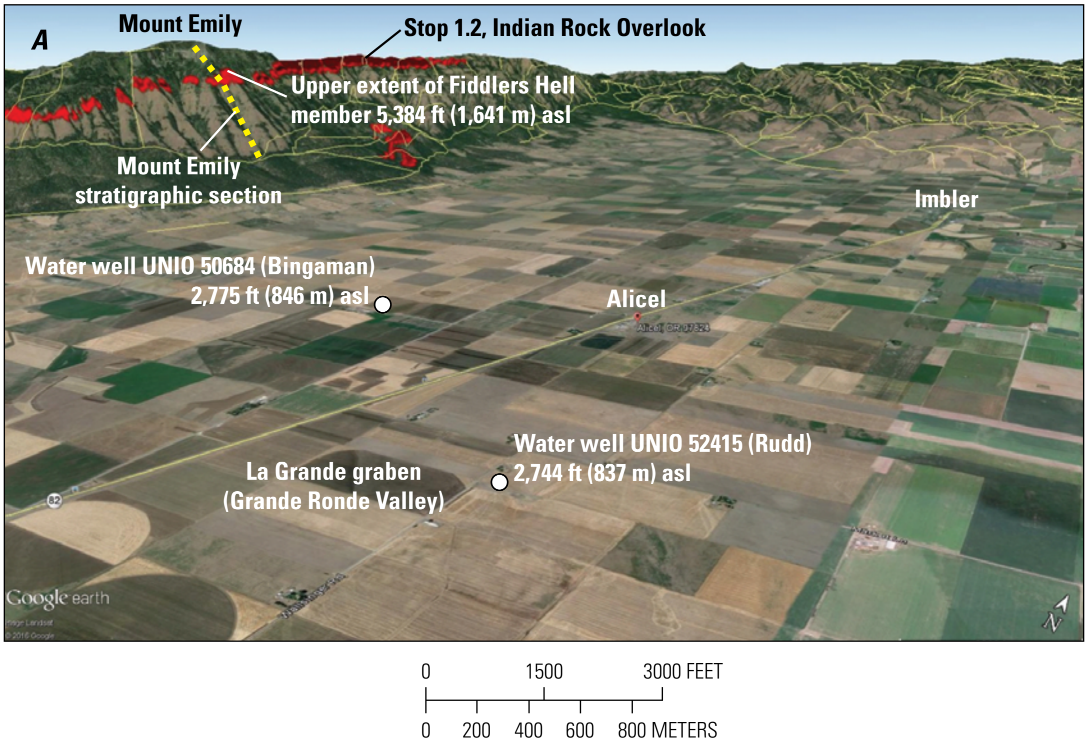

Figure 11. Lithologic- and geochemical-based correlation diagram between a mapped stratigraphic section underlying Mount Emily and the lithologies encountered in two water wells drilled in the central part of the La Grande graben (Grande Ronde Valley) near Alicel. *A*, Location photograph looking north-northwest showing (1) the location of the stratigraphic section underlying Mount Emily (dashed yellow line) that corresponds to the stratigraphy shown in figure 10*C*; (2) the location of two water wells (white-filled circles) drilled near Alicel; (3) the location of Mount Emily and Stop 1.2 (Indian Rock Overlook); (4) the mapped distribution of the Fiddlers Hell member (red shade along Mount Emily/Summit Road), including fault blocks (down to the east) exposed below Indian Rock Overlook (also red shade); (5) the upper extent of the Fiddlers Hell member at 5,384 feet (1,641 meters) above sea level (asl); (6) mapped faults from Ferns and others (2010) (thin, solid yellow lines); and (7) nearby communities. *B*, Correlation diagram for the Mount Emily stratigraphic section and two water well lithologic logs “UNIO 50684 (Bingaman)” and “UNIO 52415 (Rudd).” The location of geochemical rock samples taken from the Mount Emily stratigraphic section and the two lithologic logs are shown with red circles. The vertical center line with ticks running down the center of the diagram is true elevation (in feet). The black vertical lines with ticks next to the two respective water well logs show depth (in feet) below land surface. The red dashed line is the stratigraphic tie line at the top of the Fiddlers Hell member between the Mount Emily stratigraphic section and the two water well logs. Note that the Fiddlers Hell member is offset by significant down-to-the east faults between Mount Emily and Alicel and it appears to thin eastward, away from its source area at Indian Rock (Stop 1.2). Also note the variability and thickness of stratigraphic units in each section. The “OWRD GRID ID” is the unique identifier given by the Oregon Water Resources Department (OWRD) when the well was drilled. The OWRD GRID ID can be used to locate the original well log at the OWRD Well Log Query web site at http://apps.wrd.state.or.us/apps/gw/well_log/. Imagery for the location photograph (*A*) is from Google Earth Pro. Radiometric ages are from Ferns and others (2010). Abbreviations: bsl, below sea level; ft, feet; m, meters; ID, identification number; Ma, mega-annum (million years before present); N, normal magnetic polarity; R, reverse magnetic polarity; TRS, township, range, section, of Public Land Survey system.

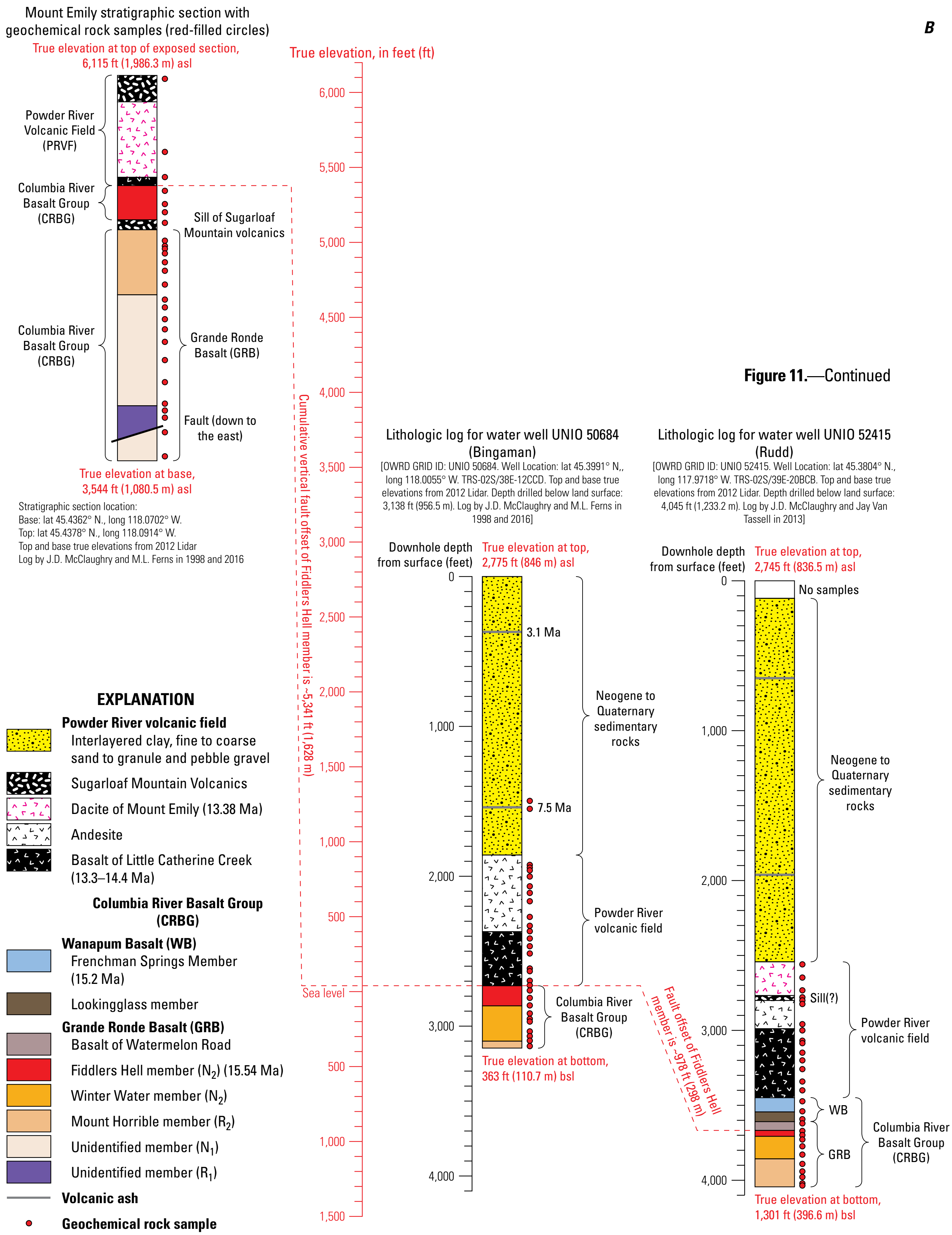

Figure 11.—Continued

extensive stage 5 and stage 6 flow sequences are not as easily correlated. Detailed geologic mapping of the Grande Ronde Valley (Ferns and others, 2010) shows the geochemically distinct Fiddlers Hell member capping a section of CRBG below Mount Emily (1.9 mi (3.1 km) south of Stop 1.2) up to an elevation of ~5,384 ft (1,641 m) (fig. 10). The Fiddlers Hell member has also been geochemically recognized in several of the deep water wells, including the UNIO 50684 (Bingaman) and UNIO 52415 (Rudd) water wells both drilled near the town of Alicel in the central part of the valley (fig. 11).

Water well "UNIO 50684 (Bingaman)" was completed in 1998 to a depth of 3,138 ft (956 m), equivalent to a land surface elevation of 2,775 ft (846 m) above sea level; the bottom of the well is 363 ft (111 m) below sea level. Southeast of Alicel, or 2.2 mi (3.5 km) southeast of the "UNIO 50684 (Bingaman) well," water well "UNIO 52415 (Rudd)" was completed in 2013 to a depth of 4,045 ft (1,233 m), equivalent to a land surface elevation of 2,744 ft (837 m) above sea level; the bottom of the well is -1,301 ft (397 m) below sea level. Geochemically distinctive flows of the Fiddlers Hell member were recovered from the 2,730 to 2,750 ft (832 to 838 m) down-hole depth interval (elevation of the top of the unit is 43 ft (13 m) above sea level) in the "UNIO 50684 (Bingaman) well," while the same lavas were encountered from the 3,680 to 3,700 ft down-hole depth interval (elevation of the top of the unit is 936 ft below sea level) in the "UNIO 52415 (Rudd)" well. The geochemically fingerprinted flow sequence (detailed from well cuttings) indicates significant cumulative vertical displacement of the section between the mapped Fiddlers Hell member flows exposed beneath Mount Emily (~5,384 ft) eastward into the central part of the La Grande graben. Cumulative vertical offsets between Mount Emily and the two wells has been determined to be ~5,341 ft (1,628 m) of apparent offset for the "UNIO 50684 (Bingaman) well," increasing eastward to ~6,320 ft (1,926 m) of apparent offset for the "UNIO 52415 (Rudd) well."

Differences in elevation between correlative Fiddlers Hell member flows in the "UNIO 50684 (Bingaman)" and the "UNIO 52415 (Rudd)" wells indicate vertical displacements of at least 979 ft (298 m) from west to east between the two subsurface stratigraphic sections. Significant vertical offsets over short distances (~2.2 mi (3.5 km)) indicate a complexly faulted and folded graben floor concealed below the thick sedimentary cover that fills the graben. Such structural complexity is consistent with detailed geologic mapping around the margins of the graben that shows a number of north-northwest-trending faults likely projecting through the valley.

Other important data include a fallout ash recovered from 1,230 ft (375 m) elevation in the "Bingaman 1984" well that gave a $^{40}Ar/^{39}Ar$ isochron age of 7.5 ± 0.11 Ma (Ferns and others, 2001). The dated ash was located 312 ft (95 m) above the top of the stage 5 sequence. Van Tassell and others (2000, 2001) report a $^{40}Ar/^{39}Ar$ age of 3.1 ± 0.3 Ma on a fallout ash deposit recovered from a depth of 361 ft (110 m) below land surface in the central part of the La Grande graben.

Continue south on U.S. Forest Service Road (toward Mount Emily) and the intersection with U.S. Forest Service Road 3120.

Cumulative Mileage
mi (km)

275.1 (442.7) Turn left onto Fox Hill Road.

275.5 (443.4) Exposures of stage 4 olivine basalt are on the right.

275.9 (444.0) Poor exposures of a rhyolite tuff, underlying olivine basalt, are in the draw on the left.

277.1 (446.0) Rock pits are developed in flows of the Fiddlers Hell member.

277.8 (447.1) Views of the West Grande Ronde Valley fault zone and the La Grande graben.

278.4 (448) Here the field-trip route crosses a large debris-flow deposit that crosses the West Grande Ronde Valley fault zone.

278.7 (449) Turn left onto Black Hawk Trail Lane and proceed west to Mt. Glenn Lane. Continue west on Mt. Glenn Lane.

279.4 (449.7) Proceed south across the Grande Ronde River into City of La Grande. Continue south onto North Sprague Street.

280.7 (451.7) Turn left and proceed to the traffic light located on Oregon Route (O.R.) 82. Turn left onto O.R. 82.

281.5 (453.0) Turn right at (Exit 261) and merge onto I–84 and proceed southeast toward Baker City.

289.7 (466.2) I–84 crosses faults on the southwest margin of the La Grande graben. The tilted section of lava flows exposed on the east are stage 5 andesites that overlie the stage 4 olivine basalt of Little Catherine Creek. Older lava flows can be seen as I–84 cuts through the section ascending Ladd Canyon. The section exposed along I–84 transitions upward from a base of stage 1 R2 and N2 Grande Ronde Basalt flows to stage 2 Fiddlers Hell member flows, stage 4 olivine basalt flows, and finally into stage 5 andesites of Ferns and McClaughry (2013). The section is cut by several small faults.

291.6 (469.3) A thick dacite lava flow, part of the Powder River volcanic field, is exposed on the left (east). The dacite overlies olivine basalt.

292.6 (470.9) A Fiddlers Hell member icelandite flow is exposed in the rock quarry to left (east).

296.0 (476.4) The cliff forming outcrop, above the broad talus field on the near skyline to the right (west), is Tamarack Mountain, a 3.18 ± 0.15 Ma late stage 6 andesite (Madin, 1998).

298.8 (480.9) Clover Creek. A Powder River volcanic field sequence of dacite and underlying olivine basalt flows is exposed on the left (east). The low hill about 2 mi (3.2 km) to the southeast is a basement high of pre-Tertiary Wallowa terrane greenstone. A southward-thinning section of stage 1 Grande Ronde Basalt flows, lap onto an erosional highland on the west that is cored by the Late Jurassic Bald Mountain batholith. Baker terrane rocks are exposed northwest of the batholith. Fiddlers Hell member lava flows in the highlands lie unconformably across a tilted surface of N1, R2, and N2 Grande Ronde Basalt flows (Madin, 1998). Scattered outcrops of middle Miocene Dinner Creek Tuff are exposed along the contact between the Fiddlers Hell member and underlying olivine basalt flows.

309.3 (497.8) Columnar-jointed outcrops of stage 5 andesite are exposed on both sides of the Powder River. The glaciated mountains to the southwest form Elkhorn Ridge, which includes the Bald Mountain batholith on the north and thrust slices of oceanic and island arc rocks on the south. Oceanic and island arc rocks are part of the Bourne subterrane of Ferns and Brooks (1995).

314.0 (505.3) Olivine basalts capping the ridge top on the east overlie Wallowa terrane greenstone.

318.0 (511.8) The far ridge line south of Baker City is Dooley Mountain, a stage 3 rhyolite vent complex. The ridge immediately south of Baker City is a tilted fault block of stage 4 olivine basalt flows and pre-Tertiary basement rocks. The bare hills on the east are fault-bounded blocks of stage 4 olivine basalt, that in places lie on the middle Miocene Dinner Creek Tuff.

324.0 (521.4) **Get off I–84 at Exit 304.** Turn right and proceed into Baker City.

After dinner, regroup for an evening excursion to the summit of Dooley Mountain. Reset vehicle mileage at the intersection of I–84 and Campbell Street. Proceed west on Campbell Street to Main Street and downtown Baker City.

1.4 (2.3) Turn left on Main Street and proceed south, traveling through Baker City. Follow the signs leading to the towns of John Day and Sumpter on O.R. 7. Main Street turns into Dewey Avenue and then becomes O.R. 7.

3.1 (5.0) Faults are present along a steeply dipping section of the olivine basalt of Little Catherine Creek.

8.0 (12.9) A thick sequence of tilted and faulted stage 4 olivine basalt flows is exposed along the Powder River.

9.7 (15.6) **Stop 1.3.** Pull off and park in the roadside pullout on the left (east) near the Powder River. The Stop 1.3 outcrop is on the opposite (west) side of the highway.

Stop 1.3. Powder River Volcanic Field Olivine Basalt Flows (lat 44.6662° N., long 117.8666° W.)

Olivine basalt flows exposed at Stop 1.3 are part of the stage 4 lavas of Ferns and McClaughry (2013) and define the base of the Powder River volcanic field of Bailey (1990) and Hooper and Swanson (1990). The olivine basalt flows are part of the basalt of Little Catherine Creek (Ferns and others, 2010) and extend north through the Grande Ronde Valley to Elgin (fig. 5*E*). The stage 4 olivine basalt flows of Ferns and McClaughry (2013) are typically diktytaxitic and form a flow-on-flow sequence as much as 492 ft (150 m) thick. The olivine basalt flows are characterized by high MgO and Al_2O_3, similar to the high alumina olivine tholeiites (HAOT) of the High Lava Plains (Carlson and Hart, 1987). The base of the flow sequence in the north is defined by hyaloclastite breccias and pillow basalts. Near-vent facies deposits of red scoria and cinder are often exposed between flows. A feeder dike at Stop 1.3 contains abundant chert xenoliths resembling the extensive chert deposits of the underlying, pre-Tertiary Elkhorn Ridge Argillite basement rocks. Bailey (1990) reports $^{40}Ar/^{39}Ar$ ages of 14.4 ± 0.2 Ma and 13.7 ± 0.1 Ma (fig. 12). The stage 4 olivine basalt flows overlie the Dooley Volcanics of Evans (1992) where here includes distal ash-flow tuffs of the middle Miocene Dinner Creek Tuff and the large rhyolite eruptive center herein referred to as the Dooley Mountain rhyolite (fig. 6).

Continue south toward Sumpter on O.R. 7 toward the intersection with O.R. 245.

Cumulative Mileage
mi (km)

10.0 (16.1) The tilted section of stage 4 olivine basalt flows exposed on the right has been cut up by faults and hydrothermally altered. Flow breccias are filled with opaline quartz and jasper. Vesicles near the faults are filled with zeolite and opaline quartz.

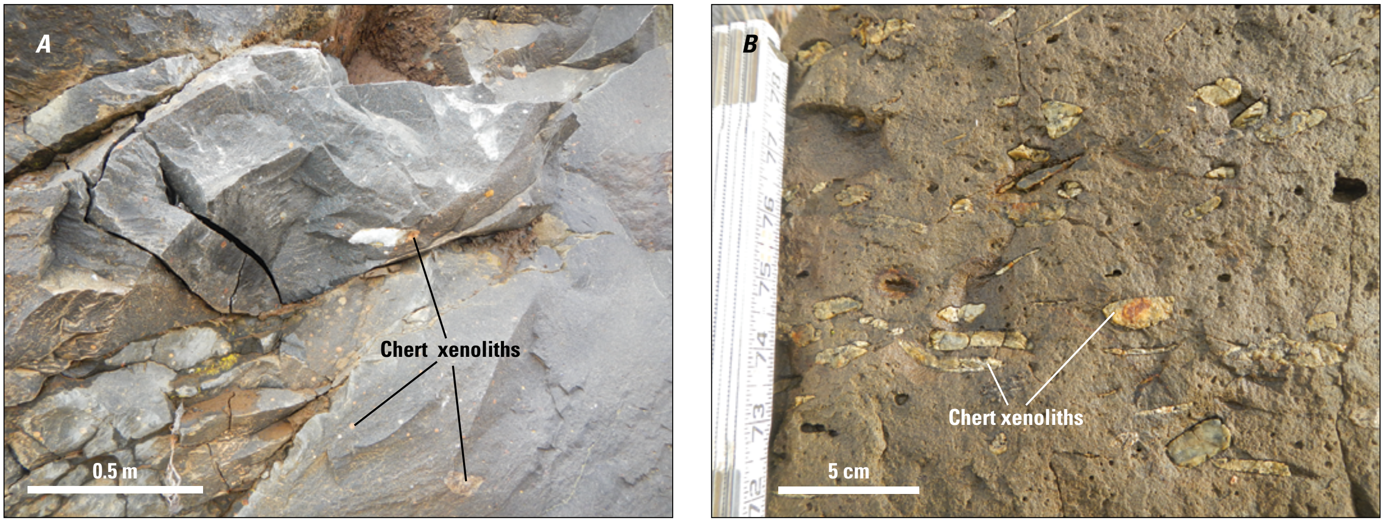

Figure 12. Photographs from Stop 1.3 showing examples of a stage 4 basalt flow and dike exposed on Oregon Route 7, south of Baker City. *A,* Olivine basalt containing a number of chert xenoliths derived from the underlying pre-Tertiary Elkhorn Ridge argillite of the Baker terrane. *B,* Elongate chert xenoliths as large as 5 cm long present in outcrop. Abbreviations: cm, centimeters; m, meters. Photographs by Jason McClaughry.

10.5 (16.9) Turn left onto O.R. 245 and proceed south into the Dooley Mountain rhyolite eruptive center. Altered stage 3 rhyolite (on left side of the road) is overlain by stage 4 olivine basalt.

16.4 (26.4) **Stop 1.4.** Pull off and park in the roadside pullout on the right (south). The Stop 1.4 outcrop is on the opposite (north) side of the highway.

Stop 1.4. Dooley Mountain Rhyolite Pyroclastic Dike (lat 44.5858° N., long 117.8487° W.)

Dooley Mountain is the northernmost stage 3 rhyolite vent complex and is considered part of the Lake Owyhee volcanic field of Rytuba and others (1985). First referred to as the Dooley Mountain rhyolite breccia by Gilully (1937), the rhyolite eruptive center at Dooley Mountain is an eroded series of nested domes and subvolcanic intrusions that are bordered by marginal debris- and block-and-ash flow deposits. The complex also includes several small, locally sourced ash-flow tuffs and fallout tuffs (Large, 2016). Rhyolite domes are locally cut up by a number of faults, and in places, are extensively altered. Many units are locally invaded by glassy rhyolite and pyroclastic dikes. Rhyolite lava flows on the north and south flanks of Dooley Mountain overlie cooling unit 1 of the Dinner Creek Tuff (cooling unit 1 defined by Streck and others, 2015). Erosional remnants of both proximal and distal facies of rhyolitic debris- and block-and-ash flow deposits originating from Dooley Mountain also overlie the Dinner Creek in the Tertiary sedimentary section exposed to the northeast of Dooley Mountain.

The rhyolite breccia exposed at Stop 1.4 is interpreted to be a vent breccia by Evans (1992). The breccia here is cut by a vertical, pyroclastic glassy dike porous along the margins with a denser interior with vertically oriented fiamme (fig. 13). The dike

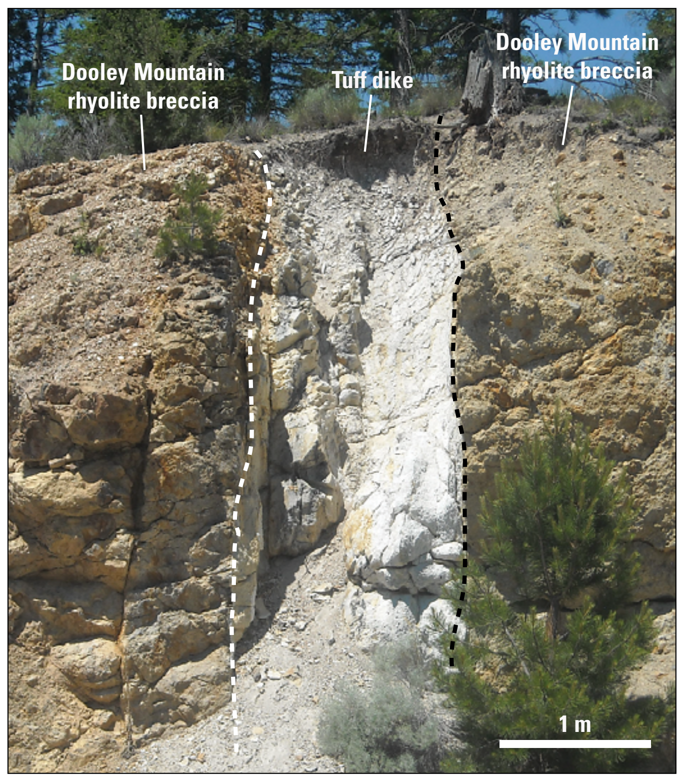

Figure 13. Photograph from Stop 1.4 near the summit of Dooley Mountain, along Oregon Route 245, showing the Dooley Mountain rhyolite breccia conspicuously crosscut by a white-colored tuff dike. The tuff dike has a well-defined vertical eutaxitic foliation defined by fresh obsidian fiamme in a devitrified vitric matrix. Abbreviation: m, meters. Photograph by Jason McClaughry.

strikes North-South and appears continuous with a glassy dike exposed along the highway to the north of Dooley Mountain. A K/Ar radiometric age of 14.7 ± 0.4 Ma is reported on a rhyolite dike near the summit of Dooley Mountain by Evans (1992). More recently, a $^{40}Ar/^{39}Ar$ age of 15.59 ± 0.04 Ma was obtained by Hess (2014) from rhyolite exposures outcropping along the highway on the south flank of Dooley Mountain. Large (2016) has identified four lithologic eruptive units within the Dooley Mountain complex that together compositionally range from low-SiO_2 rhyolites (~74 wt. percent SiO_2) to high-SiO_2 rhyolites (~76 wt. percent SiO_2). Compositionally, Dooley Mountain rhyolites are in large part "calc-alkaline" rhyolite characterized by low Y and Nb (Yttrium and Niobium, respectively).

Continue south on O.R. 245 toward Skyline Road/U.S. Forest Service Road 11.

Cumulative Mileage
mi (km)

17.9 (28.8) Turn left on U.S. Forest Service Road 11 (Skyline Road).

22.4 (36.0) Turn left onto road to the top of Beaver Mountain.

22.5 (36.2) **Stop 1.5.** Park along the road, north of the cell-tower complex.

Table 4. Major and trace element analyses, sample location, and stage for Dooley Mountain rhyolites.

[Major elements have been normalized to a 100 percent total on a volatile-free basis and recalculated as oxides, with total iron expressed as FeO*. "Older rhyolites" refer to an unnamed and undated sequence of rhyolites exposed adjacent to Dooley Mountain that may represent the earliest phase of Columbia River Basalt-related silicic magmatism. All analyses are from Ferns and McConnell (2005). Abbreviations: FRAN, Franklin and Marshall College; ID, identification number; nd, no data or not analyzed]

Formation or unit	Older rhyolite		Dinner Creek Tuff		Dooley Mountain rhyolite	
Stage	nd	nd	3	3	3	3
Field sample ID	03-B-34	03-B-36	03-B-29	03-B-06	03-B-10	03-B-11
Latitude (north)	44.5688	44.5555	44.6661	44.5071	44.5799	44.5821
Longitude (west)	118.0270	118.0260	118.2490	117.9120	117.8090	117.7850
Major elements as oxides, in weight percent						
SiO_2	71.41	73.25	66.30	73.88	73.57	74.65
Al_2O_3	16.36	14.40	14.44	13.02	13.47	13.67
TiO_2	0.23	0.31	1.19	0.24	0.29	0.29
FeO*	2.33	2.51	9.45	3.03	3.21	2.13
MnO	0.03	0.03	0.090	0.07	0.04	0.01
CaO	2.90	2.44	2.48	0.54	1.71	1.52
MgO	0.36	0.68	0.91	0.10	0.15	0.04
K_2O	1.78	2.29	2.55	5.76	3.71	3.64
Na_2O	4.50	3.94	2.32	3.34	3.80	4.00
P_2O_5	0.102	0.143	0.27	0.021	0.051	0.04
Trace elements, in parts per million						
Ni	4	10	8	4	3	4.00
Cr	9	20	8	4	5	nd
Sc	5	7	18	3	5	9
V	21	46	103	11	16	20
Ba	985	1,020	1,405	1,781	1,764	1,351
Rb	47	63	49	77	87	93
Sr	724	520	201	44	144	146
Zr	129	83	256	417	291	295
Y	8.4	10	45.8	65	43.3	40
Nb	8.7	11.4	18.2	26.6	14.7	15
Ga	16	15	18	20	17	18.0
Cu	nd	117	4	nd	nd	3
Zn	43	38	156	152	80	73
Pb	13	16	12	16	15	14
La	24	24	33	48	34	37
Ce	52	53	73	104	80	76
Th	6.4	9.6	3.8	6.7	6.8	7
Laboratory	FRAN	FRAN	FRAN	FRAN	FRAN	FRAN

Stop 1.5. Beaver Mountain Viewpoint (lat 44.5882° N., long 117.7865° W.)

The Summit of Beaver Mountain provides a 360 degree overview of the LOEA. Beaver Mountain is part of the Dooley Mountain volcanic center, the northernmost rhyolite eruptive center of the Lake Owyhee volcanic field. This area was heavily forested during the U.S. Geological Survey mapping program of the 1980s. Three large fires since that time have provided much better rock exposures.

View to the North

Both east and west escarpments of the La Grande graben are visible in the distance to the northwest, with the Baker graben in the foreground (fig. 14). Sawtooth Ridge lies in the foreground to the northeast. Sawtooth Ridge is the southernmost large andesite vent in the Powder River volcanic field. The high ground behind Sawtooth Ridge is an uplifted block of pre-Tertiary Wallowa terrane island-arc rocks that have been intruded by the Late Jurassic Wallowa Batholith. The high country is invaded and cut by numerous Grande Ronde and Imnaha Basalt dikes and is capped in places by thin Imnaha Basalt flows (fig. 3).

Sawtooth Ridge is located south of the northwest-trending Eagle Creek fault, which separates the high country farther north from a thick section of Imnaha and Grande Ronde Basalt flows. The CRBG section thickens to the east, where a sequence of Imnaha Basalt flows lie beneath the Grande Ronde Basalt, filling pre-existing topographic lows in the pre-Tertiary basement.

View to the Southwest

Existing age dates on Dooley Mountain rhyolite indicate that the main rhyolite eruptive phase at Dooley Mountain was between ~15.5 and 15 Ma; and thus, is largely co-eruptive with the younger middle Miocene Dinner Creek cooling units of Streck and others (2015). Cooling unit 2 of the Dinner Creek overlies a field of hornblende-dacite and rhyolite breccias, domes, lava and ash-flow tuffs, and shallow intrusions immediately to the south and southwest of Dooley Mountain. Older hornblende-dacites are also directly overlain by rhyolite domes and lava flows on the west flank of Dooley Mountain (Evans, 1995) and overlain at Unity Reservoir where rhyolite ash-flow tuffs and thick rhyolite lava flows occur. Recently reported radiometric ages of rhyolites at Unity Reservoir and the surrounding area, range from 17.0 to 16.5 Ma (Streck and others, 2016).

Ironside Mountain, in distance to the southwest, is interpreted to be the northern margin of the eruptive center that produced all four cooling units of the Dinner Creek and associated fallout tuffs of Streck and others (2015). This area includes the Castle Rock caldera of Rytuba and others (1985). Ironside Mountain is underlain by pre-Tertiary sedimentary rocks of the Olds Ferry-Izee terrane. Sedimentary rocks are cut by a late Eocene porphyry intrusive complex (Hooper and others, 1995).

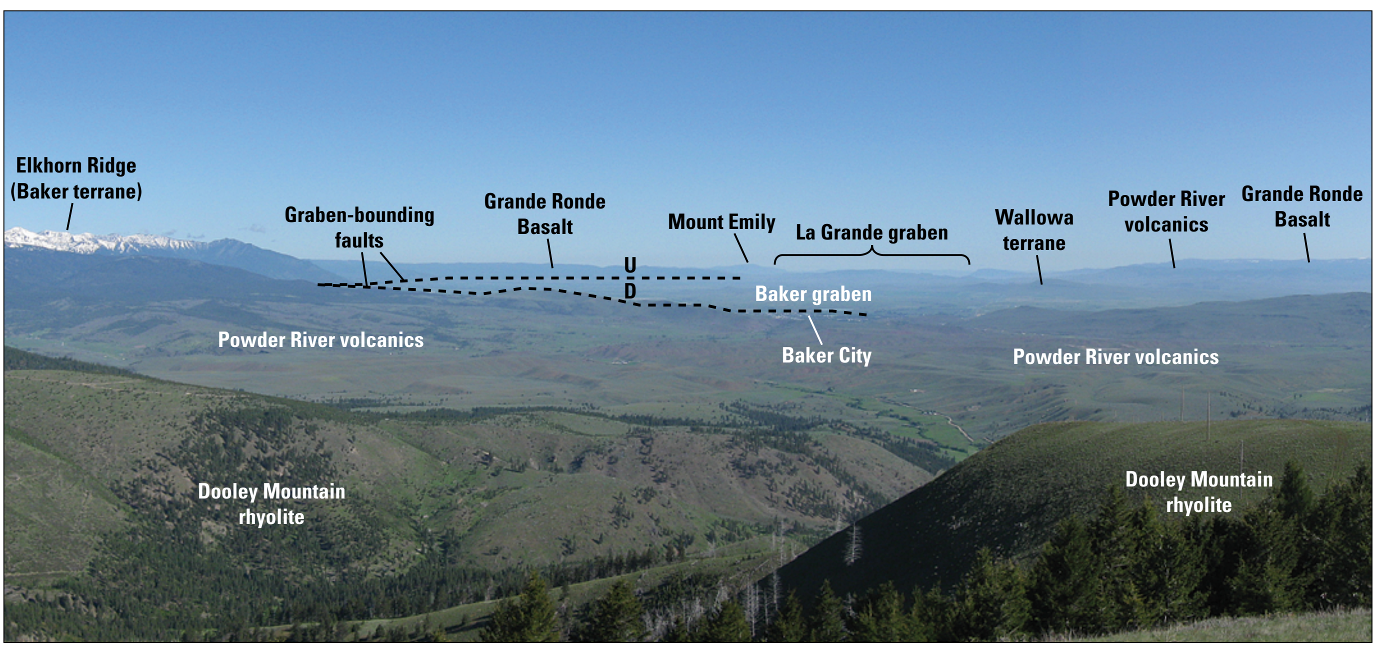

Figure 14. Photograph from Stop 1.5 looking north from Beaver Mountain into the southern part of the Baker graben. The Baker graben forms the present day boundary between the Baker and Wallowa terranes and contains a thick section of Powder River volcanics (stages 4 and 5). The Dooley Mountain rhyolite (stage 3) complex lies just south of the graben. The approximate locations of graben-bounding faults are shown by the dashed lines. Note the relationship between the Powder River volcanics and the Grande Ronde Basalt (stage 1). The bracket near the center of the photograph indicates the margins of the La Grande graben that are visible in the distance. Abbreviations: D, downthrown side; U, upthrown side. Photograph by Jason McClaughry.

Older Tertiary volcanic and subvolcanic complexes are exposed in the distance along the south flank of the ridge extending west of Dooley Mountain. The ridge itself is made up of Burnt River Schist. Older Tertiary volcanics, correlated with the Clarno Formation, include an ~41 to 36(?) Ma intertonguing sequence of calc-alkaline basalt flows, lahars, hornblende- and biotite-phyric andesite, and dacite flows and domes (Gaylord and others, 2015); south of Dooley Mountain the Tertiary sequence is cut by porphyry intrusions (Pardee and Hewitt, 1941). The older volcanic sequence displays a calc-alkaline trend and is considered to be part of the Clarno Formation of Merriam (1901).

CRBG flows that underlie the Dinner Creek Tuff to the southwest have chemically been correlated with the Picture Gorge Basalt (Large, 2016).

The Burnt River valley on the southwest separates the Baker terrane on the north from the Olds Ferry-Izee terrane on the south. Here the terrane boundary is marked by an east-west trending Quaternary fault system that is an eastern extension of the John Day fault. The rounded butte on the ridgetop to the south is the Baldy Mountain cinder cone, a trachyandesite vent (J.G. Evans, U.S. Geological Survey, unpub. data, 2009; geochemical analyses by U.S. Geological Survey, 2008). Baldy Mountain and other young alkaline lavas are part of stage 6 of Ferns and McClaughry (2013) and are part of the Kivett sequence of Lees (1994) who reported $^{40}Ar/^{39}Ar$ whole rock ages of 1.77 ± 0.31 Ma and 1.70 ± 0.44 Ma for these rocks. Preserved cinder cone and lava field morphologies indicate that these flows are subareal and postdate the Pliocene emptying of Lake Idaho.

View to the Southeast

The high ridge in the distance on the southeast is Cottonwood Mountain, a northwest-trending fault block that defines the southern margin of the western Snake River Plain. Cottonwood Mountain is capped by a large middle Miocene rhyolite, the Cottonwood Mountain rhyolite (Evans, 1999; J.G. Evans, unpub. data, 2009; Edwards, 2013; Webb and others, 2016) (fig. 6). The Cottonwood Mountain Rhyolite is also part of the middle Miocene rhyolite flare-up associated with CRBG flood basalts. The Early Cretaceous granitic intrusion at Pedro Mountain lies in the foreground to the southeast. Pedro Mountain is cut by a Grand Ronde Basalt dike swarm (Brooks, 2006).

The middle Miocene volcanic succession at Dooley Mountain proper appears to commence with local eruptions of biotite-phyric dacite flows and breccias that are followed by early CRBG-related rhyolite eruptions. Rhyolite eruptions at Dooley Mountain (fig. 5*D*) were followed in turn by marginal eruptions of stage 4 olivine basalt flows on the north and late Keeney sequence (fig. 5*F*) alkalic lavas to the south (fig. 6).

Return 22.5 mi (36.2 km) via the same route to Baker City.

Cumulative Mileage
mi (km)

22.6 (36.4) Turn left onto U.S. Forest Service Road 11 (Skyline Road). Proceed west to O.R. 245.

27.1 (43.6) Turn right onto O.R. 245. Proceed north to O.R. 7.

34.5 (55.5) Turn right onto O.R. 7. Proceed north to Baker City.

45.0 (72.4) Stop at the intersection of I–84 and Campbell Street in Baker City. **End Day 1.**

Day 2. Southern Part of the La Grande-Owyhee Eruptive Axis and Lake Owyhee Volcanic Field

Day 2 is a grand tour of the southern part of the LOEA and the Lake Owyhee volcanic field, where stage 1 rocks of the CRBG are associated in space and time with lesser known and more complex silicic volcanic stratigraphy associated with middle Miocene, large-volume, bimodal basalt-rhyolite vent complexes. Key stops will provide a broad overview of the structure and stratigraphy of the middle Miocene Mahogany Mountain caldera and middle to late Miocene calc-alkaline lavas of the Owyhee Basalt. Field discussion will include the evidence of whether there were two caldera-forming eruptions (Mahogany Mountain and Three Fingers calderas) as advocated by Rytuba and others (1985, 1989, 1991) or a single caldera-forming eruption (Rooster Comb) as suggested by Benson and Mahood (2016).

Road Log
Cumulative Mileage
mi (km)

0.0 (0.0) The road log for Day 2 begins at the intersection of I–84 and Campbell Street (Exit 304). The Always Welcome Inn fossil locality is located behind the Always Welcome Inn motel just to the east of the I–84 onramp. The tilted and faulted section of early Pliocene sedimentary rocks is an important fossil locality that has yielded a rich assemblage of small mammal, fish, reptile, and bird fossils (Van Tassell and others, 2001).

5.0 (8.1) Small quarries on the left (east) of I–84 are in the middle Miocene Dinner Creek Tuff (Streck and others, 2015) and are capped by stage 4 olivine basalt flows.

Table 5. Major and trace element analyses, sample location, and isotopic ages for late stage 6 lavas.

[Major elements have been normalized to a 100 percent total on a volatile-free basis and recalculated as oxides, with total iron expressed as FeO*. Reported isotopic ages determined by the $^{40}Ar/^{39}Ar$ method. Analyses are from Ferns and McConnell (2005)[1] and Lees (1994).[2] Abbreviations: ID, identification number; Ma, mega-annum (million years before present); nd, no data or not analyzed; WSU, Washington State University]

Location	La Grande area		Vale area	Brogan area	
	Jones Butte	Tamarack Mountain	Malheur Butte	Brogan Summit	Wendt Butte
Stage	6	6	6	6	6
Age (Ma)	nd	3.18 ± 0.15	2.78 ± 0.84	1.77 ± 0.31	nd
Field sample ID	98-MAD-3[1]	98-MAD-105[1]	KL-92-326[2]	KL-92-313[2]	KL-92-314[2]
Latitude (north)	45.6003	45.1460	44.0107	44.3456	44.3667
Longitude (west)	117.9450	118.0310	117.8491	117.6742	117.7500
Major elements as oxides, in weight percent					
SiO_2	62.68	61.02	59.44	50.24	61.12
Al_2O3	18.82	18.92	18.02	16.87	17.59
TiO_2	0.48	0.53	0.940	1.71	0.88
FeO*	3.99	4.62	5.65	10.03	5.68
MnO	0.08	0.08	0.120	0.18	0.12
CaO	6.09	6.64	2.31	8.14	5.47
MgO	2.29	2.96	1.45	6.12	2.32
K_2O	0.93	1.28	2.02	2.57	2.04
Na_2O	4.46	3.73	2.95	3.44	4.46
P_2O_5	0.19	0.18	0.29	0.7	0.33
Trace elements, in parts per million					
Ni	22	39	24	77	16
Cr	27	31	29	213	21
Sc	12	14	14	20	11
V	60	102	88	143	90
Ba	593	578	805	846	946
Rb	10	11	60	62	32
Sr	897	689	650	551	593
Zr	104	94	280	222	145
Y	8	11	17	24	18
Nb	4	3.7	64.6	72.1	24.7
Ga	20	21	18	12	18
Cu	39	22	21	13	21
Zn	60	58	57	62	64
Pb	6	6	3	nd	6
La	8	9	32	41	32
Ce	33	23	82	64	37
Th	1	2	4	5	2
Laboratory	WSU	WSU	WSU	WSU	WSU

12.0 (19.3) Quarries on the left (north) at Pleasant Valley are the sources of tuff stone used in many older buildings in Baker City. The Quarries are developed in cooling unit 2 of the Dinner Creek Tuff of Streck and others (2015), but cooling units 1, 2, and 4 have been found in the greater vicinity of Pleasant Valley.

14.2 (22.9) A stage 4 olivine basalt flow fills a channel that is incised into pre-Tertiary Baker terrane basement rocks. Fiebelkorn and others (1982) report a K/Ar age of 12.3 Ma for this flow.

14.7 (23.7) U.S. Highway (U.S.) 30 on the west cuts through an outcrop of Dinner Creek Tuff that has been folded. The ridge line on the west is capped by the Dinner Creek.

16.0 (25.7) Iron Mountain, a small stage 6 andesite volcano, can be seen on the left (east). The ridgeline in the distance is capped by Imnaha Basalt, the second oldest (~16.7–16.5 Ma) (Jarboe and others, 2010; Baksi, 2013; Barry and others, 2013) of the main CRBG units (stage 1 of CRBG flows). The CRBG section on the ridgeline dips to the northeast;

younger onlapping Grande Ronde Basalt flows are capped by Dinner Creek Tuff. Palagonitic breccias lower in the section on the south, mark Imnaha Basalt vents. A south-tilted section of Grande Ronde Basalt flows overlain by Dinner Creek Tuff is variably exposed across the top of pre-Tertiary Baker terrane basement rocks in the low hills west of the freeway.

21.6 (34.8) Zeolitized, middle to late Miocene tuffaceous sediments are exposed to the left (east) in a series of terraces. Highlands on the south are Burnt River Schist. Faceted spurs along the foot of the ridge on the west mark a series of faults. The high hills in the foreground are ancient hot spring travertine mounds.

26.0 (41.8) Dinner Creek Tuff is exposed at the base of the sedimentary section on the east, where the unit is cut by precious opal and fibrous zeolite veins. The old opal mine in this area is the type locality for the fibrous zeolite mineral identified as erionite (Sheppard and Gude, 1986).

27.0 (43.5) I–84 begins the descent down the Burnt River, cutting through a steeply dipping section of marble and carbonaceous phyllite (Burnt River Schist). This area is cut by a series of faults that drop isolated exposures of Grande Ronde Basalt to river level.

30.8 (49.6) I–84 crosses the poorly exposed Connor Creek fault, the terrane-bounding structure that separates the Burnt River Schist (Baker terrane) on the north from the Weatherby Formation (Olds Ferry-Izee terrane) on the south. Prospect tunnels on the right (south) are from the exploration of mineralized zones in serpentinite along the Baker terrane side of the fault.

31.0 (49.9) Weatherby Rest Area.

31.7 (51.0) Steeply dipping marine turbidites are exposed along the railroad on the west.

32.6 (52.5) Crossing Burnt River. Rust brown Columbia River dikes and sills are exposed on the right (south) at the railroad tunnel.

34.0 (54.7) The south-dipping tablelands on the ridge to the south are capped by stage 6 lava flows that erupted between 2 and 1 Ma. The top of the ridge (not visible from the freeway) is marked by a preserved cinder cone.

36.6 (58.9) The dark-brown outcrops on both sides of I–84 are a stage 6 trachyandesite with a reported $^{40}Ar/^{39}Ar$ whole-rock age of 7.96 ± 0.50 Ma (Lees, 1994).

39.4 (63.4) CRBG dikes are exposed in road and railroad cuts constructed in limestone at the base of the Weatherby Formation. Dikes are part of the Chief Joseph dike swarm (fig. 2).

43.0 (69.2) I–84 leaves the Burnt River, climbing the low ridge west of the town of Huntington. The light-colored rocks along I–84 are lake deposits from Pliocene Lake Idaho.

47.0 (75.6) Flat-lying sediments on the right (south) are Bonneville flood deposits.

48.4 (77.9) Community of Farewell Bend and Snake River to the left.

50.1 (80.6) CRBG lava flows exposed on the right (south) are cut by chalcedonic quartz and zeolite veins. These flows are part of the Birch Creek and underlying upper Pole Creek units of Lees (1994) (fig. 6). Birch Creek lava flows chemically resemble Grande Ronde Basalt while the underlying upper Pole Creek contains flows that more closely resemble the Imnaha Basalt. Nearby exploration drill holes have penetrated at least 300 m of CRBG flows.

64.0 (102.9) I–84 descends into the modern day Snake River Plain, which can be followed eastward through Idaho to the western margin of Yellowstone. The broad depression is believed to result from the eastward passage of the Yellowstone hot spot. This part of the Western Snake River Plain is believed to be a pull-apart graben that formed adjacent to the hot-spot track (Bonnichsen and Godchaux, 2002).

64.5 (103.8) The high mountains to the west are part of the Late Cretaceous Idaho Batholith, which intrudes the old North American craton.

64.8 (104.3) Faulted terrace deposits in roadcut to left.

70.5 (113.5) **Leave I–84 at Exit 374.** On the outskirts of the City of Ontario, turn right onto O.R. 201 (Yturri Beltline) following the signs to Vale and Nyssa.

75.9 (122.1) Proceed south through the stop light and past the intersection with U.S. 26. Follow signs to the town of Nyssa.

83.7 (134.7) Turn right at the stoplight in Nyssa onto O.R. 201 (Adrian Boulevard.) and proceed south toward the town of Adrian.

96.0 (154.5) Town of Adrian. The low-standing bluffs visible on the west are silicified sandstone and conglomerate.

97.0 (156.1) The processing plant for Teague Minerals is on the right to the west.

104.3 (167.9) Turn right onto Succor Creek Cutoff Road (gravel road), following signs leading to Succor Creek State Park.

108.7 (174.9) The prospect pit on the left exposes steeply dipping Spring Creek tuff. Ridges on the east are tilted fault blocks of stage 1 lava flows, stage 3 ash-flow tuffs, and stage 4 olivine basalts (Ferns and McClaughry, 2013) (fig. 6). Olivine basalt flows are thin with locally pillowed bases (lobate pillows) enclosed in palagonitic sediment. The tilted fault blocks are unconformably overlain by a sedimentary sequence of bentonitic clays, arkosic and tuffaceous sandstone, and conglomerate. Sedimentary stratigraphy is constrained by extensive exploration and development drilling associated with mining of bentonite clay deposits.

110.0 (177.0) Owyhee Ridge on the west is capped by a series of stage 5 basalt, basaltic andesite, and andesite lava flows (fig. 6) that are part of the Owyhee Basalt of Bryan (1929).

110.5 (177.8) Davis Road on the left (east).

110.6 (177.9) Camp Kettle Creek Road on the right (west).

111.4 (179.3) Turn left (east) off of Succor Creek Road onto an unimproved side road and proceed 0.4 mi (0.6 km) to Stop 2.1.

111.8 (179.9) **Stop 2.1.** Park in rock pit.

Stop 2.1. Leslie Gulch Ash-Flow Tuff Outflow (lat 43.5499° N., long 117.1028° W.)

An outflow sheet of the Leslie Gulch Ash-Flow Tuff (Kittleman and others, 1965) is exposed atop the Bishops Ranch lava flows at this locality (fig. 15). The outflow tuff is sparsely phyric, with sodic sanidine, quartz, and rare pyroxene phenocrysts. Considering the outcrop's close proximity to the source caldera at Mahogany Mountain, it is not especially thick. Benson and Mahood (2016) report an $^{40}Ar/^{39}Ar$ age of 15.84 ± 0.05 Ma from this locality. The top of ridge above the zeolite mine is capped by a stage 4 olivine basalt flow (fig. 15).

The lower cliff face in the distance to the southeast is an arkosic conglomerate derived from the Idaho Batholith. The conglomerate is in the upper part of the Sucker Creek Formation of Kittleman and others (1965, 1967). Here, the Sucker Creek Formation consists of arkosic sediments and bentonitic clays that unconformably overlie a tilted sequence of mafic lava flows and interbedded rhyolite lava flows and ash-flow tuffs. The arkose-clay sequence is overlain by the Jump Creek Rhyolite to the south.

The low-lying, dark-colored outcrops in the middle ground to southeast are part of the Graveyard Point sill. The sill is a late Miocene intrusion that records the bottom to top continuous fractional crystallization of a tholeiitic parent magma that culminated in the development of granophyre pods. White (2007) considers the sill to be an intrusion of Snake River Plain basalt emplaced at shallow depths and undergoing crystal fractionation. Snake River Plain basalt fractionating minerals are olivine (Fo_{73} to Fo_2), clinopyroxene (X_{Fe} = 0.95 to X_{Fe} = 0.18), feldspars ($An_{80}Or_1$ to An_1Or_{62}), and Fe-Ti oxides (Ti-rich magnetite to ilmenite), and apatite (Markl and White, 1999). Ferns (1989a) reports a K/Ar age of 6.7 ± 0.4 Ma from the chilled margin.

Return 0.4 mi (0.6 km) to Succor Creek Road. Turn left and proceed south toward Succor Creek State Park.

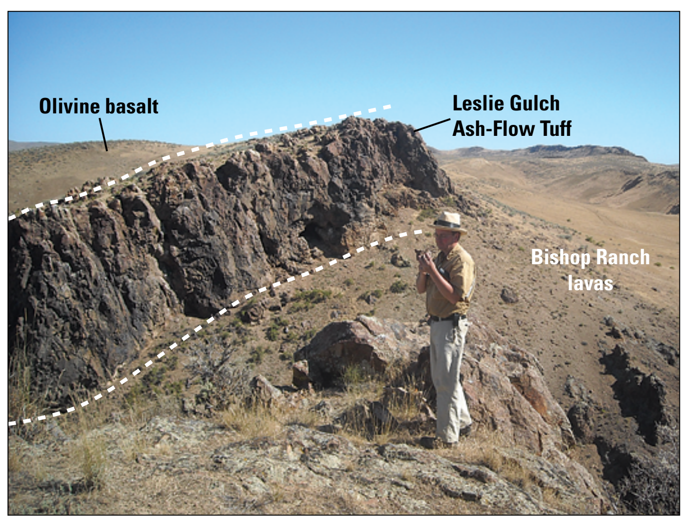

Figure 15. Photograph from Stop 2.1 of a stratigraphic section exposing (from bottom to top) the Bishop Ranch lavas (stage 2), the Leslie Gulch Ash-Flow Tuff (stage 3), and overlying olivine basalts (stage 4). The photograph is looking northwest of Succor Creek, near Graveyard Point. For scale, the person in the photograph (Martin Streck) is 1.7 meters tall. Photograph by Mark Ferns.

Cumulative Mileage
mi (km)

113.0 (181.9) The cliff forming rock (lower on the ridge on the right (west)) is a rhyolite lava flow that overlies Stage 1 lavas and is overlain by Stage 4 olivine basalt flows.

114.0 (183.5) The road crosses into a well-exposed part of the Sucker Creek Formation. The Sucker Creek Formation here consists of a lower tilted sequence of interbedded airfall tuff, sandstone, and diatomite, and an unconformably overlying upper sequence of bentonite clays and arkosic sandstone. The upper sequence is a well-known vertebrate fossil locality. Downing and Swisher (1993) report $^{40}Ar/^{39}Ar$ ages of 14.93 ± 0.08 Ma and 15.13 ± 0.2 Ma from the upper section and 15.46 ± 0.07 Ma from the lower tilted section.

115.6 (186.0) **Stop 2.2.** An unimproved dirt road takes off to the right (west), just as Succor Creek Road descends downward toward Succor Creek State Park. Turn right and park along the edge of the dirt road.

Stop 2.2. Mahogany Mountain Caldera Margin Overlook (lat 43.51217° N., long 117.13916° W.)

The parking area for Stop 2.2 is on weathered arkosic conglomerate that is part of the sedimentary sequence that unconformably overlies tilted fault blocks of stage 1 lavas and stage 3 ash-flow tuffs (fig. 16). Ash-flow tuff visible on the south and east from Stop 2.2 corresponds with the Spring Creek tuff of Rytuba and others (1985) and here includes at least three cooling units marked by dense black basal vitrophyres (fig. 16). The Spring Creek tuff is metaluminous (table 6) with alkali feldspars (An_6,Ab_{52},Or_{42}) (Marcy, 2014) and now is considered to be a later outflow sheet from the Mahogany Mountain caldera (Marcy and others, 2013). Conformable mapped contact relationships indicate that the underlying mafic unit is a stage 1 lava flow and not a mafic intrusion as mapped by Ferns (1989a).

The northern margin of the Three Fingers caldera of Rytuba and others (1988) runs through the small canyon to the west (fig. 16). The caldera margin is marked by a series of post-collapse domes that have been emplaced into caldera-fill deposits exposed on the south. The Devils Gate rhyolite lava flow lies north of the rim where it overlies stage 1 Bishops Ranch lava flows (fig. 16). A 100-ft-thick (30 m) section of caldera-fill deposits is exposed between the Bishops Ranch and Devils Gate along the caldera margin. Farther to the west, the caldera margin is characterized by a sequence of reworked tuffaceous moat deposits. Across the margin, stage 4 olivine basalt dikes underlie a series of olivine basalt flows (fig. 16). Recent work by Marcy (2014) and Benson and Mahood (2016) suggests that the Mahogany Mountain and Three Fingers calderas of Rytuba and others (1985) are part of a single large, vigorous rhyolite eruptive center active for 200 to 300 thousand years.

Benson and Mahood (2016) consider the Spring Creek tuff and the Leslie Gulch Ash-Flow Tuff Member of the Sucker Creek Formation to be different facies of a single ash-flow that erupted from their single large "Rooster Comb" caldera. We prefer to retain the original name of "Mahogany Mountain caldera" first used by Rytuba and others (1985) to define the larger composite rhyolite complex that generated at least two separate ash-flow tuffs, both of which have limited areal extent. The Leslie Gulch and Spring Creek ash-flow tuffs are in the same general stratigraphic position, atop stage 1 basalt of Bishops Ranch and beneath stage 4 olivine basalt. Geochemical analyses (table 6) and radiometric ages indicate

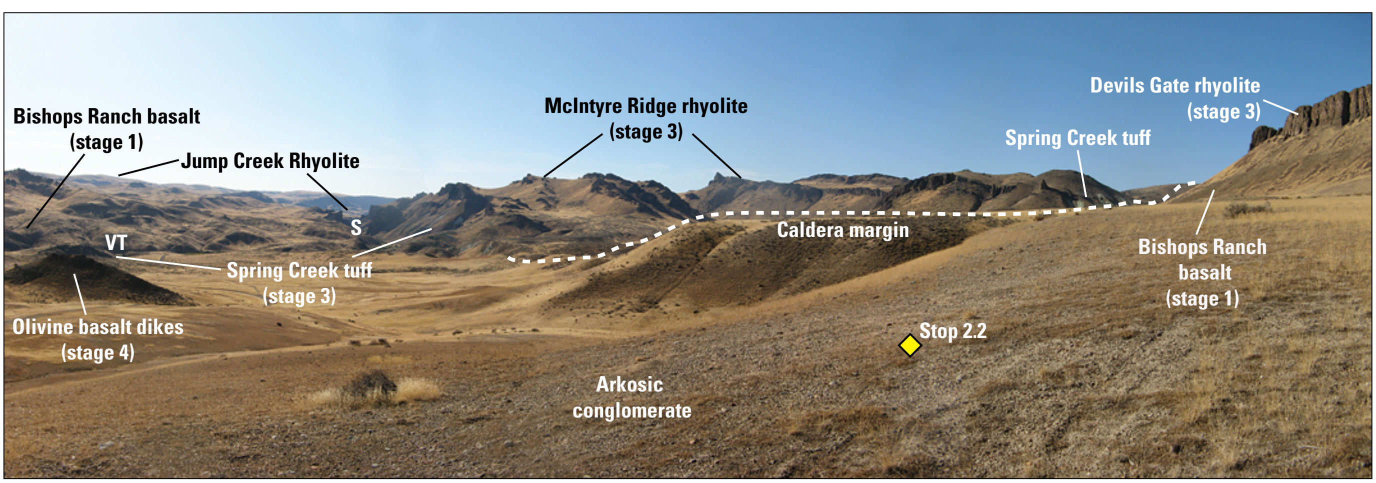

Figure 16. Photograph from Stop 2.1 showing the view of the northern margin to the Mahogany Mountain caldera and distribution of units discussed in the text. The abbreviation "VT" shows the location of a steeply dipping section of Spring Creek outflow tuff vitrophyre. The location of Stop 2.2 is shown with a yellow diamond. The photograph is looking south up Succor Creek. Photograph by Jason McClaughry.

Table 6. Major and trace element analyses, sample location, isotopic age, and stage for lava flows from the Mahogany Mountain caldera.

[Major elements have been normalized to a 100 percent total on a volatile-free basis and recalculated as oxides, with total iron expressed as FeO*. The Leslie Gulch tuff is formally known as the "Leslie Gulch Ash-Flow Tuff Member of Sucker Creek Formation." Analyses are from Ferns and McConnell (2005),[1] Benson and Mahood (2016),[2] Streck (2014),[3] and Marcy (2013).[4] Reported isotopic ages determined by the $^{40}Ar/^{39}Ar$ method. Abbreviations: FRAN, Franklin and Marshall College; ID, identification number; Ma, mega-annum (million years before present); nd, no data or not analyzed; WSU, Washington State University; XRAL, X-Ray Assay Laboratories (Toronto, Canada)]

Formation unit	Basalt of Bishops Ranch		Leslie Gulch tuff		Spring Creek tuff		
Flow characteristic	**Pre-caldera**	**Pre-caldera**	**Outflow**	**Caldera fill**	**Caldera fill**	**Outflow**	**Caldera fill**
Stage	1	1	3	3	3	3	3
Age (Ma)	nd	nd	15.84 ± 0.05	15.81 ± 0.03	nd	15.64 ± 0.09	15.64 ± 0.08
Field sample ID	AXB-519[1]	AVB-106[1]	TB-109[2]	TB-161[2]	TB-171[2]	MS-11-15-SCT[3]	TF-88A[4]
Latitude (north)	43.2380	43.5547	43.5499	43.3188	43.3178	43.511967	nd
Longitude (west)	117.0552	117.0827	117.1021	117.3170	117.2122	117.1235	nd
Major elements as oxides, in weight percent							
SiO_2	60.36	54.43	75.85	72.70	74.89	73.35	77.19
Al_2O_3	14.67	15.93	12.31	13.29	12.30	12.67	11.58
TiO_2	1.51	1.45	0.27	0.32	0.260	0.359	0.16
FeO*	7.46	5.66	1.96	4.43	3.19	3.50	1.88
MnO	0.31	0.20	0.02	0.02	0.100	0.083	0.03
CaO	4.74	7.07	0.10	1.85	0.53	1.00	0.32
MgO	1.69	3.54	0.04	0.02	0.07	0.13	n.d.
K_2O	2.07	1.77	4.92	2.50	4.93	5.23	5.51
Na_2O	4.96	3.71	4.13	4.41	3.31	3.64	3.34
P_2O_5	0.64	0.58	0.04	0.03	0.03	0.03	0.01
Trace elements, in parts per million							
Ni	11	39	3	2	4	3	1.9
Cr	14	11	6	4	3	3	2.1
Sc	nd	nd	nd	nd	nd	2	nd
V	nd	nd	27	31	27	5	28
Ba	3,190	771	1,299	1,546	1,656	1,880	1,306
Rb	76	41	142	122	151	140	146.2
Sr	358	515	20	40	32	25	3
Zr	629	93	774	903	726	681	670.5
Y	57	12	80	88	108	95	121.6
Nb	38	24	52	51	42	43.2	47.1
Ga	nd	nd	29	32	30	24	26.1
Cu	10	72	5	4	2	5	5.2
Zn	156	118	116	261	186	175	193.1
Pb	nd	nd	27	17	12	23	27.7
La	nd	nd	72	90	83	64	73.4
Ce	nd	nd	222	232	228	134	153
Th	nd	nd	17	29	15	14	16.6
Laboratory	XRAL	XRAL	FRAN	FRAN	FRAN	WSU	WSU

that two ash-flow tuffs were erupted in close succession. Marcy and others (2013) reports an $^{40}Ar/^{39}Ar$ age of 15.64 ± 0.09 Ma (recalculated to 15.76 ± 0.09 Ma using the Fish Canyon Tuff sanidine age of 28.203 Ma, reported by Kuiper and others (2008)) for the Spring Creek cooling unit that is slightly younger than an $^{40}Ar/^{39}Ar$ age of 15.84 ± 0.05 that Benson and Mahood (2016) report for the Leslie Gulch Ash-Flow Tuff outflow.

Continue south on Succor Creek Road, proceeding south to Succor Creek State Park.

Cumulative Mileage
mi (km)

118.3 (190.4) The prominent cliff forming rock on the west is part of the rhyolite of McIntyre Ridge of Vander Meulen and others (1989). We have divided the rhyolite of McIntyre Ridge into two units, while Benson and Mahood (2016) consider this to be only one pre-caldera unit. The lower unit was erupted before the Leslie Gulch Ash-Flow Tuff and forms part of the eastern margin to the Mahogany Mountain caldera. Hess (2014) and Benson and Mahood (2016) report $^{40}Ar/^{39}Ar$ sanidine ages of 15.94 ± 0.16 Ma and 15.91 ± 0.27 Ma, respectively, on the older McIntyre Ridge rhyolite (fig. 16). We have obtained an $^{40}Ar/^{39}Ar$ age of 15.76 ± 0.02 Ma on the younger McIntyre Ridge rhyolite (M.J. Streck and W.C. McIntosh, unpub. data, 2016) that likely post-dated intracaldera rhyolites of the Three Fingers area (Marcy, 2014).

120.2 (193.4) **Stop 2.3.** Succor Creek State Park. Pull off and park in the developed parking area on the right (east) side of the road. The parking area has restroom facilities.

Stop 2.3. Succor Creek State Park (lat 43.4537° N., long 117.1202° W.)

Spectacular outcrops to the southeast are part of the Jump Creek Rhyolite (figs. 16 and 17), a composite rhyolite lava flow and dome sequence with lobes that overlie arkosic sandstone and bentonite clays of the upper Sucker Creek Formation. The Jump Creek Rhyolite forms a broad plateau with cliff faces as much as 985 ft (300 m) high and is flanked by large landslide complexes. Radiometric ages for the Jump Creek Rhyolite include (1) K/Ar ages of 10.6 ± 0.3 Ma (Ferns and others, 1993a,b) and 11.1 ± 0.2 Ma (Armstrong and others, 1980), and (2) $^{40}Ar/^{39}Ar$ ages of 11.69 ± 0.06 Ma and 11.56 ± 0.25 Ma (Bonnichsen and others, 2004). A series of north-trending faults juxtapose the younger Jump Creek rhyolite against older McIntyre Ridge rhyolite, making for difficult mapping (figs. 16 and 17).

Continue south on Succor Creek Road, ascending to the top of the McIntyre Ridge rhyolite.

Cumulative Mileage
mi (km)

122.3 (196.8) Succor Creek Road crosses a landslide area where a block of Jump Creek Rhyolite overlies bentonitic clays of the upper Sucker Creek Formation.

123.1 (198.1) Bedded airfall tuff and tuffaceous sedimentary rocks, exposed on the left, mark the noted Succor Creek fossil leaf locality. Downing and Swisher (1993) reported an initial $^{40}Ar/^{39}Ar$ age of 15.46 ± 0.07 Ma (recalculated to 15.55 Ma for the Lough ash, the basal fallout tuff at this locality). Nash and Perkins (2012) correlate the Lough ash with the tuff of Bully Creek. Streck and others (2015) consider the Lough ash and the tuff of Bully Creek to be part of cooling unit 3 of the Dinner Creek Tuff.

Figure 17. Photograph of Stop 2.3 (shown with a yellow diamond) from the south, looking down Succor Creek (lat 43.4467° N., long 117.1198° W.). Photograph by Jason McClaughry.

129.0 (207.6) The mountains on the southeast are the Silver City Range and South Mountain in Idaho. The lowlands between South Mountain and the Silver City Range are occupied by the Juniper Mountain volcanic center. The intervening area between the two areas of pre-Tertiary outcrop is covered by the enigmatic Swisher Mountain Tuff (Ekren, 1982). Manley and McIntosh (2002) report $^{40}Ar/^{39}Ar$ ages ranging from 13.65 ± 0.04 to 14.48 ± 0.04 Ma for the Swisher Mountain Tuff. The Swisher Mountain tuff may be the first of the very large rhyolite lava flow (rheomorphic tuff) components of the Owyhee-Humboldt volcanic center that define the track of the Yellowstone hot spot.

129.3 (208.1) Turn right onto Leslie Gulch Road and proceed west.

135.6 (218.2) **Stop 2.4.** Pull off and park in the turnout area on the left (east) side of the road.

Stop 2.4. Leslie Gulch Overlook (lat 43.3151° N., long 117.2159° W.)

Leslie Gulch Road begins the descent into the thick caldera-fill deposits of Leslie Gulch. The timbered highlands on the southwest is Mahogany Mountain, a large composite rhyolite flow-dome complex that forms the south rim of the Mahogany Mountain caldera (Rytuba and others, 1991). Benson and Mahood (2016) report a $^{40}Ar/^{39}Ar$ sanidine age of 15.63 ± 0.05 Ma from a sample in the upper part of the rhyolite of Mahogany Mountain, indicating the unit includes postcaldera ring fracture rhyolites. This relationship is similar to the McIntyre Ridge rhyolite on the east margin of the caldera. MacLeod (1990a,b) describes basalt, and iron-rich andesite flows associated with mafic hyaloclastite lapilli tuff and breccia deposits beneath the eastern and southern distal edges of the rhyolites on Mahogany Mountain.

Continue west on Leslie Gulch Road, descending into Leslie Gulch.

Cumulative Mileage
mi (km)

138.8 (223.4) **Stop 2.5.** Pull off and park on the road shoulder on the right (north) side of the road.

Stop 2.5. Dago Gulch Dikes (lat 43.2941° N., long 117.2530° W.)

The road has descended through a thick sequence of picturesque outcrops of intracaldera facies to the ash-flow tuff of Leslie Gulch within the Mahogany Mountain caldera. The intracaldera facies at Dago Gulch is cut by a number of north-trending rhyolite dikes (fig. 18). These rhyolite dikes have compositions identical to intracaldera rhyolites of the Three Fingers area that erupted shortly after the eruption of the tuff of Spring Creek (Marcy, 2014). The intracaldera facies contains lithic fragments, ~5 percent phenocrysts with sodic sanidine, and rare quartz and oxidized mafic minerals. Benson and Mahood (2016) report $^{40}Ar/^{39}Ar$ ages ranging from 15.75 ± 0.05 to 15.87 ± 0.37 Ma from variably altered samples of the intracaldera facies.

Continue west on Leslie Gulch Road, descending farther into Leslie Gulch.

Cumulative Mileage
mi (km)

141.2 (227.2) **Stop 2.6.** Pull off and park on in the wide turnout on the right (north) side of the road. This is the trailhead for Yellowjacket Trail. Leave the vehicle and hike north on Yellowjacket Trail, north into Yellowjacket Gulch.

Figure 18. Photograph looking north at the Leslie Gulch Ash-Flow Tuff exposed in Dago Gulch (near Stop 2.5) within the Mahogany Mountain caldera (lat 43.2911° N., long 117.2561° W.). Here the intracaldera tuff is cut by numerous rhyolite dikes marking part of the central vent complex of Vander Meulen (1989). Photograph by Jason McClaughry.

Stop 2.6. Yellowjacket Gulch (lat 43.2987° N., long 117.2706° W.)

We will hike up the Yellowjacket Trail for a look at the intracaldera facies of the Leslie Gulch Tuff. Vander Meulen and others (1987a,b,c) used color differences and weathering characteristics to map what they considered to be a younger Spring Creek tuff from an older tuff of Leslie Gulch in the central part of the Mahogany Mountain caldera (fig. 19). Detailed geochemical and X-ray diffraction (XRD) analyses by Benson and Mahood (2016) show the color differences along the Leslie Gulch road result from differential alteration. The characteristic green color of what was mapped here as Spring Creek tuff is from an alteration mineral assemblage of clinoptilotite±mordenite±minor smectite, and the characteristic orange color of the Leslie Gulch Tuff is from an alteration mineral assemblage of quartz±albite±phylosilicate (fig. 19).

Continue west on Leslie Gulch Road to the Bureau of Land Management (BLM) campground near Owyhee Reservoir at the end of the road.

Cumulative Mileage
mi (km)

143.5 (230.9) BLM campground at the end of Leslie Gulch Road. Restrooms are available at the campground. Turn around and proceed east, back up Leslie Gulch Road.

154.2 (248.2) Turn left onto an unimproved BLM road and proceed north for an overview of the northern part of the Mahogany Mountain caldera.

155.6 (250.4) **Stop 2.7.** Pull off and park in the wide turnout on the right (north) side of the road.

Stop 2.7. Mahogany Ridge Overlook (lat 43.3436° N., long 117.1888° W.)

The northwest margin of the Mahogany Mountain caldera is occupied by a dome complex centered on Three Fingers Rock. Marcy (2014) and Benson and Mahood (2016) report $^{40}Ar/^{39}Ar$ ages on rhyolites from the Three Fingers Rock area of 15.64 ± 0.08 Ma (recalculated to 15.76 ± 0.08 Ma using the Fish Canyon Tuff sanidine age of 28.203 Ma, reported by Kuiper and others (2008)) and 15.61 ± 0.05 Ma, respectively. On the basis of descriptions given by Marcy (2014), the dome complex appears to be a series of coulee domes cored by devitrified rhyolite that is rimmed by banded devitrified-vitrophyre, perlitic rinds, and variably altered vitrophyre breccia. A sequence of welded tuffs, tuffaceous sedimentary rocks, and mafic lavas is locally exposed beneath the domes. Marcy (2014) reports an analysis of an underlying mafic lava flow that resembles the stage 1 Bishops Ranch lava. Mafic inclusions entrained in some of the domes are heavily enriched in rare earth elements (REEs) (Marcy, 2014).

The eruptive sequence at Mahogany Mountain caldera is recorded by major rock units including from oldest to youngest: (1) rhyolite flows of Devils Gate, (2) intracaldera and outflow facies of the Leslie Gulch Tuff, (3) intracaldera and outflow facies of the Spring Creek tuff, (4) intracaldera rhyolite domes and intrusion of rhyolite dikes, and (5) postcaldera rhyolite lava flow of McIntyre Ridge and others along caldera margins. These units collectively define a major and vigorous rhyolite eruptive center, active over a 200 to 300 thousand year time span between ~15.9 Ma and 15.6 Ma, during the waning stages of Grande Ronde Basalt and Littlefield Rhyolite magmatism on the north. Scattered outcrops of Columbia River Basalt lava flows underlying the rhyolite of Mahogany Mountain (MacLeod, 1990a,b) chemically resemble lavas associated with a maar complex at Crissman Hill (Gilbert, 1988; Macleod, 1990a) on the south and may be correlative with the upper Pole Creek basalt of Lees (1994) (fig. 6).

Figure 19. Photograph looking east at variably altered Leslie Gulch Ash-Flow Tuff exposed ~1.5 kilometers north of Yellowjacket Gulch (Stop 2.6) within the Mahogany Mountain caldera (lat 43.3156° N., long 117.2967° W.). Vander Meulen and others (1987a,b,c) used color differences and weathering characteristics to map what they considered to be a younger tuff (light tan) from an older tuff of Leslie Gulch (darker brown) in the central part of the Mahogany Mountain caldera. Benson and Mahood (2016) show the color differences along the Leslie Gulch dirt road resulting from differential alteration. Photograph by Jason McClaughry.

Reverse course and return to Leslie Gulch Road.

Cumulative Mileage
mi (km)

157.0 (252.7) Turn left on Leslie Gulch Road. Proceed east to Succor Creek Road.

160.4 (258.0) Turn left on Succor Creek Road. Return 25 miles on Succor Creek Road to O.R. 201.

185.4 (298.3) Turn left onto O.R. 201 and proceed north toward Adrian.

193.0 (310.6) The ridge top on the left (west) is capped by an arkosic conglomerate with black chert pebbles that marks a slight angular unconformity between the Glenns Ferry Formation and underlying Chalk Hills Formation of the Idaho Group. Kimmel (1982) reports a fission track age of 6.6 ± 1.0 Ma on an ash deposit near the top of the lower Chalk Hills Formation. The Glenns Ferry and Chalk Hills Formation and underlying Banbury Basalt, also of the Idaho Group, are part of the Pliocene Lake Idaho section of the western Snake River Plain.

197.5 (317.8) Turn left on Owyhee Avenue and follow the signs west to Lake Owyhee.

201.4 (324.0) Turn left onto Owyhee Lake Road. Proceed south to Lake Owyhee.

203.6 (327.7) Mitchell Butte, an erosional remnant of Glenns Ferry Formation sandstone and conglomerate is visible on the right. Many of the small buttes that ring the southwest margin of the Western Snake River Plain are erosional remnants formed where permeable sandstones have been hardened by mineralizing hot spring fluids. Mitchell Butte is underlain by stage 4 olivine basalt flows (Ferns and Urbanczyk, 1990) that resemble the Banbury Basalt of Malde and Powers (1962). Fiebelkorn and others (1982) report a K/Ar age of 7.4 Ma from these rocks. The olivine basalts record a mafic magmatic pulse that followed silicic volcanism in the Western Snake River Plain between ~9 and 7 Ma (Bonnichsen and Godchaux, 2002).

206.3 (332.0) Lake Owyhee Road crosses a series of north-trending faults and enters the mouth of a canyon that is carved into older stage 5 lavas (fig. 6). The upper part of the sequence is defined by a series of basalt and basaltic andesite flows equivalent to the Blackjack Basalt of Bryan (1929) which are equivalent to the capping flows of the Owyhee basalt of Corcoran and others (1962) and Kittleman and others (1965).

207.9 (334.6) Snively Hot Springs. The high butte visible on the west is Deer Butte, a hot springs-hardened sedimentary section in the Idaho Group.

209.5 (337.2) The massive cliffs capping the canyon walls to the right (west) are heavily silicified arkosic sandstone and conglomerate, that are part of the Deer Butte Formation (Corcoran and others, 1962). The Deer Butte Formation is overlain by the 12.6 ± 0.6 Ma Kern Basin tuff (Ferns and Cummings, 1992). The Kern Basin tuff is part of the Kern Basin Formation and once considered to be part of the Idaho Group (Corcoran and others, 1962).

220.0 (354.1) **Stop 2.8.** Drive just past Owyhee Dam, and pull off and park in the turnout on the right (south).

Stop 2.8. Owyhee Dam—Dam Rhyolite, Owyhee Basalt, Maar Hyaloclastite Units, and Feeder Dikes to the Owyhee Basalt (lat 43.6422° N., long 117.2409° W.)

Lava flows exposed along the Owyhee River belong to stage 5 of Ferns and McClaughry (2013) (figs. 5*F*, 6, and 20) and are part of the Owyhee basalt of Bryan (1929), Corcoran (1962), and Kittleman and others (1965).

The Owyhee Basalt forms a >1,310-ft (400-m)-thick complexly coalescing sequence of basalt, basaltic andesite, and andesite lava flows and associated vent deposits consisting of scoria, agglutinate and hyaloclastic deposits. Lava flows are calc-alkaline in composition and range from basalt to andesite (Brown and Petros, 1985; Cummings and others, 2000). Vents are associated with north-south trending feeder dikes that are in places cut by north-south trending faults. The base of the section exposed on the south along the Owyhee Reservoir is marked by a thick section of brown palagonitic maar complexes that locally grades upward in red and black scoria and spatter deposits. The southern maar sequence is disrupted by numerous mafic dikes and sills (Ferns and Cummings, 1992).

Individual lava flows pinch, swell, and in places appear invasive into underlying pyroclastic deposits. To the south, the Owyhee basalt transitions to a flow-on-flow stack of basalt, basaltic andesite and andesite flows that are interbedded with distal flows and breccias of the Dam rhyolite. The capping lava flow has yielded K/Ar ages of 15.3 ± 0.6 Ma (Brown and Petros, 1985) and 13.1 ± 0.3 Ma (Watkins and Baksi, 1974). Radiometric ages for the underlying rhyolite include whole rock dates of 22.8 ± 2.6 Ma (Brown and Petros, 1985) and 13.5 ± 3.4 Ma (Ferns and Cummings, 1992). Although early workers, including Ferns (1989a,b,c), Brown and Petros (1985),

Table 7. Major and trace element analyses, sample location, and isotopic age for stage 5 lavas.

[Major elements have been normalized to a 100 percent total on a volatile-free basis and recalculated as oxides, with total iron expressed as FeO*. The "tuff of Kern Basin" refers to the "Kern Basin Formation of the Idaho Group." Analyses are from Ferns and McConnell (2005),[1] Lees (1994),[2] Edwards (2013),[3] and Bailey (1990),[4] Reported isotopic ages determined by the K/Ar method. Abbreviations: FRAN, Franklin and Marshall College; ID, identification number; Ma, mega-annum (million years before present); nd, no data or not analyzed; WSU, Washington State University; XRAL, X-Ray Assay Laboratories (Toronto, Canada)]

Formation, unit, or location	Dam rhyolite	Owyhee Basalt		Freezeout Mountain	Kern Basin	Vines Hill	Mount Fanny	La Grande	Sawtooth Ridge
Stage	5	5	5	5	5	5	5	5	5
Age (Ma)	13.5 ± 3.4	nd	nd	nd	12.6 ± 0.6	nd	11.8 ± 0.9	nd	13.0 ± 0.1
Field sample ID	AXB-301[1]	AXB-309[1]	KL-92-286[2]	AYB-210[1]	AWB-100[1]	CNHS-08[3]	99-LCC-98[1]	98MAD130[1]	DB87-3104[4]
Latitude (north)	43.6080	43.6141	43.6833	43.8114	43.7267	nd	45.3075	45.3020	44.9712
Longitude (west)	117.2689	117.2950	117.1833	117.5575	117.2555	nd	117.7300	118.1112	117.5446
Major elements as oxides, in weight percent									
SiO_2	69.18	55.51	55.16	55.99	71.90	60.13	67.61	58.35	61.32
Al_2O_3	15.37	16.57	17.07	17.12	14.91	17.77	17.06	17.04	16.78
TiO_2	0.49	1.38	1.15	0.97	0.28	0.91	0.53	1.32	0.99
FeO*	2.24	9.06	7.84	6.98	1.99	5.92	3.44	6.82	6.21
MnO	0.08	0.18	0.14	0.18	0.07	0.14	0.05	0.15	0.10
CaO	2.61	7.31	8.12	8.38	2.63	5.83	4.16	6.51	5.85
MgO	0.87	3.75	4.99	5.12	0.81	2.31	0.82	3.28	2.45
K_2O	4.00	1.73	1.42	1.23	3.97	2.24	1.75	2.02	1.55
Na_2O	4.64	4.01	3.74	3.37	3.27	4.27	4.33	3.87	4.27
P_2O_5	0.13	0.49	0.38	0.29	0.10	0.46	0.25	0.64	0.47
Trace elements, in parts per million									
Ni	6	nd	39	93	7	47	4	25	27
Cr	nd	29	87	131	21	67	16	49	50
Sc	nd	nd	23	nd	nd	19	12	18	19
V	nd	nd	194	nd	nd	132	64	138	102
Ba	1,700	771	633	655	1,440	1,192	638	845	673
Rb	98	22	20	134	94	30.3	27	26	20
Sr	305	565	493	518	386	605	535	596	502
Zr	246	150	158	133	137	201	160	208	190
Y	27	29	22	nd	16	24.7	13	27	24
Nb	31	40	11.7	nd	22	16.5	6.9	25.1	18
Ga	nd	nd	16	nd	nd	18.2	20	19	17
Cu	11	nd	39	62	18	53	23	29	44
Zn	49	nd	82	84	42	77	75	86	78
Pb	nd	nd	3	nd	nd	2	8	5	nd
La	nd	nd	16	nd	nd	31	36	30	29.8
Ce	nd	nd	52	nd	nd	60	52	71	52.2
Th	nd	nd	2	nd	nd	nd	3	2	2
Laboratory	XRAL	XRAL	WSU	XRAL	XRAL	FRAN	WSU	WSU	WSU

Figure 20. Photograph from Stop 2.8 looking north from Owyhee Dam. Stacked calc-alkaline lavas and vent deposits of the Owyhee basalt (stage 5) here overlie a complexly flow banded and flow folded calc-alkaline rhyolite dome. Photograph by Jason McClaughry.

Corcoran and others (1962), and Kittleman and others (1965, 1967) considered the Owyhee basalt to be part of the CRBG, the Owhyee basalt is now recognized as a suite of younger stage 5 calc-alkaline flows (Ferns and McClaughry, 2013).

Owyhee Dam is anchored in a >1,080-ft (330-m)-thick section of low-silica rhyolite, known as the Dam rhyolite (fig. 20). At the dam, observed flow breccia constitutes the top of the rhyolite. The base of the rhyolite is not exposed here. On the southwest side of the reservoir, the rhyolite consists of two lobes separated by block-and-ash flow deposits. Farther south, the rhyolite is interbedded with Owyhee basalt lava flows (Ferns and Cummings, 1992).

Owyhee basalt lava flows also overlie mafic hyaloclastite lapilli tuffs and tuffaceous sandstone that are interpreted as mafic surge deposits formed in a maar setting. Similar deposits that underlie the rhyolite to the south, grade laterally into a sequence of intertonguing basaltic andesite and andesite lava flows, mudflow breccias, and mafic hyaloclastite lapilli tuffs (Ferns and Cummings, 1992) that are interpreted as a series of overlapping maar volcanoes. The maar sequence to the south is cut by numerous basalt dikes and sills and overlies a sequence of interbedded white airfall tuff, lapilli tuff, and coal-shale that resembles lower Sucker Creek Formation deposits east of Mahogany Mountain.

Reverse course and return 18.6 mi (29.9 km) to Owyhee Avenue.

Cumulative Mileage
mi (km)

238.6 (384.0) Turn right on Owyhee Avenue and proceed east to Owyhee and the junction with O.R. 201.

243.2 (391.4) At the town of Owyhee, turn left (north) onto O.R. 201 and proceed north to Ontario.

250.7 (403.5) Town of Nyssa. Turn left at the stop light and continue north on O.R. 201 to Ontario.

261.0 (420.0) Stop light. Turn right on SW 4th Avenue (Olds Ferry/Ontario Highway) and proceed east into Ontario.

262.9 (423.1) Turn left on SW 2nd Street and proceed 4 blocks north to E. Idaho Avenue.

263.2 (423.6) Turn right on E. Idaho Avenue and proceed east to the I–84 interchange.

264.0 (424.9) Cross I–84 interchange and turn left at the 2nd stop light into the motel complex. **End Day 2.**

Day 3. Transect from Western Margin of La Grande-Owyhee Eruptive Axis and Oregon-Idaho Graben through Southern Margin of Strawberry Volcanics to John Day

Day 3 will progress westward from the eastern margin of the LOEA, examining a transition linking the Columbia River Basalt/Yellowstone province with a northwestward-younging magmatic trend of silicic volcanism that underlies the High Lava Plains of eastern Oregon. Initial field stops on Day 3 will examine key outcrops demonstrating the intercalated nature of middle Miocene tholeiitic CRBG flood basalts, prominent ash-flow tuffs, and “Snake River-type” large-volume rhyolite lava flows exposed along the Malheur River. Subsequent stops on Day 3 will focus on the emerging volcanic stratigraphy northeast of Burns which includes middle to late Miocene ash-flow tuffs, and lava flows assigned to the Strawberry Volcanics.

Road Log
Cumulative Mileage
mi (km)

0.0 (0.0) The road log for Day 3 begins at America's Best Value Inn, located at the intersection of Lincoln Avenue and Goodfellow Avenue in Ontario. Proceed south to E. Idaho Ave.

0.2 (0.3) Turn right (west) onto E. Idaho Avenue. Proceed west to I–84.

0.4 (0.6) At the I–84 interchange, take Exit 376. Merge onto I–84 and proceed westbound to Exit 374.

2.6 (4.2) City of Ontario. **Leave I–84 at Exit 374.**

2.9 (4.7) Turn right (Exit 374) onto O.R. 201 (Yturri Beltline), following signs to the towns of Vale and Nyssa. Proceed south through stoplight to Cairo Junction.

8.0 (12.9) Cairo Junction. Turn right onto O.R. 26 and proceed west to Vale.

10.7 (17.2) Siphon Drive The butte on the right is Malheur Butte, a small, composite high-silica andesite/dacite vent that protrudes through Glenns Ferry Formation sediments. Lees (1994) reports a poor resolution K/Ar age of 2.78 ± 0.84 Ma for the vent rocks. Tilted pebble conglomerate in the top of the Glenns Ferry Formation, exposed just north of the butte, are interbedded with near-vent mafic surge deposits of dark-gray lapilli tuff (Madin and Ferns, 1997). The age of the top of the Glenns Ferry Formation is believed to be about 1.76 Ma (Othberg and others, 1995).

18.0 (29.0) Vale Buttes on the left is a mound of Glenns Ferry Formation sediments that have been cemented by hydrothermal fluids.

18.5 (29.8) The steam rising along the Malheur River, on the right, is a hot-spring vent.

18.8 (30.3) Town of Vale. Continue west through Vale.

20.0 (32.2) The butte in the foreground on the left (southwest) is Double Mountain, a late stage 5 high-silica, dacite dome complex. The Double Mountain dome appears to lie on the axis to the thickest part of the Oregon-Idaho graben. Fiebelkorn and others (1982) report a whole rock K/Ar age of 8.07 ± 0.21 Ma for the Double Mountain dome.

20.2 (32.5) The long, high ridge to the right (north) is Cottonwood Mountain, a fault block of pre-Tertiary basement rocks overlain by a thick sequence of CRBG flows and stage 3 rhyolite lava flows.

30.0 (48.3) U.S. 20 crosses out of the western Snake River Plain, ascending Vines Hill.

30.9 (49.7) A series of exposed, north-south trending faults cut the Glenns Ferry Formation shoreline gravels and older Chalk Hills Formation algal limestones.

31.5 (50.7) A fault contact is visible to the right (north) between the Chalk Hills Formation algal limestone and stage 5 hypersthene andesite of Vines Hill. Edwards (2013) reports $^{40}Ar/^{39}Ar$ ages of 11.45 ± 0.17 Ma and 10.87 ± 0.08 Ma for Vines Hill andesite at Neal Hot Springs.

34.3 (55.2) Crossroad at Little Valley. Neal Hot Springs lies out of sight behind the ridge to the north, along a major down-to-the-east fault that may extend through this area. The ridge on the south is Freezeout Mountain, a series of stage 5 andesite and basaltic andesite lava flows that are overlain by olivine basalt flows that cap the top of the Bully Creek Formation section.

36.1 (58.1) A small anticline in olivine basalt is present on the left.

37.3 (60.0) The contact between olivine basalt flows and the underlying Bully Creek Formation (Kittleman and others, 1965, 1967) comes into view on both sides of the highway. The Bully Creek Formation is a sedimentary sequence of interbedded diatomite and airfall tuff.

39.1 (62.9) The low hills on the left (south) are silicified siltstone and arkosic sandstone. Hot spring systems include densely silicified, finely laminated siltstones that are interpreted to be exhalative chert deposits.

41.3 (66.5) Turn right onto Harper Road at Harper Junction and proceed north toward the town of Harper.

41.8 (67.3) Turn right on "A Street" (Harper-Westfall Road), proceeding northeast through the small town of Harper.

42.2 (67.9) Leaving the town of Harper, near the football field, bear left onto the Harper-Westfall Road, proceeding north.

43.3 (69.7) At the intersection with Old Mail Road, keep left, and continue proceeding west on Harper-Westfall Road.

47.4 (76.3) Turn to the right and proceed onto an unimproved dirt road. If weather and fire hazard conditions allow, follow the dirt road up to the cliff-forming outcrops to the north.

47.8 (76.6) **Stop 3.1**. Pull off and park alongside the dirt track. Outcrops are off to the left (northwest).

Stop 3.1. Dinner Creek Tuff, Cooling Unit 3 (lat 43.9182° N., long 117.6508° W.)

The ash-flow tuff exposed in the cliff face, first referred to as the tuff of Bully Creek, is the type locality for cooling unit 3 of the Dinner Creek Tuff (Streck and others, 2015) (fig. 21). The Dinner Creek is the most extensive ignimbrite in the CRBG province and includes at least four discrete cooling units that erupted from a common source area over a time span of approximately 1 million years between ~16 and 15 Ma (Streck and others, 2015) (figs. 5*C* and 22). All four cooling units of the Dinner Creek lie at or near the top of the Grande Ronde Basalt (figs. 3 and 6; individual cooling units not shown on figs. 3 and 6) and together extend over an area in excess of 7,722 mi^2 (20,000 km^2) (fig. 5*C*). Streck and others (2015) note that three of the ignimbrite sheets cannot be confidently distinguished from one another in the field, sharing similar lithological characteristics, as well as showing similar lateral facies changes typical of other widespread ignimbrites in eastern Oregon (see Streck and Grunder, 1995), and they display only very subtle compositional differences (Streck and others, 2015) (fig. 22).

Haddock (1967) and Wood (1976) were the first to propose a source vent in the vicinity of Castle Rock where Rytuba and others (1991) later placed the Castle Rock caldera. The Dinner Creek cooling units appear to thicken back toward what is believed to be a common vent area located between Castle Rock and Ironside Mountain (see Streck and others, 2015).

The areal extent of cooling unit 3 has yet to be determined. Evans and Binger (1999) describe a possibly correlative sequence (“Tps”) of tuff, welded tuff, lapilli tuff, and tuff breccia to the northwest that contains Dinner Creek blocks as much as 2 m across. The “Tps” unit of Evans and Binger (1999) interfinger with underlying stage 2 Hunter Creek Basalt lava flows that have upper Grand Ronde Basalt compositions (fig. 6).

The lower Bully Creek Formation is exposed between north-south trending, linear hyaloclastite ridges of Hunter Creek Basalt. There are two possible explanations for the linear ridges. They could be erosional remnants of linear Hunter Creek vents on which the Bully Creek Formation was deposited. Alternatively, Hunter Creek Basalt vents may have formed after the Dinner Creek tuffs were emplaced. The lower part of the Bully Creek Formation includes thick airfall tuffs as well as cooling unit 3 of the Dinner Creek Tuff.

Sedimentary rocks and tuff in the upper part of Bully Creek Formation are capped by an olivine basalt flow that can be traced south to the Harper Gold Prospect where exploration drill holes

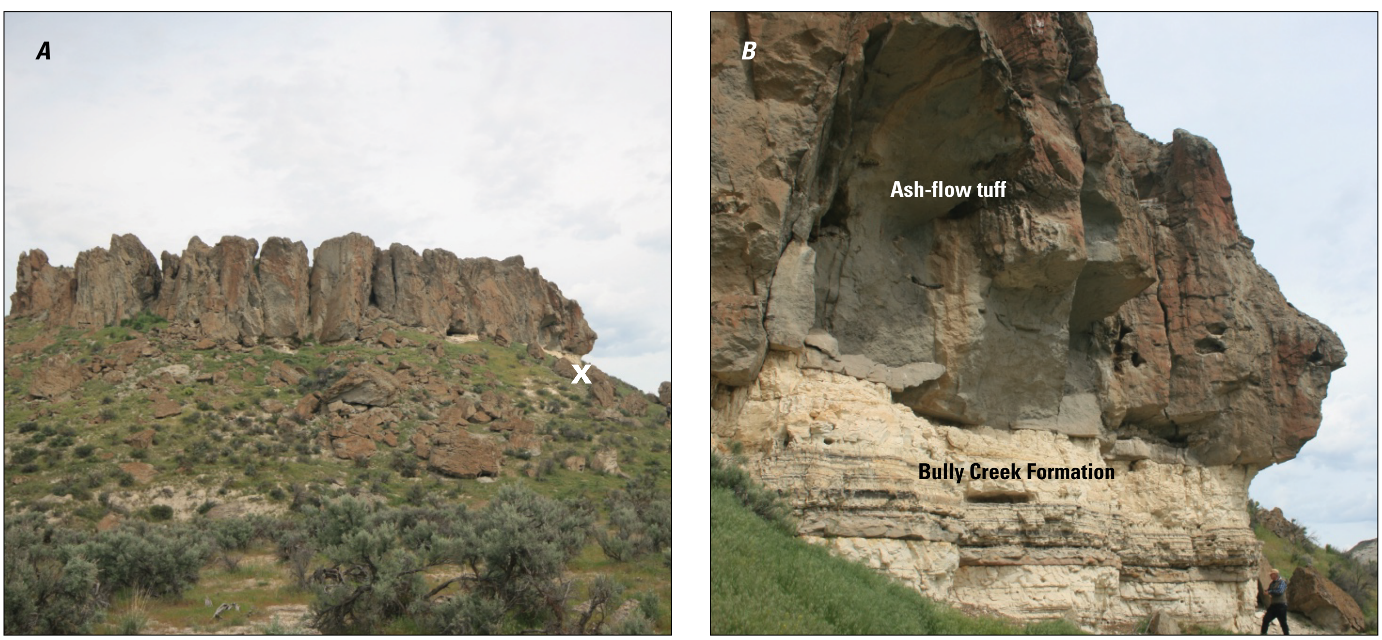

Figure 21. Photographs of ash-flow tuff looking east-northeast from Stop 3.1. *A*, Ash-flow tuff exposed in a cliff face that was first referred to as the tuff of Bully Creek, but now is the type locality for cooling unit 3 of the Dinner Creek Tuff. The “X” marks the location of the photograph shown in B. *B*, the base of ash-flow tuff showing the underlying lower Bully Creek Formation. Photographs by Jason McClaughry.

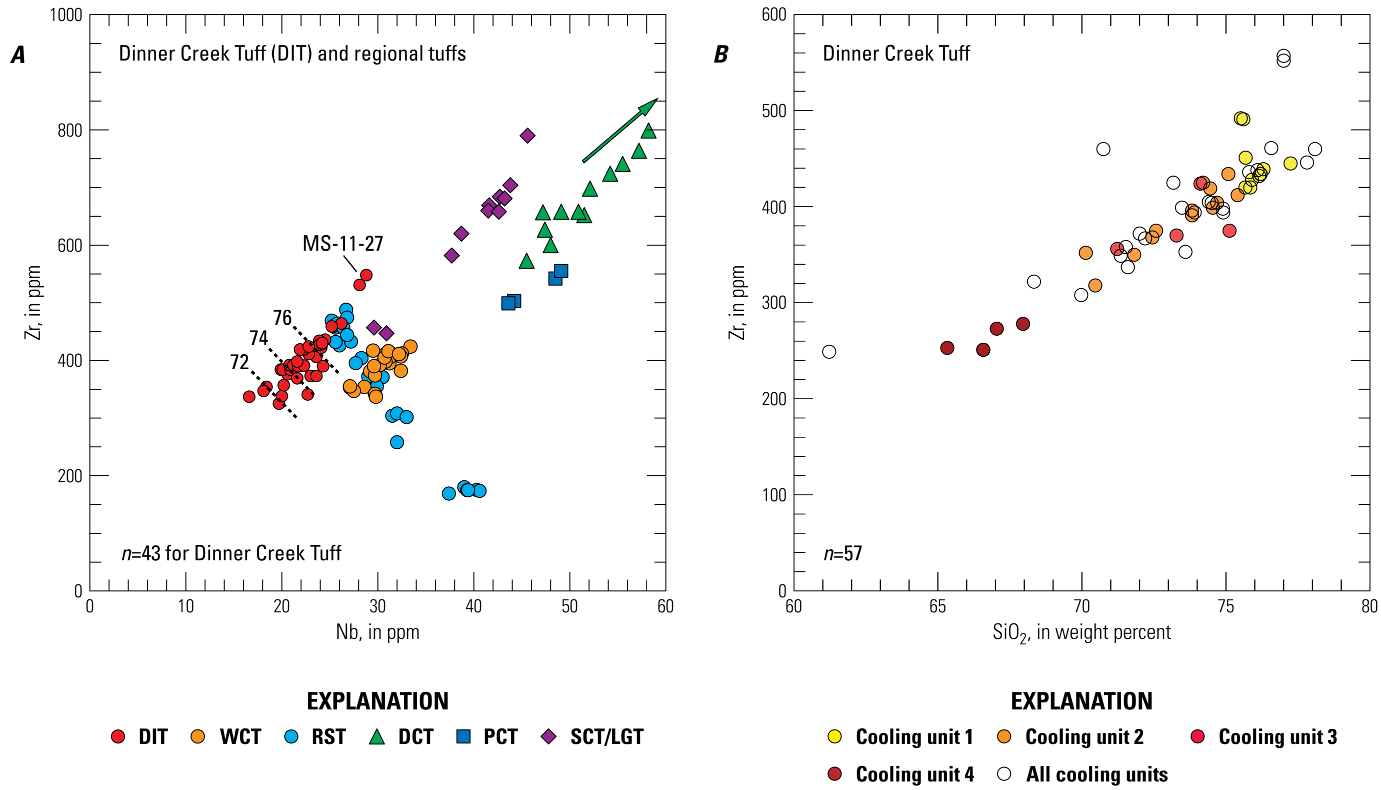

Figure 22. Geochemistry plots showing results from the Dinner Creek Tuff (DIT) and regional tuffs. *A,* Zirconium (Zr) vs. niobium (Nb) for the Dinner Creek Tuff relative to regional tuffs (all rhyolites) (from Streck and others, 2015). Numbers 72, 74, and 76 are SiO_2 weight percent and dashed lines are approximate contour variations within the Dinner Creek Tuff samples (all cooling units); green arrow indicates the Dinner Creek Tuff compositions extend beyond range shown; sample MS-11-27 is from a distal location that yielded the highest Nb and Zr concentrations. Data sources for other tuffs include: Wildcat Creek Welded Tuff (WCT) from Hooper and others (2002); Rattlesnake tuff (RST) from Streck and Grunder (1997); Devine Canyon Ash-Flow Tuff (DCT) from S. Wacaster and M.J. Streck (unpub. data, 2016); Prater Creek Ash-Flow Tuff (PCT), Spring Creek tuff (SCT), and Leslie Gulch Tuff Member (LGT) from Marcy (2014), Streck (2014), and M.J. Streck (unpub. data, 2016). *B,* Zr vs. SiO_2 showing the compositional spread of cooling units of the Dinner Creek Tuff (from Streck and others, 2015). Abbreviations: n, number of analyses; ppm, parts per million.

have penetrated basalt and a gray tuff that overlie a mineralized section of arkosic sandstone and stage 5 basaltic andesite and andesite flows. An underlying stage 5 basaltic andesite has a $^{40}Ar/^{39}Ar$ whole rock age of 11.5 ± 0.99 Ma (Lees, 1994). This series of calc-alkaline lava flows, interbedded with arkosic sandstone, and maar and hot spring deposits is similar to the section exposed along the Owyhee Reservoir (Stop 2.8).

Reverse course and return 0.4 mi (0.6 km) to Harper-Westfall Road.

Cumulative Mileage
mi (km)

48.2 (77.6) Turn right onto Harper-Westfall Road, and proceed north.

51.1 (82.2) Turn right on Dahle Road. Outcrops in the foreground to left (north) and right (south) are the tuff of Bully Creek. North-south trending ridges in the middle ground on the left (north) are Hunter Creek Basalt hyaloclastite deposits (fig. 6).

53.4 (85.9) Bully Creek. Turn right on Old Stage Road. The hill immediately to the north is a mound of Hunter Creek hyaloclastite breccia and lapilli tuff.

54.2 (87.2) Hunter Creek Basalt with a K/Ar age of 15.78 ± 0.6 Ma (Lees, 1994) (fig. 6).

54.6 (87.9) **Stop 3.2**. Pull off and park alongside the left (north) side of the road. Outcrops are off to the left (north).

Stop 3.2. Hunter Creek Vent Complex (lat 43.9823° N., long 117.6274° W.)

Proceed on foot a short distance north of the parking area to look at a Hunter Creek Basalt hyaloclastite complex (figs. 6 and 23). A similar complex in the foreground on the west is cut by a glassy rhyolite dike that is probably correlative to the Littlefield Rhyolite (fig. 6). The ridge in the distance is capped by Hunter Creek Basalt and Dinner Creek Tuff. The Dinner Creek thickens to the northwest, toward the presumed source vent near Castle Rock (fig. 5*C*).

Massive outcrops downstream on Bully Creek are the Cottonwood Mountain rhyolite and overlying Hunter Creek Basalt (fig. 6). The Neal Hot Springs Geothermal plant is located 7 mi (11.3 km) west of Stop 3.1 on Bully Creek. Geophysical surveys, accompanied by geologic mapping and geochemical analyses of samples recovered during development of the hot springs has provided a wealth of subsurface data (Colwell, 2013; Edwards, 2013). Geochemical analyses show a CRBG sequence ~5,248 ft (1,600 m) thick that correlates with the Malheur gorge basalt of Evans (1990a,b) (fig. 6). Well-field analyses can be correlated with the three-fold division of the Malheur gorge basalt by Lees (1994) and Hooper and others (2002) into lower Pole Creek, upper Pole Creek, and Birch Creek units (fig. 6). At Neal Hot Springs, the basalt of Malheur gorge is overlain by the Cottonwood Mountain Rhyolite which in turn is overlain by a section of Hunter Creek Basalt flows and interbedded volcaniclastic rocks (fig. 6).

Edwards (2013) describes an overlying sequence of volcaniclastic, fluvial and lacustrine deposits equivalent to the Drip Spring Formation that contains diabase-textured basalt that may be largely intrusive. Edwards (2013) shows an overlying basaltic andesite flow can be correlated with surface outcrops that have yielded $^{40}Ar/^{39}Ar$ ages of 12.13 ± 0.02 Ma and 12.29 ± 0.09 Ma. These flows are in turn overlain by the andesite of Vines Hill which has yielded $^{40}Ar/^{39}Ar$ ages of 11.46 ± 0.17 Ma and 10.87 ± 0.08 Ma (Edwards, 2013).

A small mafic vent complex near Neal Hot Springs yielded a $^{40}Ar/^{39}Ar$ age of 8.81 ± 0.05 Ma (Edwards, 2013). The top of the volcanic sequence is marked by two small dacite breccia mounds for which no isotopic ages have been determined. The deepest exploration well penetrated Mesozoic granitic basement at a depth of 6,727 ft (2,051 m) (Edwards, 2013). A preliminary zircon age of ~145 Ma is reported for the granite at depth (J.H. Edwards, oral commun., 2012).

Reverse course and return 12.5 mi (20.1 km) to U.S. 20 through Harper.

Cumulative Mileage
mi (km)

55.8 (89.8) Turn left onto Dahle Road.

56.0. (90.1) The sharp peak on the west is Castle Rock, part of the eruptive center that produced the four

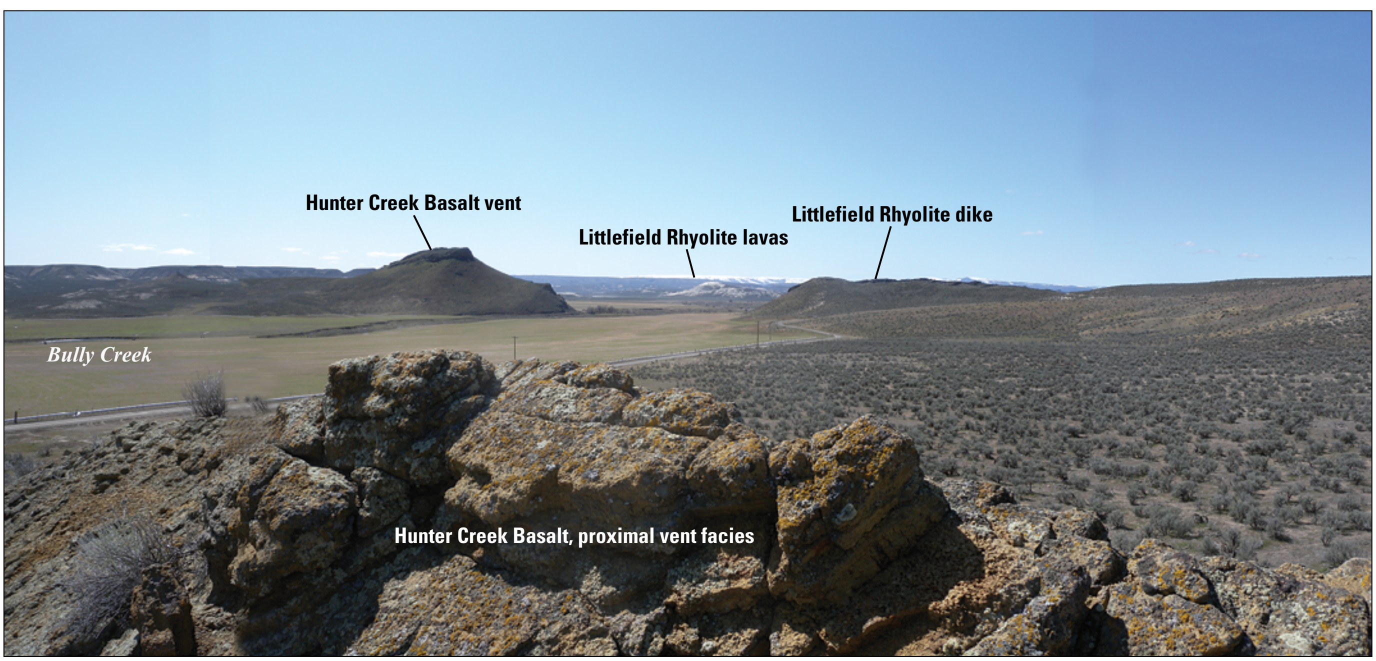

Figure 23. Photograph from Stop 3.2 of the Hunter Creek Basalt vent complex. The view is looking west across a series of north-trending Hunter Creek Basalt (stage 2) vents and Littlefield Rhyolite (stage 3) dikes that cross Bully Creek near the west margin of the Oregon-Idaho graben. On the skyline in the distance is an east-dipping sequence of younger Littlefield Rhyolite lavas. Photograph by Jason McClaughry.

identified cooling units of the Dinner Creek Tuff (fig. 5*C*).

56.6. (91.1) Ironside Mountain comes into view farther to the north of Castle Rock. This is possibly also part of the Castle Rock caldera. The highlands farther to the south mark the western margin of the Oregon-Idaho graben. The ridge in the foreground is Littlefield Rhyolite. Brooks and O'Brien (1992b) show the Littlefield Rhyolite overlying what they called the rhyolite of Bully Creek. The lower Littlefield Rhyolite has a composition similar to that of the Cottonwood Mountain rhyolite residing in the highlands farther west.

58.0 (93.3) The low hill to the immediate west is capped by a thin outcrop of 9.8 Ma Devine Canyon Ash-Flow Tuff. The distinctive high-Zr, low-Ba signature of the Devine Canyon Tuff contrasts sharply with the high-Ba signature of the middle Miocene Dinner Creek Tuff.

58.1 (93.3) Turn left onto Harper-Westfall Road, and proceed south through the town of Harper.

66.6 (107.1) Turn left onto Harper Road.

67.1 (108.0) Turn right onto U.S. 20 at Harper Junction.

69.8 (112.3) The yellow-weathering hills on both sides of U.S. 20 are part of the Drip Spring Formation (Kittleman and others, 1965, 1967; Ferns and O'Brien, 1992). In the type area to the south, the Drip Spring Formation is a sequence of interbedded arkosic sandstones, shales, and mafic hyaloclastite deposits, with intercalated basaltic andesite and andesite flows. The yellowish color here results from alteration associated with large basaltic sills. The margins of the sills are marked by pepperite rinds, and rafts of porcelain-like material occur within some of the mafic intrusives. Limited geochemical analyses indicate that the sills are olivine basalts that resemble the diabase and basalt encountered above the Hunter Creek Basalt at Neal Hot Springs. Analyses from this section and the Neal Hot Springs wells show these to be high-alumina olivine tholeiites that are likely equivalent to the Timms Peak basalt, a series of stage 4 olivine basalt flows (fig. 6).

73.4 (118.1) Mouth of Squaw Creek. The ridge on the south is made up of two or more low-silica Littlefield Rhyolite lava flows. The rhyolites exhibit ambiguous textural features similar to the high-temperature rhyolites in the Bruneau-Jarbidge and Juniper eruptive centers of southwest Idaho (Bonnichsen, 1982, Bonnichsen and Kaufman, 1987; Ekren and others, 1982).

74.0 (119.1) Thick outcrops of Littlefield Rhyolite occur on both sides of the highway at the entrance to the Malheur gorge.

75.7 (121.8) Carefully turn right onto the dirt road and continue southward for about 0.3 mi (0.5 km). **Use extreme caution exiting and entering the highway here; the speed limit on U.S. 20 is 65 mph and visibility here is limited.**

75.9 (122.1) **Stop 3.3a.** Pull off and park along the dirt road and walk up the slope to the cliff face for ~100 m. This is an overview stop looking at the exposed section across the Malheur River, to the south and east (figs. 24, 25) as well as at the section seen in figure 26.

Stop 3.3a. Overview of Namorf Section, Littlefield Rhyolite, Basalt of Malheur Gorge and Hunter Creek Basalt, and Dinner Creek Tuff (lat 43.7775° N., long 117.7364° W.)

Lees (1994) and Hooper and others (2002) highlighted the bimodal nature of the section by including the Dinner Creek Tuff, Hunter Creek Basalt, and the Littlefield Rhyolite of Kittleman and others (1967) in their Hog Creek formation. The base of the cliff face to the east is marked by two tholeiitic basalt flows at the top of the Malheur gorge basalt that are part of the Birch Creek basalt of Lees (1994). These flows closely resemble flows of the Grande Ronde Basalt (figs. 24 and 25) and are overlain by cooling unit 1 of the Dinner Creek Tuff, which is in turn overlain by the lower Littlefield Rhyolite, a lobe-forming rhyolite lava flow. Based on new work by Webb and others. (2016), the rhyolite is overlain by agglutinated spatter of Hunter Creek Basalt (fig. 26) and three lava flows of Hunter Creek Basalt (fig. 24). Dense agglutination of the spatter forms a vitrophyre that is interpreted to be a very proximal vent spatter deposit. These vent/near vent deposits are overlain by thin epiclastic deposits and a thick upper Littlefield Rhyolite lava flow (fig. 25) that is chemically distinct from the lower Littlefield Rhyolite (Webb and others, 2016).

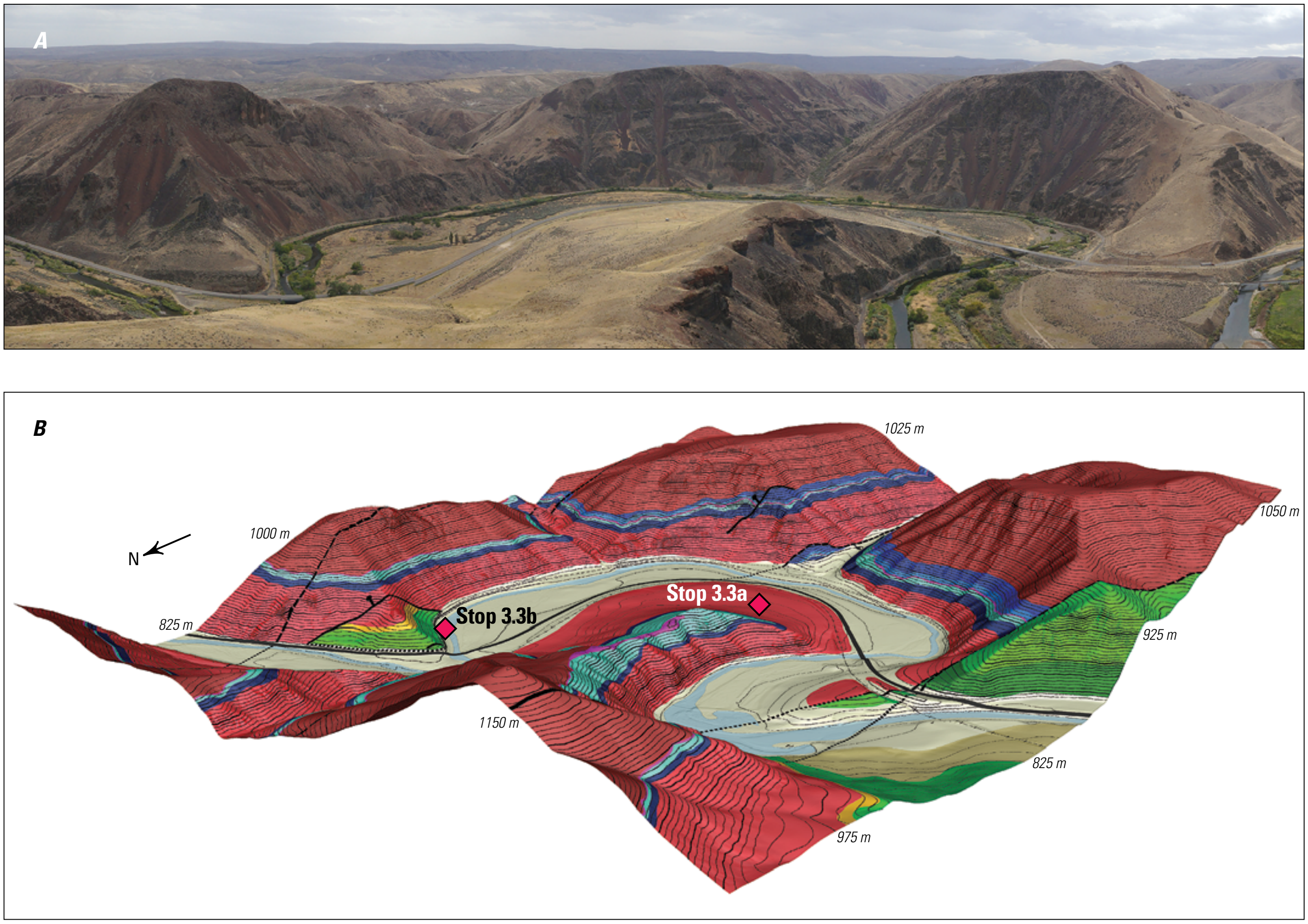

Universal Transverse Mercator, zone 11
North American Vertical Datum of 1988, GEOID 12A
5 m contours, 25 m index contours

0 200 400 600 METERS
0 600 1200 1800 FEET

EXPLANATION

- **Quaternary alluvium**
- **Quaternary colluvium**
- **Upper Littlefield Rhyolite**
- **Lava flow of Hunter Creek Basalt**
- **Lava flow of Hunter Creek Basalt**
- **Epiclastic tuff**
- **Pyroclastic spatter of Hunter Creek Basalt**
- **Lava flow of Hunter Creek Basalt**
- **Lower Littlefield Rhyolite**
- **Dinner Creek Tuff**
- **Malheur Gorge basalt (Birch Creek unit)**
- **Malheur Gorge basalt (upper Pole Creek member)**
- **Fault**
- **Fault inferred**
- **Fault concealed**

Figure 24. Photograph looking southeast of a panoramic view of the Namorf location (*A*), and a generalized geologic map of the Namorf location (*B*) showing volcanic units present in A. Note that here the Malheur gorge basalt is referred to as the Imnaha basalt. The locations of stops 3.3a and 3.3b are shown with red diamonds. Figure modified from Webb and others (2016). Photograph by Brian Webb, Portland State University.

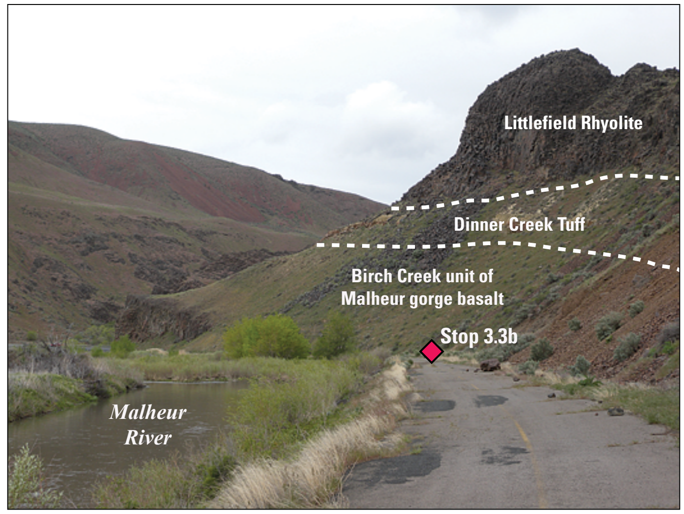

Figure 25. Photograph near Stop 3.3b (red diamond) looking north-northeast along the Malheur River where a stacked succession exposes (from bottom to top) the Birch Creek unit of the Malheur gorge basalt (stage 1), the Dinner Creek Tuff (stage 3), and the Littlefield Rhyolite (stage 3). An automobile is shown for scale along the road near the right-center of the photograph. Photograph by Mark Ferns.

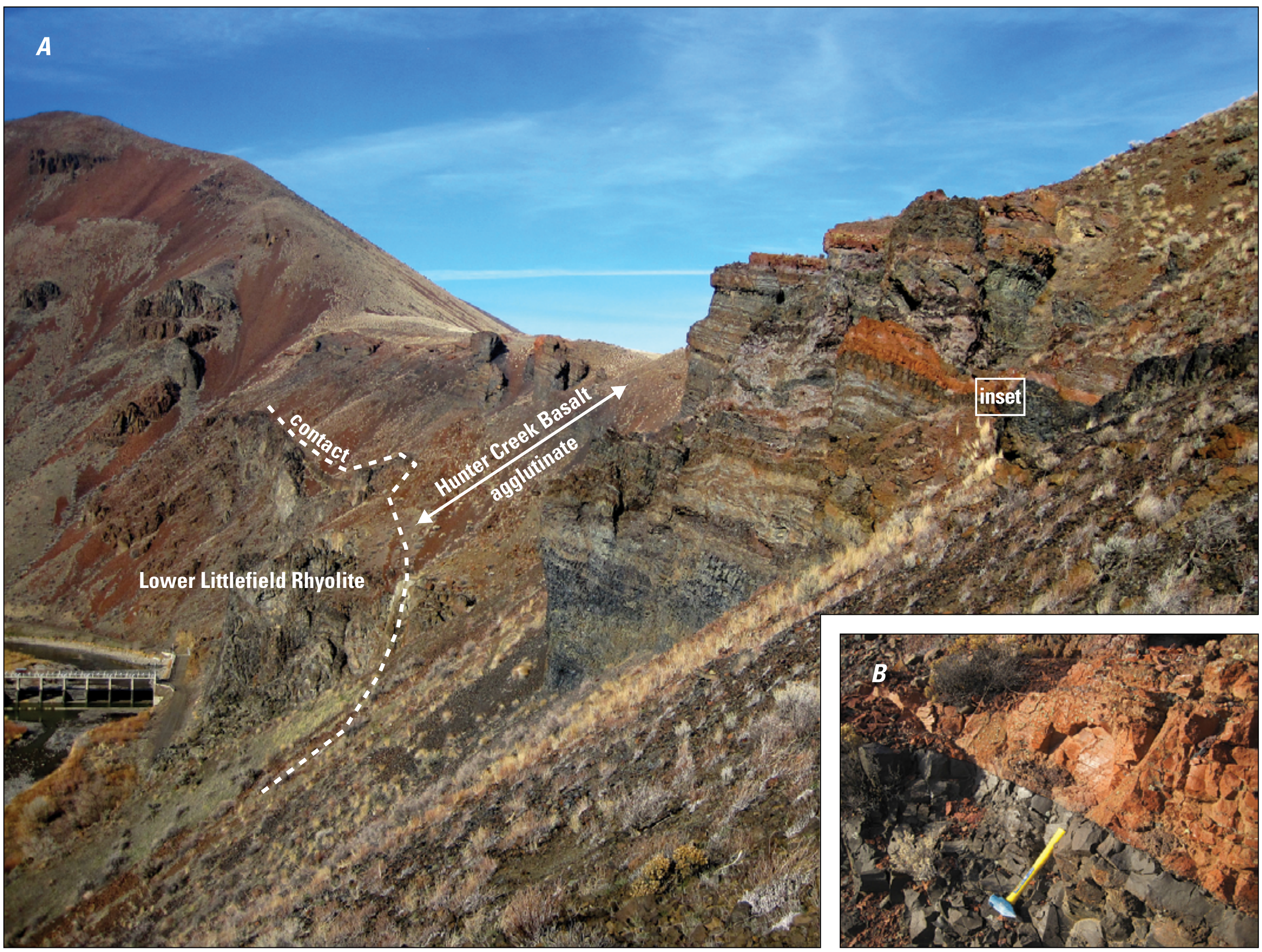

Figure 26. Photograph looking north from Stop 3.3a of proximal-vent, welded spatter deposits (Webb and others, 2016) of the Hunter Creek Basalt near Stop 3.3b at the Namorf location. The dashed line in *A* shows the contact between the Littlefield Rhyolite and the Hunter Creek Basalt. The inset (*B*) shows a close up of basaltic andesitic agglutinate (at hammer) (composed of dense black glass) with a sharp contact with overlying devitrified agglutinate (above hammer). Photographs by Brian Webb, Portland State University, and Martin Streck.

Return to the car and drive back 0.2 mi (0.4 km) towards U.S. 20. Turn left at mile 75.8 to immediately get off of U.S. 20 (at coordinates lat 43.7833° N., long 117.7326° W.) crossing the highway.

Cumulative Mileage
mi (km)

76.1 (122.5) Turn left onto U.S. 20. In less than 0.1 mi (0.1 km) you will make an immediate right. The route to the next stop essentially crosses the highway to the east. **Use extreme caution exiting and entering the highway here; the speed limit on U.S. 20 is 65 mph and visibility here is limited.**

76.2 (122.6) **Stop 3.3b.** Turn right onto gravel road, just after crossing the Malheur River. Pull off and park along the access road below outcrops of Dinner Creek Tuff and away from U.S. 20.

Stop 3.3b. Namorf Section, Littlefield Rhyolite, Malheur Gorge and Hunter Creek Basalt, and Dinner Creek Tuff (lat 43.7833° N., long 117.7326° W.)

Cooling unit 1 of the Dinner Creek Tuff here sits on upper lava flows of Malheur gorge basalt that were misidentified as Hunter Creek Basalt by Ferns and O'Brien (1992) (figs. 6 and 25). The ash-flow tuff is overlain by a thick rhyolite lava flow in the lower part of the Littlefield Rhyolite of Kittleman and others (1965, 1967). The base of the lower rhyolite lava flow is marked by well-defined large vitrophyre flow lobes. Webb and others (2016) report single crystal $^{40}Ar/^{39}Ar$ ages of 16.12 ± 0.07 and 16.20 ± 0.08 Ma from the lower rhyolite flow.

Webb and others (2015, 2016) shows that the lower rhyolite of the Littlefield here is in the same stratigraphic position as the Cottonwood Mountain Rhyolite (Evans, 1999) is on Bully Creek, where it lies beneath the Hunter Creek Basalt. The rhyolite lava flow in the lower cliff face is separated from an overlying Littlefield Rhyolite flow by a >165-ft (50-m)-thick sequence of Hunter Creek Basalt and interbedded agglutinated mafic pyroclastic deposits (fig. 25). Welded agglutinate spatter seen at Stop 3.3a, and consistent with near vent deposits, strongly thins between Stop 3.3a and here (fig. 24).

Geochemical analyses of the Malheur gorge lava flow beneath the Dinner Creek Tuff, strongly resemble analyses reported by Evans and Binger (1999) for Hunter Creek flows to the north that overlie the Dinner Creek. Lava flows that have been mapped as Hunter Creek Basalt range in composition from ~55 wt. percent SiO_2 to flows that are as silicic as ~63 wt. percent SiO_2. The Hunter Creek Basalt icelandites show remarkable similarities to the Fiddlers Hell icelandites at Indian Rock (Stop 1.2).

The Littlefield Rhyolite flow that overlies the Hunter Creek Basalt has yielded $^{40}Ar/^{39}Ar$ ages of 16.05 ± 0.04 and 16.01 ± 0.06 Ma (Webb and others, 2016). This effectively places an age of the Hunter Creek Basalt (upper Grand Ronde Basalt) between 16.15 to 16.05 Ma. Geochemical modeling by Webb and others (2015) indicates that higher silica variants of Hunter Creek Basalt (~61 wt. percent SiO_2) can be derived by mixing of Grande Ronde Basalt and Littlefield Rhyolite magmas.

Return to U.S. 20 and carefully turn left, proceeding west toward Burns. Go 1.1 mi (1.8 km) and pull off on the left side of the highway for Stop 3.4.

Cumulative Mileage
mi (km)

77.3 (124.4) **Stop 3.4.** Pull off and park along the left (south) side of U.S. 20. Continue walking west, to where U.S. 20 leaves the Owyhee River and cuts through the neck of an oxbow.

Stop 3.4. Littlefield Rhyolite Dike (parking at lat 43.7719° N., long 117.7549° W; stop at lat 43.7697° N., long 117.7563° W.)

Here, U.S. 20 cuts through a rhyolite dike. The glassy rubbly outcrop in the roadcut to the right is interpreted as a feeder dike to the Littlefield Rhyolite (Ferns and McClaughry, 2013) (fig. 27). The chemical composition of the rhyolite here associates the dike to the lower Littlefield Rhyolite seen at Stop 3.3b (Webb, 2016). The rhyolite dike and Hunter Creek Basalt are situated along the north-trending Hog Creek fault (Evans, 1990b), which cuts across the Malheur River and separates a thick section of Littlefield Rhyolite/Hunter Creek Basalt on the east from a much thinner section on the west. The Hog Creek fault marks the west margin of the Oregon-Idaho graben (Cummings and others, 2000). Geologic relationships suggest that the Littlefield Rhyolite erupted from a series of north-trending vents during the initial development of the Oregon-Idaho graben.

Proceed west on U.S. 20 to Stop 3.5.

Cumulative Mileage
mi (km)

82.1 (132.1) Gold Creek. A thick section of the basalt of Malheur gorge is exposed to the left. The lower slope is made up of coarse plagioclase-phyric flows of the lower Pole Creek unit of Lees (1994). Camp and others (2003) consider these flows to be part of the lower Steens Basalt. Gold Creek got its name from the large chalcedonic quartz vein that forms the light colored outcrops on the hill side to the left. The mineralized zone trends west-northwest and intersects a warm spring at the foot of the hill.

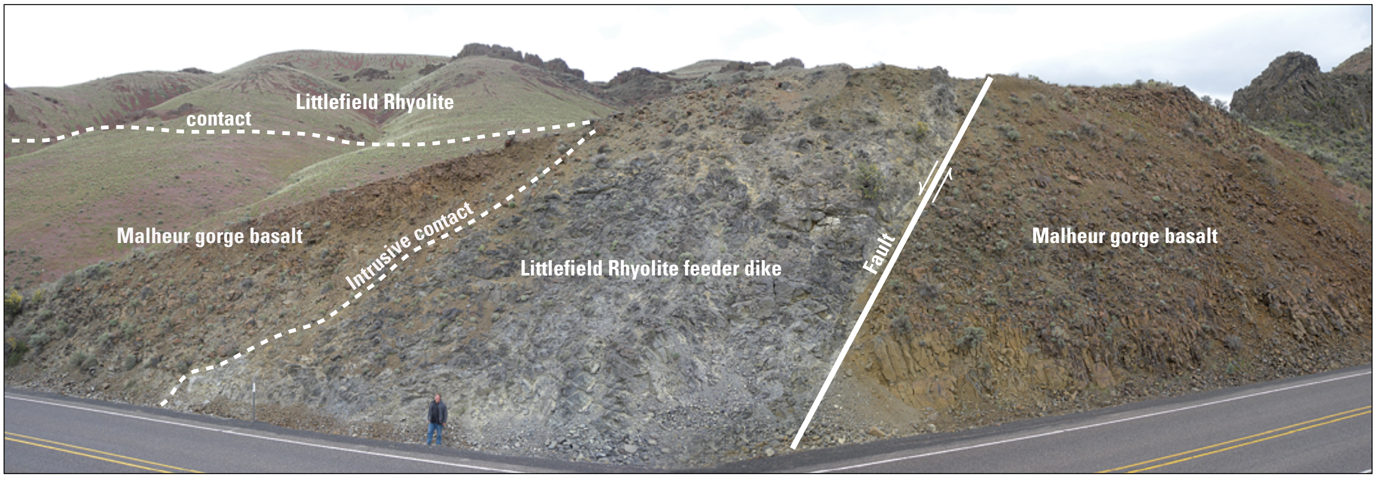

Figure 27. Photograph looking north from Stop 3.4 of a Littlefield Rhyolite dike cutting Malheur gorge basalt. A person is shown for scale. Photograph by Jason McClaughry.

82.7 (133.1) Gold Creek hot spring (to the left) is located on a northwest-trending fault that crosses the Malheur River on the right and drops the Dinner Creek Tuff and Hunter Creek Basalt to form a half graben.

85.4 (137.4) An outcrop of Devine Canyon Tuff caps sediments on the right.

90.8 (146.1) Cliff forming ledges to left and right of welded Dinner Creek Tuff are overlain by rubbly weathering Hunter Creek Basalt.

97.1 (156.3) **Stop 3.5.** Pull off and park along the right side of U.S. 20. Proceed across the highway to the southeast to examine a faulted Dinner Creek Tuff exposure.

Stop 3.5. Dinner Creek Tuff, Cooling Unit 1 (lat 43.7669° N., long 118.0298° W.)

The outcrop at Stop 3.5 is the type locality of cooling unit 1 of the Dinner Creek Tuff (fig. 28). This is the only Dinner Creek cooling unit prominently exposed in the Malheur gorge. The welded tuff is about 66 ft (20 m) thick and is marked by a basal vitrophyre. The devitrified core to the ash-flow tuff is marked by irregular ovoid cavities and spherulites filled with chalcedonic quartz near the fault.

Cooling unit 1 is a high-silica rhyolite with plagioclase composition of An_{10} and 1,300 to 1,600 parts per million (ppm) barium. It is probably the most regionally widespread of the Dinner Creek cooling units (fig. 5*C*), with exposures as far to the northwest as the Snake and Powder River divide. Streck and others (2015) correlate cooling unit 1 with the Mascall Formation ignimbrite of Davenport (1971) and the Brogan tuff of Lees (1994). The most precise and stratigraphically consistent $^{40}Ar/^{39}Ar$ age reported by Streck and others (2015) for cooling unit 1 is 16.16 ± 0.02 Ma.

Cooling unit 2 outcrops typically contain two color varieties of pumice; low-silica rhyolite and dacite. Glass shards in cooling unit 2 typically contain SiO_2 in excess of 75.0 wt. percent. Feldspars are less albitic than those in cooling unit 1, with compositions typically of $An_{20}Ab_{75}Or_5$, and 0.26 wt. percent BaO. Trace element compositional ranges are broader in cooling unit 2, with 1100 to 1700 ppm barium (Ba), 35 to 80 ppm rubidium (Rb), 87 to 270 ppm strontium (Sr), and 49 to 86 ppm yttrium (Y). $^{40}Ar/^{39}Ar$ ages of 15.45 ± 0.15 Ma, 15.48 ± 0.13 Ma

Figure 28. Photograph from Stop 3.5 of the Dinner Creek Tuff (stage 3) and overlying Hunter Creek Basalt (stage 2) along the Malheur River near Jonesboro. View is looking south from U.S. 20. Photograph by Jason McClaughry.

and 15.53 ± 0.15 Ma are reported for cooling unit 2 by Streck and others (2015).

Cooling unit 4, although not seen here at Stop 3.5, is worth mentioning because it contains vesicular globules of tholeiitic andesite glass that resemble Hunter Creek Basalt (Streck and others, 2015). Evans and Binger (1997) describe a gradational contact between the upper Dinner Creek Tuff that grades from a rhyolitic tuff to an andesitic tuff at the base of the Hunter Creek Basalt near Westfall Butte. Their geologic mapping indicates that the Hunter Creek Basalt is absent over what is mapped as Dinner Creek Tuff north of Westfall Butte.

Distal tuffs correlative with cooling unit 2 have been found (1) on Lookingglass Creek north of Elgin, (2) north of the Grande Ronde River west of La Grande, and (3) beneath the Strawberry Volcanics on the North Fork of the Burnt River. Evans and Binger (1997) show that the Dinner Creek Tuff north of Westfall Butte thickens to as much as 120 m.

Proceed west on U.S. 20 to Stop 3.6.

Cumulative Mileage
mi (km)

100.4 (161.6)	Town of Juntura.
104.6 (168.3)	Outcrops of Devine Canyon Tuff can be seen north of the highway.
104.7 (168.5)	Castle Rock is visible in distance to the right (north).
105.4 (169.6)	The Timms Peak Basalt is to the left. The younger rhyolitic Black Butte eruptive center (in foreground to the southeast) is part of a calc-alkaline volcanic suite broadly correlative with stage 5 lavas of Ferns and McClaughry (2013). Five distinct petrochemical volcanic successions recognized by Camp and others (2003) in the western Malheur gorge are the (1) Oligocene-Miocene calc-alkaline dacite; (2) mafic to bimodal (rhyolitic) rocks associated associated with middle Miocene, tholeiitic flood-basalt volcanism (~16–15.3 Ma); (3) early diktytaxitic olivine basalts (~13.5 Ma); (4) calc-alkaline intermediate to felsic rocks associated with Basin and Range extension; and (5) late diktytaxitic olivine basalts (~7 Ma to 32,000 years before present).
107.7 (173.3)	Mafic flows distal to the Black Butte eruptive center are exposed here along U.S. 20 and are mapped correlative to the Strawberry Volcanics (Greene and others, 1972).
113.0 (181.9)	**Stop 3.6.** Pull off and park along the right side of U.S. 20.

Stop 3.6. Drinkwater Pass Vantage Point and Devine Canyon Ash-Flow Tuff (lat 43.7827° N., long 118.2823° W.)

Here, a non-welded zone of the Devine Canyon Tuff of Greene (1973) underlies a welded zone. The Devine Canyon Tuff is one of the largest late Miocene ash-flow tuffs in eastern Oregon, extending over an area in excess of 20,000 km^2 (Wacaster and others, 2011). The Devine Canyon Tuff is a slightly peralkaline rhyolite characterized by high zirconium (Zr) and low Ba contents. More proximal outcrops are crystal rich, with alkali feldspar and quartz phenocrysts, in addition to minor amounts of hedenbergite pyroxene and fayalite olivine. Wacaster and others (2011) reports feldspar compositions of $Ab_{34.7–61.8}Or_{34.7–61.8}$. Wacaster and others (2011) reports streaks of comingled mafic glass in select pumices contain 63.4 wt. percent SiO_2 and 10.2 wt. percent FeO*, indicating that underlying, strongly differentiated tholeiitic magmas (icelandites) may have provided a thermal input. An $^{40}Ar/^{39}Ar$ age of 9.74 ± 0.02 Ma is reported for the Devine Canyon Tuff by Jordan and others (2004).

U.S. 20 goes over Stinkingwater Pass atop the ridge in the distance to the west. The ridge is capped by flows of the Stinkingwater Basalt, a high-alumina olivine basalt that is correlative to the Timms Peak and Little Catherine Creek basalts. Wright and others (2016) report a weighted $^{40}Ar/^{39}Ar$ plateau age of 13.79 ± 0.09 Ma.

The low-relief hills on the east slope of the ridge are older small rhyolite domes that are in some cases mineralized. Gold, mercury, and antimony mineralization are aligned along a southeast-trending zone that extends through Warm Springs Reservoir to the Duck Creek Buttes area.

Proceed west on U.S. 20 to Drewsey Road.

Cumulative Mileage
mi (km)

117.8 (189.6)	Turn right onto Drewsey Road and proceed north.
119.6 (192.5)	Town of Drewsey. Proceed north through the small town of Drewsey.
120.1 (193.3)	Turn left and proceed west on Van-Drewsey Road.
122.3 (196.8)	Tuffaceous sediments of the Drewsey Formation crop out to the north of the road. The Drewsey Formation consists mainly of fine-grained tuffaceous sediments with interbedded diatomite deposits, resembling the Bully Creek Formation.
137.7 (221.6)	A small hyaloclastite vent is on the left (west).
143.7 (231.3)	This is an optional stop to an outcrop of a platy, aphyric dacite flow. Turn right onto U.S. Forest

Service Road 15 and proceed 0.5 mi (0.8 km) to the optional stop.

Optional Stop: Strawberry Volcanics (lat 44.0138° N., long 118.6965° W.)

The platy, jointed aphyric lava flow exposed here typifies the Strawberry Volcanics (fig. 29) and has a high-silica dacite composition. Strawberry Volcanic lavas identified by Steiner and Streck (2013) include basaltic andesite and more commonly andesite (compositional analyses shown on fig. 8). Aphyric andesite and dacite lavas of similar age are the dominant rock types in both the main sequence of the southern part of the Strawberry volcanic field (fig. 7) and stage 5 lavas of the Powder River volcanic field (fig. 6).

Retrace the side route back to the intersection with U.S. Forest Service Road 17.

Cumulative Mileage mi (km)

143.7 (231.3) Continue west on U.S. Forest Service Road 17. For the next 14 mi (22.5 km) we will be on U.S. Forest Service Road 17, which winds through the Malheur National Forest. Outcrops along U.S. Forest Service Road 17 include various cooling units of the Dinner Creek Tuff, intermediate and rhyolitic lava flows of the Strawberry Volcanics, overlying clastic deposits composed of debris eroded from the Strawberry Volcanics, mafic pyroclastic deposits, and erosional remnants of younger regional ash-flow tuffs such as the 9.7 Ma Devine Canyon Tuff and 7.1 Ma Rattlesnake Tuff (Streck and Grunder, 1995; Streck and Ferns, 2004). The exact

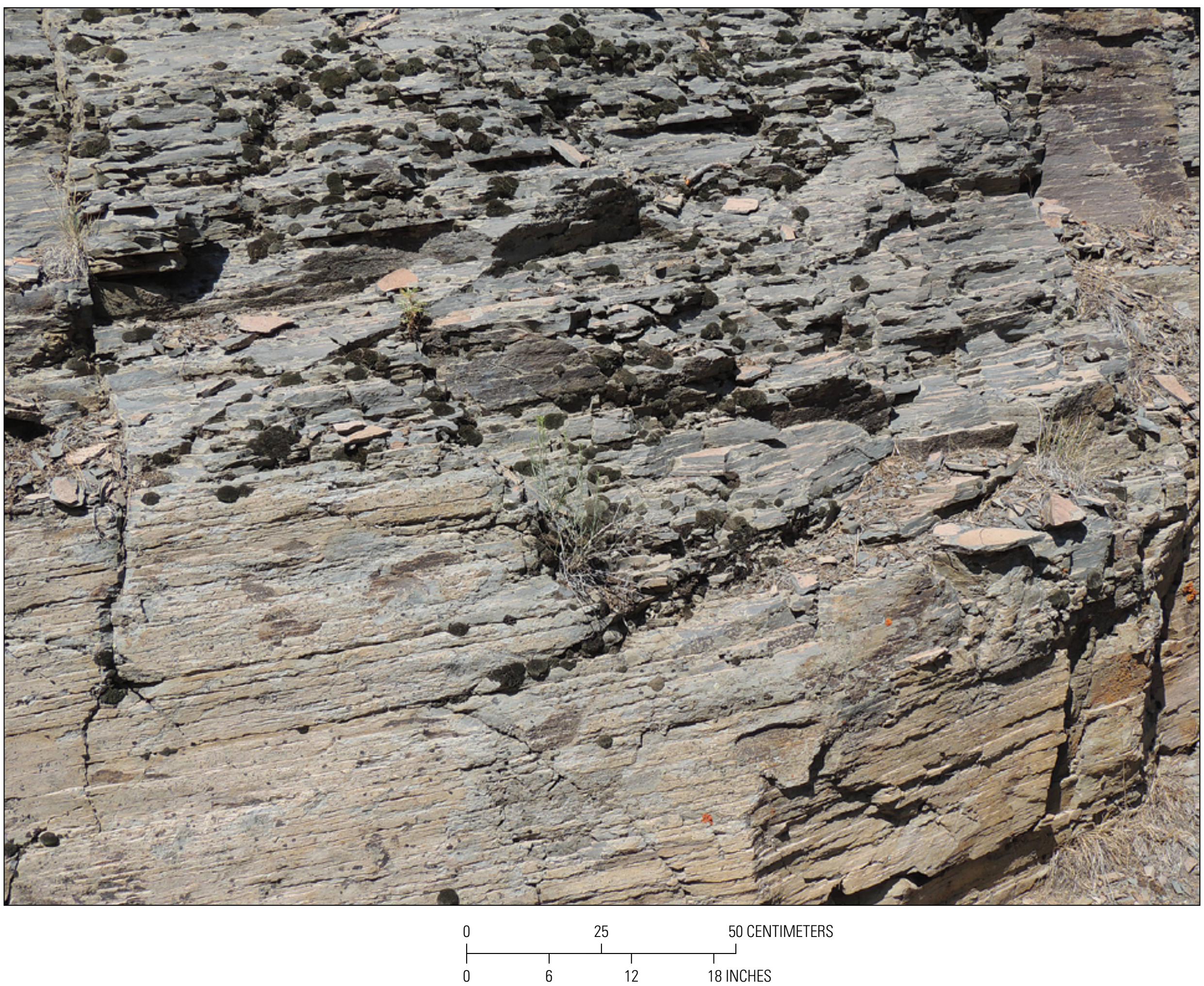

Figure 29. Photograph looking north from Optional Stop showing platy dacite exposed along U.S. Forest Service Road 15, just north of the intersection with U.S. Forest Service Road 17. The dacite here typifies the Strawberry Volcanics. The vertical dimension of the picture is approximately 1.5 meters. Photograph by Martin Streck.

stratigraphic relationships amongst units mapped here as part of the Strawberry volcanic field have not yet been fully established, but the basal unit appears to be cooling unit 1 of the Dinner Creek Tuff and possibly intercalated rhyolite lava flows. This basal silicic sequence is overlain by main sequence Strawberry volcanic field intermediate lava flows, that are in turn overlain by more mafic pyroclastic and air-fall deposits possibly related to cooling unit 4 of the Dinner Creek. **Continue on U.S. Forest Service Road 17.**

144.0 (231.7) A plagioclase-phyric, calc-alkaline andesite flow can be seen to left (south) side of the road.

144.5 (232.6) Float of the 7.1 Ma Rattlesnake Tuff can be seen along the roadside. The Rattlesnake Tuff is the youngest of the large ignimbrites that erupted from near the town of Burns (Streck and Grunder, 1995). Underlying tuffaceous sediments are reworked rhyolitic pyroclastics derived from rhyolites of the Strawberry volcanic field.

144.9 (233.2) Dacite and andesite flows with intercalated tuffaceous sediments are present along both sides of the road.

145.5 (234.2) A tilted section of Devine Canyon Ash-Flow Tuff is visible to the left (southeast).

145.7 (234.5) Strawberry volcanic field andesite flows are located to the right (north).

148.7 (239.3) **Stop 3.7.** Pull off and park along the right side of U.S. Forest Service Road 17.

Stop 3.7. Basal Rhyolite Sequence of the Strawberry Volcanic Field (lat 44.0132° N., long 118.7819° W.)

Streck and Steiner (2013a) define the base of the Strawberry volcanic field in the south to be the series of rhyolite lava flows and breccias that likely overlie cooling unit 1 of the Dinner Creek Tuff. Tuffs and ash-flow tuffs that correspond to the various cooling units of the Dinner Creek were first used by Pardee and Hewitt (1914) and Pardee and others (1941) as stratigraphic markers to distinguish between younger (Strawberry Volcanics) and older mafic lava flows. The rhyolitic pyroclastic flow and underlying reworked block-and-ash flow deposit (exposed here at Stop 3.7) is considered to be in the lower part of the Strawberry volcanic field. Charcoal chips can be identified in the non-welded pyroclastic flow here at Stop 3.7.

Continue on U.S. Forest Service Road 17.

Cumulative Mileage
mi (km)

149.5 (240.6) Basal vitrophyre of cooling unit 1 of the Dinner Creek Tuff. Without geochemical and thin section analyses, it is sometimes difficult to distinguish between devitrified Strawberry rhyolites and devitrified Dinner Creek cooling units. Correlation of exposed tuff (sample MS-15-38, fig. 30, table 8) with cooling unit 1 is established by geochemical data.

151.0 (243.0) Mafic scoria.

152.0 (244.6) Devitrified Dinner Creek Tuff.

152.5 (245.4) **Stop 3.8.** Pull off and park along the right side of U.S. Forest Service Road 17.

Stop 3.8. Dinner Creek Tuff (lat 44.0092° N., long 118.8238° W.)

Hand samples of Dinner Creek Tuff cooling units 1, 2, and 3 strongly resemble one another, and when devitrified appear nearly identical to hand samples of devitrified rhyolite lava flows considered to be part of the lower Strawberry Volcanics. The base of the cooling unit here is the bottom of the section and is defined by a vitrophyre that indicates a high degree of welding. The strongly welded zone grades upward from a more poorly welded tuff to a non-welded tuff. The presence of large, dark-colored, scoriaceous pumic fragments (up to 30–40 centimeters (cm)) and obsidian lithic fragments (up to 15 cm) suggest close proximity to the Dinner Creek vent. Trace element geochemistry implies a correlation with cooling unit 2 of the Dinner Creek Tuff (figs. 22*B* and 30; table 8). Dark-colored pumices are iron-rich, low silica rhyolite with 70.4 wt. percent SiO_2 and 5.2 wt. percent FeO* (table 8).

Continue on U.S. Forest Service Road 17.

Cumulative Mileage
mi (km)

153.0 (246.2) **Stop 3.9.** Pull off and park along the right side of U.S. Forest Service Road 17.

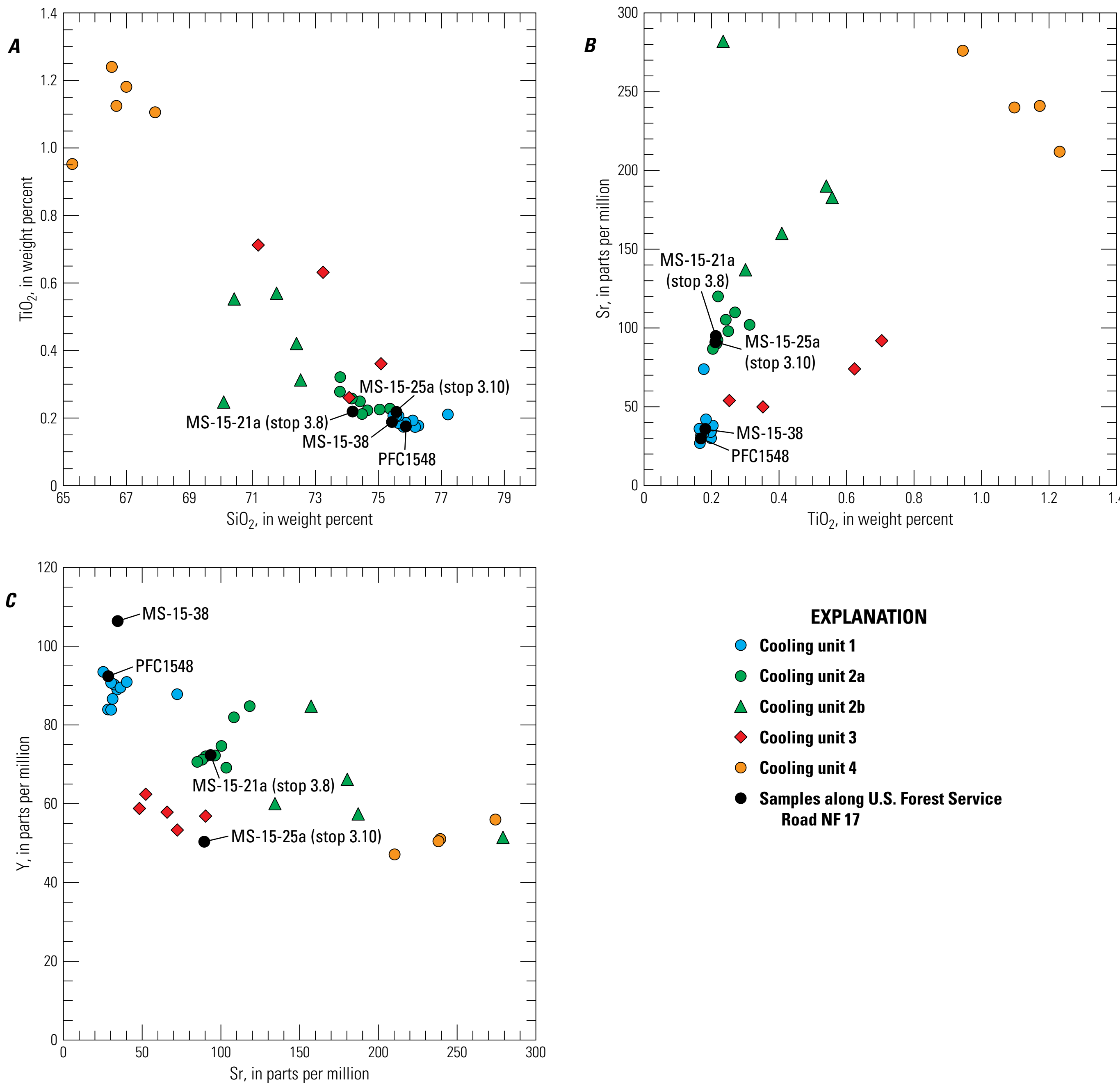

Figure 30. Trace element geochemistry plots of Dinner Creek Tuff along U.S. Forest Service Road 17 relative to data of Streck and others (2015). *A*, SiO_2 vs. TiO_2. *B*, TiO_2 vs. strontium (Sr). *C*, Sr vs. yttrium (Y). The sample identification numbers (this report) are for Dinner Creek Tuffs along U.S. Forest Service Road 17 (black filled circles). Sample data are located in table 8. Samples location coordinates: MS-15-38 (lat 44.01055° N., long 118.7819° W.); PFC1548 (lat 44.0068° N., long 118.8324° W.).

Table 8. Major and trace element analyses and sample location for Strawberry Volcanics, Dinner Creek Tuff, and icelandite lavas along U.S. Forest Service Road 17.

[Major elements have been normalized to a 100 percent total on a volatile-free basis and recalculated as oxides, with total iron expressed as FeO*. Location of sample "MS-15-37" was at field-trip cumulative mileage 149.5 miles (240.6 kilometers) and the location of sample "PFC1548" was along road 17. Abbreviations: ID, identification number; Ma, mega-annum (million years before present); na, not applicable; nd, no data or not analyzed; WSU, Washington State University]

Formation or lava type	Strawberry Volcanics		Dinner Creek Tuff					Icelandite	
Unit	na	na	Cooling unit 1 (~16.1 Ma)		Cooling unit 2 (~15.5 Ma)			Unit 1	Unit 3
Stage	5	5	3	3	3	3	3	2	2
Field-trip stop or location	Optional	Sidetrip along road NF 1705	3.7–3.8	After 3.9	3.8	3.8	3.10	3.9	3.9
Material	Bulk rock	Bulk rock	Bulk rock	Bulk rock	Bulk rock	Scoria	Bulk rock	Scoria	Scoria
Field sample ID	MS-15-17	MS-15-37	MS-15-38	PFC1548	MS-15-21a	MS-15-21b	MS-15-25a	MS-15-23a	MS-15-23c
Latitude (north)	44.0082	43.9650	44.0106	44.0068	44.0092	44.0092	44.0049	44.0086	44.0086
Longitude (west)	118.6989	118.8352	118.7819	118.8324	118.8238	118.8238	118.8377	118.8280	118.8280
Major elements as oxides, in weight percent									
SiO_2	68.64	60.25	75.46	75.90	74.21	70.42	75.60	59.59	57.91
Al_2O_3	15.22	16.43	12.68	12.34	12.88	13.54	13.30	15.30	16.09
TiO_2	0.63	0.91	0.18	0.17	0.22	0.53	0.21	1.86	1.84
FeO*	4.05	6.75	2.45	2.14	0.06	5.18	1.55	8.92	9.36
MnO	0.15	0.12	0.06	0.06	0.94	0.12	0.02	0.18	0.19
CaO	3.07	6.43	0.66	0.54	0.94	1.92	0.44	5.38	5.77
MgO	0.87	3.10	0.15	0.05	0.07	0.29	0.09	1.79	1.51
K_2O	2.95	1.73	5.85	5.96	5.96	3.96	4.06	3.87	4.32
Na_2O	4.26	3.96	2.50	2.82	2.96	3.90	4.72	5.38	5.77
P_2O_5	0.16	0.12	0.02	0.01	0.01	0.14	0.02	1.12	1.40
Trace elements, in parts per million									
Ni	3	8	2	1	4	3	2	5	8
Cr	4	11	1	4	1	15	2	1	nd
Sc	9	18	4	4	2	12	3	23	24
V	56	181	6	5	2	12	6	114	66
Ba	1,170	818	1,372	1,445	1,567	1,416	1,665	1,005	1,106
Rb	64	32	91	82	84	71	73	45	12
Sr	274	448	35	29	94	168	90	407	411
Zr	219	164	449	442	392	351	423	196	208
Y	26	24	106	92	72	67	50	43	52
Nb	10.9	7.6	24.4	23.9	21.3	20.5	23.1	13.4	15.2
Ga	16	18	21	21	22	21	23	19	20
Cu	8	25	4	3	3	6	2	8	10
Zn	62	86	169	151	137	159	113	124	123
Pb	11	8	18	20	16	14	15	6	7
La	27	18	56	48	41	36	31	27	31
Ce	49	45	99	93	89	83	64	61	67
Th	5	4	7	8	8	7	8	4	4
Laboratory	WSU	WSU	WSU	WSU	WSU	WSU	WSU	WSU	WSU

Stop 3.9. Mafic Pyroclastic Flow and Scoria Fall Deposits (lat 44.0086° N., long 118.8280° W.)

The outcrops here are interpreted to be made up of near-vent mafic pyroclastic flow deposits, followed by deposits from typically strombolian activity (fig. 31). The dark scoria throughout the entire outcrop are icelandites that are compositionally nearly indistinguishable.

Outcrops can be divided into three main units: (1) The lowest (oldest) deposit (unit 1 and 1b in fig. 31), is a poorly sorted lithic tuff that contains small, light-colored juvenile pumices, large juvenile scoria, and lithic clasts that include obsidian and vitrophyre that are likely derived from local rhyolite lavas and from vitrophyres of welded tuffs. Rhyolite(?) pumices and icelandite lapilli and bombs indicate co-eruption of silicic and intermediate magmas. (2) The middle deposit (unit 2 in fig. 31) is a poorly sorted, clast-supported tuff that lacks light colored rhyolite pumice. Deposition is likely from a pyroclastic flow, but less fragmentation suggests less explosivity and therefore less energetic emplacement. The outcrops of units 1 and 2 appear to record a transition upward from more matrix-rich to less matrix-rich deposits. (3) The upper (youngest) deposit (unit 3 in fig. 31) is a classical near-source strombolian fallout deposit with some lithic fragments. Compositionally, this unit deviates only slightly from units 1 and 2 that lie below it; for example higher P_2O_5. Here at Stop 3.9, the mafic pyroclastic flows may represent an eruptive phase that followed the eruption of cooling unit 4 of the Dinner Creek Tuff at ~15 Ma. This abundant intermediate to mafic juvenile component (compositionally similar to the icelanditic composition of scoria clasts) is a distinctive feature of cooling unit 4 of the Dinner Creek Tuff of Streck and others (2015).

Cumulative Mileage mi (km)

153.1 (246.4) Intersection with U.S. Forest Service Road 1705 (optional side trip). The unimproved road leading to the south will take you to a platy andesite flow located at “lat 43.9650° N., long 118.8352° W” along U.S. Forest Service Road 2860. The exposed lava flows are more examples of intermediate lava flows of the Strawberry Volcanics. The composition of the Strawberry Volcanics lava flow here from field sample identification (ID) number MS-15-37 is approximately 60 wt. percent SiO_2 and 6.8 wt. percent FeO* (table 8). **Continue on U.S. Forest Service Road 17.**

154.0 (247.8) **Stop 3.10.** Pull off and park along the right side of U.S. Forest Service Road 17.

Stop 3.10. Cooling Unit 2 of the Dinner Creek Tuff (lat 44.0049° N., long 118.8377° W.)

Two ledges of devitrified Dinner Creek Tuff are exposed along the road here.

Cumulative Mileage mi (km)

154.2 (248.2) An outcrop of vertically flow-banded rhyolite lava is exposed along the right (north) side of the road. The outcrop is part of the rhyolite

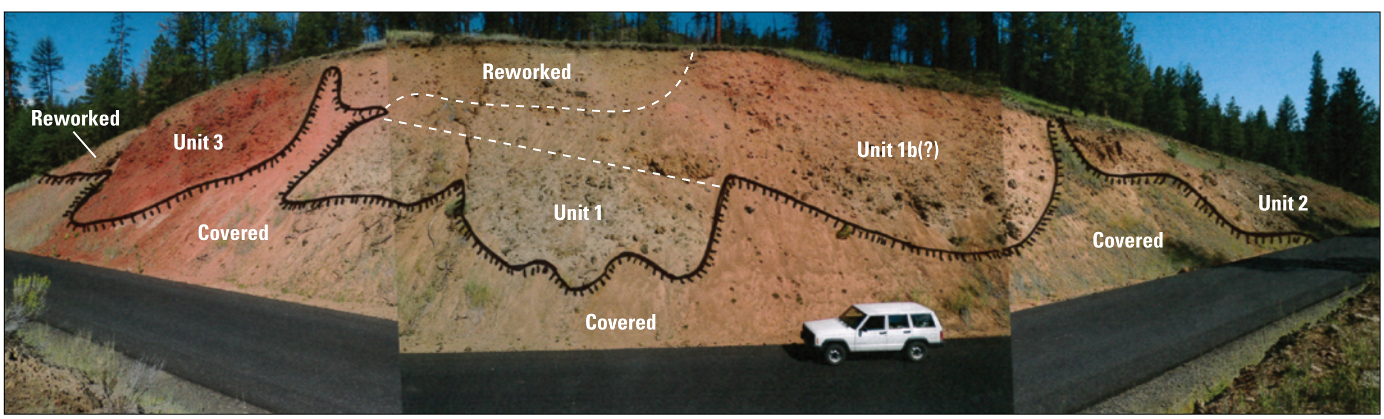

Figure 31. Photograph looking north from Stop 3.9 of mafic pyroclastic flow (units 1, 1b, and 2) and scoria fall deposits (unit 3). “Covered” means talus conceals outcrop; the black line is the upper extent of talus. “Reworked” means the unit is slightly modified from subsequent processes. The dashed white line is the presumed contact between units. Unit “1b” is uncertain (?). Photograph by Martin Streck.

sequence at the base of the Strawberry volcanic field.

154.5 (248.6) U.S. Forest Service Road 56 leads north to an outcrop of a biotite-phyric rhyolite in the base of the Strawberry Volcanics located at lat 44.0133° N., long 118.8410° W.

156 (251.1) Devine Canyon Tuff.

159.5 (256.7) Turn right onto U.S. 395 and proceed north toward the City of John Day.

167.0 (268.8) Basement rocks of fine-grained, Mesozoic, fore-arc basin sedimentary rocks to the right.

168.0 (270.4) A sill of porphyritic basalt is located on the right.

170.0 (273.6) Town of Seneca. The high peak on the skyline to the right (northeast) is Strawberry Mountain, the type locality for the Strawberry volcanic field.

176.7 (284.4) Outcrops of the 7.1 Ma Rattlesnake tuff and the 9.7 Ma Devine Canyon Tuff are on both sides of U.S. 395.

179.0 (288.1) U.S. 395 begins its descent into Canyon Creek, cutting through a section of pre-Tertiary, basement fore-arc sedimentary rocks of the Izee terrane. The sedimentary rocks are unconformable and in fault contact with ophiolitic rocks of the Baker terrane. The skyline to northeast is formed by the Canyon Mountain Complex, which is a classical alpine ophiolite with peridotite, gabbro, and sheeted dike complexes.

187.8 (302.2) Canyon Mountain Complex pyroxenites are located on the right.

190.0 (305.8) Canyon Mountain Complex gabbros are located on the right.

190.4 (306.4) Serpentinte-matrix mélange exposed on both sides of the highway.

191.2 (307.7) U.S. 395 crosses the John Day Fault and enters the John Day Valley.

193.2 (310.9) Outcrops of Picture Gorge Basalt are located on the right.

194.0 (312.2) Intersection of U.S. 395 and U.S. 26 in the town of John Day.
End Day 3.

Day 4. Picture Gorge Basalt, Southern Columbia River Basalt Group, Monument Dike Swarm, and John Day Fossil Beds

The return route to Portland on Day 4 traverses across the western axis of the Blue Mountains, highlighting exposures of the widespread, middle Miocene Dinner Creek Tuff and aspects of Picture Gorge Basalt flows and associated northwest-trending feeder dikes situated in the central part of the CRBG province.

Road Log
Cumulative Mileage
mi (km)

0.0 (0.0) The road log for Day 4 begins at the intersection of U.S. 395 and U.S.26 in the town of John Day. Proceed east on U.S. 26 through the city of John Day toward Baker City.

5.0 (8.0) “Southern” CRBG facies are exposed on the north. Here, the light-colored, ledge-forming rocks to the left are Dinner Creek Tuff, which are overlain by olivine basalt flows.

8.2 (13.2) **Stop 4.1.** Pull off and park along the right side of U.S. 26.

Stop 4.1. “Marginal Facies” of the Columbia River Basalt Group (lat 44.4325° N., long 118.8371° W.)

Rocks here are part of what was initially mapped as “marginal facies” of the Columbia River Basalt by Brown and Thayer (1967) before the formal CRBG flow stratigraphy was developed. Here, olivine basalt flows overlie cooling unit 2 of the Dinner Creek Tuff. Lava Flows correlative with the Picture Gorge Basalt are believed to underlie cooling unit 2 of the Dinner Creek.

Reverse course and return west 8.2 mi (13.2 km) on U.S. 26 through John Day and continue to Mount Vernon.

Cumulative Mileage mi (km)

14.0 (22.5)	A thick, dipping section of cooling unit 2 of the Dinner Creek Tuff crops out on the hillside north of the City of John Day.
15.5 (24.9)	The Rattlesnake Tuff is exposed in the low hill to the left (south), interbedded with coarse gravels.
20.5 (33.0)	Town of Mount Vernon. Continue west on U.S. 26 at the intersection with U.S. 395.
28.9 (46.5)	U.S. 26. A steeply dipping section of Picture Gorge Basalt flows is on the left (south).
30.3 (40.8)	Fields Creek. Deformed late Miocene sedimentary rocks to the left are cut by strands of the John Day Fault.
35.5 (57.1)	Picture Gorge Basalt on both sides of the highway.
43.5 (70.0)	Town of Dayville. The rimrock on the north side of the valley is Rattlesnake Tuff.
47.6 (76.6)	Turn left onto Grant County Road 40 and follow the signs to the Mascall Overlook.
48.0 (77.2)	Turn right onto the access road for the Mascall Overlook and proceed to the parking area.
48.4 (77.9)	**Stop 4.2.** Arrive at the parking area for the Mascall Overlook (Mascall Formation Overlook). Walk a short distance north to the overlook. Restrooms are available.

Stop 4.2. Mascall Formation Overlook (lat 44.5004° N., long 119.6221° W.)

The Picture Gorge Basalt is one of the main formations in the CRBG (fig. 3). Picture Gorge flows are confined to the region south of the Blue Mountain uplift and were fed by the Monument dike swarm (fig. 2). The youngest flows are considered to be age equivalent to R2 Grande Ronde Basalt flows (Bailey, 1989) (fig. 3). Here at Stop 4.2, the Picture Gorge Basalt is overlain by tuffaceous sedimentary rocks of the middle Miocene Mascall Formation, which includes rhyolitic units of the Dinner Creek Tuff (Streck and others, 2015) (fig. 32). The section is in turn overlain with an angular unconformity and the 7.1-Ma Rattlesnake Tuff, which dips approximately 5 degrees in a southerly direction.

Reverse course and return west 0.8 mi (1.3 km) to U.S. 26.

Cumulative Mileage mi (km)

49.1 (79.0)	Turn right onto U.S. 26 and proceed west into Picture gorge.
51.4 (82.7)	Picture gorge. This is the type locality for the Picture Gorge Basalt (fig. 3).
52.1 (83.8)	Turn right onto O.R. 19 and proceed north down the John Day River, through the Sheep Rock unit of the John Day fossil beds.
54.2 (87.2)	**Stop 4.3.** Turn left into the parking area for the Thomas Condon Paleontology Center at the Sheep Rock unit of the John Day Fossil Beds National Monument. Restrooms are available.

Stop 4.3. Thomas Condon Paleontology Center, Sheep Rock Unit of the John Day Fossil Beds National Monument (lat 44.5525° N., long 119.6461° W.)

The Thomas Condon Paleontology Center in the Sheep Rock unit of the John Day Fossil Beds National Monument features exhibits that showcase some of the spectacular paleontological specimens that have been recovered from the Eocene-Oligocene John Day Formation. A short hike up the trail that begins near the south end of the parking area ascends to an overlook of Sheep Rock and the John Day River. Sheep Rock is formed from a well-exposed section of the Turtle Cove Member of the John Day Formation, which here consists of an assemblage of blue-green and tan, variably zeolitized siltstones, paleosols, and interbedded tuffs (Bestland, 1995). The Picture gorge ignimbrite (“member H tuff”) forms a prominent marker bed at the midpoint of the stratigraphic section (Bestland, 1995). The section at Sheep Rock is capped by a remnant of middle Miocene Picture Gorge Basalt. There is some speculation that the older John Day rhyolites and basalts record an earlier phase of Yellowstone plume-related volcanic activity (Seligman and others, 2014; Wells and others, 2014).

Return to O.R. 19. Turn left and proceed north.

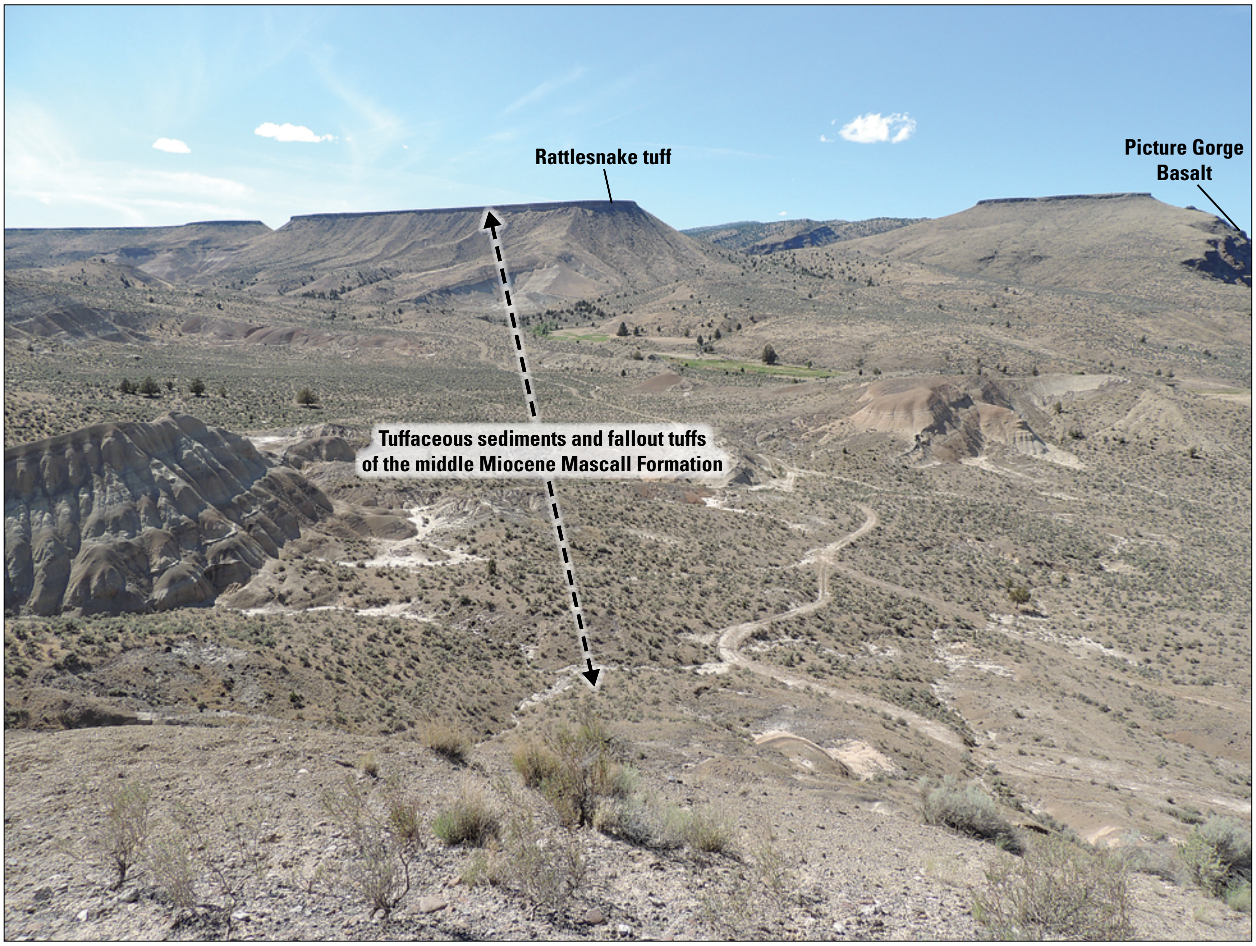

Figure 32. Photograph looking west-northwest from Stop 4.2, at the Mascall overlook, showing a tilted section of the middle Miocene Mascall Formation that overlies the Picture Gorge Basalt. The Mascall Formation section includes one rhyolitic unit of the Dinner Creek Tuff. The section is unconformably overlain by the cap-forming, 7.1-Ma Rattlesnake Tuff. Abbreviation: Ma, mega-annum (million years before present). Photograph by Martin Streck.

Cumulative Mileage
mi (km)

55.7 (89.6)	Outcrops of Cretaceous marine sedimentary rocks to the left.
71.7 (115.4)	Stop 4.4. Pull off and park on the roadside of O.R. 19.

Stop 4.4. Monument Dike Swarm (lat 44.7447° N., long 119.6440° W.)

A feeder dike to the Picture Gorge Basalt (fig. 2) is exposed here on the northwest edge of the Monument dike swarm. The Monument Dike Swarm occupies a northwest trending zone 15 mi (24.1 km) wide that extends more than 50 mi (80.1 km). Dikes within the swarm generally trend N 30° W to N 40° W.

Continue north on O.R. 19.

Cumulative Mileage
mi (km)

73.4 (118.1)	Bear to the left on O.R. 19 at the town of Kimberly.
74.5 (119.9)	A dike of the Picture Gorge Basalt, west of the town of Kimberly, is located on the right (north).
83.2 (133.9)	Turn right onto O.R. 207 and proceed north.

90.7 (146.0) A contact between the upper John Day Formation and Picture Gorge Basalt is present along the side of the road.

102.7 (165.3) Picture Gorge Basalt flows are banked up against old volcanic highlands that include rhyolite flows and dome complexes. The volcanic highlands to the right includes This is also a precious opal locality at Opal Butte.

109.7 (176.5) R2 Grande Ronde Basalt flows on both sides of the highway.

111.4 (179.3) N2 Grande Ronde Basalt flows on both sides of the highway.

115.7 (186.2) Town of Hardman.

124.3 (200.0) Intersection of O.R. 207 and O.R. 206, continue into the town of Ruggs.

124.5 (200.4) Turn left on Rhea Creek Road and proceed toward the town of Ione.

142.9 (230.0) Turn left onto O.R. 74, east of Ione.

173.5 (279.2) Intersection of O.R. 74 and I–84 (Exit 147). Merge onto I–84 westbound and proceed 147 mi (236.5 km) west back to Portland.

320.5 (515.8) End of I–84 in Portland. **End of Day 4. End of field trip.**

Acknowledgments

The authors would like to thank Brett Rudd, staff of the Oregon Water Resources Department, and the drill crew from Boart Longyear for supplying the many well cuttings obtained from the "UNIO 52415 (Rudd)" water well. The collaboration of Dr. Jay Van Tassell and students in identifying the stratigraphy from well cuttings is deeply appreciated. New research during the development of this field-trip guidebook was in part supported by the National Science Foundation grants EAR–1220676 and EAR–1551495 to Streck.. We would also like to thank Bill Bonnichsen and Steve Self for their constructive reviews that significantly helped to improve this U.S. Geological Survey publication.

References Cited

Anderson, J.L., 1987, The structure and ages of deformation of a portion of the southwest Columbia Plateau, Washington and Oregon: Los Angeles, Calif., University of Southern California, Ph.D. dissertation, 272 p.

Anderson, J.L., and Tolan, T.L., 1986, Ages of wrench faulting in interridge basins, southwest Columbia Plateau, Washington and Oregon [abs.]: Geological Society of America Abstracts with Programs, v. 18, no. 2, p. 82.

Anderson, J.L., Tolan, T.L., and Wells., R.E., 2013, Strike-slip faults in the western Columbia River flood basalt province, Oregon and Washington, *in* Reidel, S.P., Camp, V., Ross, M.E., Wolff, J.A., Martin, B.E., Tolan, T.L., and Wells, R.E., eds., The Columbia River flood basalt province: Geological Society of America Special Paper 497, p. 325–347. [Also available at http://dx.doi.org/10.1130/2013.2497(13).]

Anderson, J.L., and Vogt, B.F., 1987, Intracanyon flows of the Columbia River Basalt Group in the southwestern part of the Columbia Plateau and adjacent Cascade Range, Oregon and Washington, *in* Schuster, J.E., ed., Selected papers on the geology of Washington: Washington Department of Natural Resources, Division of Geology and Earth Resources Bulletin 77, p. 249–267.

Armstrong, R.E., Harakal, J.E., and Neil, W.M., 1980, K-Ar dating of Snake River plain (Idaho) volcanic rocks–New results: Isochron/West, v. 27, p. 5–10.

Aseto, C.O., 2012, Geology, geochemistry and geochronolgy of the mid-Miocene, low-sulfidation epithermal gold-silver ores on War Eagle Mountain, Silver City District, Idaho: Auburn, Ala., Auburn University, M.S. thesis, 170 p.

Bailey, D.G., 1990, Geochemistry and petrogenesis of Miocene volcanic rocks in the Powder River volcanic field, northeastern Oregon: Pullman, Wash., Washington State University, Ph.D. dissertation, 341 p.

Bailey, M.M., 1989, Revisions to stratigraphic nomenclature of the Picture Gorge Basalt Subgroup, Columbia River Basalt Group, *in* Reidel, S.P., and Hooper, P.R., eds., Volcanism and tectonism in the Columbia River flood-basalt province: Geological Society of America Special Paper 239, p. 67–84.

Barry, T.L., Kelley, S.P., Reidel, S.P., Camp, V.E., Self, S., Jarboe, N.A., Duncan, R.A., and Renne, P.R., 2013, Eruption chronology of the Columbia River Basalt Group, *in* Reidel, S.P., Camp, V.E., Ross, M.E., Wolff, J.A., Martin, B.S., Tolan, T.L., and Wells, R.E., eds., The Columbia River flood basalt province: Geological Society of America Special Paper 497, p. 45–66. [Also available at http://dx.doi.org/10.1130/2013.2497(02).]

Beeson, M.H., Fecht, K.R., Reidel, S.P., and Tolan, T.L., 1985, Regional correlations within the Frenchman Springs Member of the Columbia River Basalt Group—New insights into the middle Miocene tectonics of northwest Oregon: Oregon Geology, v. 47, no. 8, p. 87–96.

Beeson, M.H., Perttu, R., and Perttu, J., 1979, The origin of the Miocene basalt of coastal Oregon and Washington—An alternative hypothesis: Oregon Geology, v. 41, no. 10, p. 159–166.

Beeson, M.H., and Tolan, T.L., 1990, The Columbia River Basalt Group in the Cascade Range—A middle Miocene reference datum for structural analysis: Journal of Geophysical Research, v. 95, no. B12, p. 19,547–19,559.

Beeson, M.H., Tolan, T,L., and Anderson, J.L., 1989, The Columbia River Basalt Group in western Oregon—Geologic structures and other factors that controlled flow emplacement patterns, *in* Reidel, S.P., and Hooper, P.R., eds., Volcanism and tectonism in the Columbia River flood-basalt province: Geological Society of America Special Paper 239, p. 223–246.

Benson, T.R., and Mahood, G.A., 2016, Geology of the mid-Miocene Rooster Comb caldera and Lake Owyhee volcanic field, eastern Oregon—Silicic volcanism associated with Grande Ronde flood basalt: Journal of Volcanology and Geothermal Research, v. 309, p. 96–117.

Betsland, E.A., 1995, Stratigraphy of the Turtle Cove Member of the John Day Formation at Sheep Rock: U.S. National Park Service Open-File Report, 14 p.

Binger, G.B., 1997, The volcanic stratigraphy of the Juntura region, eastern Oregon: Pullman, Wash., Washington State University, M.S. thesis, 206 p.

Bishop, E.M., 1995, Mafic and ultramafic rocks of the Baker terrane, eastern Oregon, and their implications for terrane origin, *in* Vallier, T.L., and Brooks, H.C., eds., Geology of the Blue Mountains region of Oregon, Idaho, and Washington—Petrology and tectonic evolution of pre-Tertiary rocks of the Blue Mountains region: U.S. Geological Survey Professional Paper 1438, p. 221–246. [Also available at https://pubs.er.usgs.gov/publication/pp1438.]

Bonnichsen, B., 1982, Rhyolite lava flows in the Bruneau-Jarbidge eruptive center, southwestern Idaho, in Bonnichsen, B., and Breckenridge, R.M., eds., Cenozoic geology of Idaho: Idaho Bureau of Mines and Geology Bulletin 26, p. 283–320.

Bonnichsen, B., and Godchaux, M.M., 2002, Late Miocene, Pliocene, and Pleistocene geology of southwestern Idaho with emphasis on basalts in the Bruneau-Jarbidge, Twin Falls, and Western Snake River Plain regions, *in* Bonnichsen, B., White, C.M., and McCurry, M., eds., Tectonic and magmatic evolution of the Snake River plain volcanic province: Idaho Geological Survey Bulletin 30, p. 233–312.

Bonnichsen, B., and Kaufman, D.F., 1987, Physical features of rhyolite lava flows in the Snake River plain volcanic province, southwestern Idaho, *in* Fink, J.D., ed., The emplacement of silicic domes and lava flows: Geological Society of America Special Paper 212, p. 119–145.

Bonnichsen, B., McCurry, M., and Godchaux, M.M., 2004, Miocene Snake River plain rhyolites of the Owyhee front, Owyhee County, Idaho, *in* Haller, K.M., and Wood, S.H., eds., Geological field trips in southern Idaho, eastern Oregon, and northern Nevada: U.S. Geological Survey Open-File Report 2004–1222, p. 157–175. [Also available at http://pubs.usgs.gov/of/2004/1222/.]

Brandon, A.D., and Goles, G.G., 1988, A Miocene subcontinental plume in the Pacific Northwest—Geochemical evidence: Earth and Planetary Science Letters, v. 88, nos. 3–4, p. 273–283. [Also available at http://dx.doi.org/10.1016/0012-821X(88)90084-2.]

Brandon, A.D., and Goles, G.G., 1995, Assessing subcontinental lithospheric mantle sources for basalts—Neogene volcanism in the Pacific Northwest, USA, as a test case: Contributions to Mineralogy and Petrology, v. 121, no. 4, p. 364–379. [Also availableat http://dx.doi.org/10.1007/s004100050102.]

Branney, M.J., Bonnichsen, B., Andrews, G.D.M., Ellis, B., Barry, T.L., and McCurry, M., 2008, “Snake River (SR)-type” volcanism at the Yellowstone hotspot track—Distinctive products from unusual high-temperature silicic super-eruptions: Bulletin of Volcanology, v. 70, no. 3, p. 293–314, accessed at http://dx.doi.org/10.1007/s00445-007-0140-7.

Brooks, H.C., 1979, Geologic map of the Huntington and part of the Olds Ferry quadrangles, Baker and Malheur Counties, Oregon: Oregon Department of Geology and Mineral Industries Geologic Map Series GMS–13, 11-p. text, 1 sheet, scale 1:62,500.

Brooks, H.C., 2006, Preliminary geologic and mineral resources map of the Mormon basin quadrangle, Baker and Malheur Counties, Oregon: Oregon Department of Geology and Mineral Industries Open-File O–06–25, scale 1:24,000.

Brooks, H.C., and O’Brien, J.P., 1992a, Geology and mineral resources map of the Westfall quadrangle, Malheur County, Oregon: Oregon Department of Geology and Mineral Industries Geological Map Series GMS–71, scale 1:24,000.

Brooks, H.C., and O’Brien, J.P., 1992b, Geology and mineral resources map of the Little Valley quadrangle, Malheur County, Oregon: Oregon Department of Geology and Mineral Industries Geological Map Series GMS–72, scale 1:24,000.

Brown, C.E., and Thayer, T.P., 1967, Geologic map of the Canyon City quadrangle, northeastern Oregon: U.S. Geological Survey Miscellaneous Geologic Investigations Map I–447, scale 1:250,000.

Brown, D.E., and Petros, J.R., 1985, Geochemistry, geochronology, and magnetostratigraphy of a measured section of the Owhyee Basalt, Malheur County: Oregon Geology, v. 47, no. 2, p. 15–20.

Bryan, K., 1929, Geology of reservoir and dam sites, with a report on of the Owyhee irrigation project, Oregon: U.S. Geological Survey Water Supply Paper 597–A, 72 p.

Bunker, R.C., Farooquiel, S.M., and Thoms, R.E., 1982, K/Ar dates for volcanic rocks associated with Neogene sedimentary deposits in north-central and northeastern Oregon: Isochron/West, no. 33, p. 21–22.

Camp, V.E., 1995, Mid-Miocene propagation of the Yellowstone mantle plume head beneath the Columbia River Basalt source region: Geology, v. 23, no. 5, p. 435–438. [Also available at http://geology.gsapubs.org/content/23/5/435.full.pdf+html.]

Camp, V.E., 2013, Origin of the Columbia River Basalt–Passive rise of shallow mantle or active upwelling of a deep mantle plume?, *in* Reidel, S.P., Camp, V.E., Ross, M.E., Wolff, J.A., Martin, B.S., Tolan, T.L., and Wells, R.E., eds., The Columbia River flood basalt province: Geological Society of America Special Paper 497, p. 181–199. [Also available at http://dx.doi.org/10.1130/2013.2497(07).]

Camp, V.E., and Hanan, B.B., 2008, A plume-triggered delamination origin for the Columbia River Basalt Group: Geosphere, v. 4, no. 3, p. 480–495, accessed at http://dx.doi.org/10.1130/GES00175.1.

Camp, V.E., and Ross, M.E., 2004, Mantle dynamics and genesis of mafic magmatism in the intermontane Pacific Northwest: Journal of Geophysical Research, v. 109, no. B8, accessed at http://dx.doi.org/10.1029/2003JB002838.

Camp, V.E., Ross, M.E., Duncan, R.A., Jarboe, N.A., Coe, R.S., Hanan, B.B., and Johnson, J.A., 2013, The Steens Basalt–Earliest lavas of the Columbia River Basalt Group, *in* Reidel, S.P., Camp, V.E., Ross, M.E., Wolff, J.A., Martin, B.S., Tolan, T.L., and Wells, R.E., eds., The Columbia River flood basalt province: Geological Society of America Special Paper 497, p. 87–116. [Also available at http://dx.doi.org/10.1130/2013.2497(04).]

Camp, V.E., Ross, M.E., and Hanson, W.E., 2003, Genesis of flood basalts and Basin and Range volcanic rocks from Steens Mountain to the Malheur River gorge, Oregon: Geological Society of America Bulletin, v. 115, no. 1, p. 105–128.

Carlson, R.W., and Hart, W.K., 1987, Crustal genesis on the Oregon Plateau: Journal of Geophysical Research, v. 92, no. B7, p. 6,191–6,206. [Also available at http://dx.doi.org/10.1029/JB092iB07p06191.]

Christiansen, R.L., Foulger, G.R., and Evans, J.R., 2002, Upper mantle origin of the Yellowstone hotspot: Geological Society of America Bulletin, v. 114, no. 10, p. 1,245–1,256.

Christiansen, R.L., and Yeats, R.S., 1992, Post-Laramide geology of the U.S. Cordilleran region, *in* Burchfiel, B.C., Lipman, P.W., and Zoback, M.L. eds., The Cordilleran orogen—Conterminous U.S., v. G–3 of The geology of North America: Boulder, Colo., Geological Society of America, p. 261–406.

Coble, M.A., and Mahood, G.A., 2012, Initial impingement of the Yellowstone plume located by widespread silicic volcanism contemporaneous with Columbia River flood basalts: Geology, v. 40, no. 7, p. 655–658. [Also available at http://dx.doi.org/10.1130/G32692.1.]

Colwell, C.R., 2013, Integrated geophysical exploration of a known geothermal resource—Neal Hot Springs: Boise, Idaho, Boise State University, M.S. thesis, 105 p.

Conrey, R.M., Taylor, E.M., Donnelly-Nolan, J.M., and Sherrod, D.R., 2002, North-central Oregon Cascades—Exploring petrologic and tectonic intimacy in a propagating intra-arc rift, in Moore, G.W., ed., Field guide to geologic processes in Cascadia: Oregon Department of Geology and Mineral Industries Special Paper 36, p. 47–90.

Corcoran, R.E., Doak, R.A., Porter, P.W., Pritchett, F.I., and Privrasky, V.C., 1962, Geology of the Mitchell Butte quadrangle, Oregon: Oregon Department of Geology and Mineral Industries Geological Map Series GMS–2, 14-p. text, 1 sheet, scale 1:125,000.

Cummings, M.L., Evans, J.G., Ferns, M.L., and Lees, K.R., 2000, Stratigraphic and structural evolution of the middle Miocene synvolcanic Oregon-Idaho graben: Geological Society of America Bulletin, v. 112, no. 5, p. 668–682. [Also available at http://gsabulletin.gsapubs.org/content/112/5/668.]

Davenport, R,E., 1971, Geology of the Rattlesnake and older ignimbrites in the Paulina Basin and adjacent area, central Oregon: Corvallis, Oreg., Oregon State University, Ph.D. dissertation, 132 p.

Dodson, A., Kennedy, B.M., and DePaolo, D.J., 1997, Helium and neon isotopes in the Imnaha Basalt, Columbia River Basalt Group—Evidence for a Yellowstone plume source: Earth and Planetary Science Letters, v. 150, nos. 3–4, p. 443–451. [Also available at http://dx.doi.org/10.1016/S0012-821X(97)00090-3.]

Downing, K.F., 1992, Biostratigraphy, taphonomy, and paleoecology of vertebrates from the Sucker Creek Formation (Miocene) of southeastern Oregon: Tempe, Ariz., University of Arizona, Ph.D. dissertation, 482 p.

Downing, K.F., and Swisher, C.C.J., 1993, New 40Ar/39Ar dates and refine geochronology of the Sucker Creek Formation, Oregon [abs.]: Journal of Vertebrate Paleontology, v. 13, no. 3, p. 33A.

Draper, D.S., 1991, Late Cenozoic bimodal magmatism in the northern Basin and Range province of southeastern Oregon: Journal of Volcanology and Geothermal Research, v. 47, nos. 3–4, p. 229–328. [Also available at http://dx.doi.org/10.1016/0377-0273(91)90006-L.]

Duncan, R.A., 1982, 40Ar/39Ar dating of Columbia River basalts: Rockwell/Hanford Report M29–SBB–258874, 10 p.

Edwards, J.H., 2013, Structural controls of the Neal Hot Springs geothermal system, eastern Oregon: Reno, Nev., University of Nevada-Reno, M.S. thesis, 83 p.

Ekren, E.B., McIntyre, D.H., Bennett, E.H., and Marvin, R.F., 1982, Cenozoic stratigraphy of Western Owyhee County, Idaho, *in* Bonnichsen, B., and Breckenridge, R.M., eds., Cenozoic geology of Idaho: Idaho Bureau of Mines and Geology Bulletin 26, p. 215–236.

Evans, J.G., 1990a, Geology and mineral resources map of the Jonesboro Quadrangle, Malheur County, Oregon: Oregon Department of Geology and Mineral Industries Geological Map Series GMS–66, scale 1:24,000.

Evans, J.G., 1990b, Geology and mineral resources map of the South Mountain Quadrangle, Malheur County, Oregon: Oregon Department of Geology and Mineral Industries Geologic Map Series GMS–67, scale 1:24,000.

Evans, J.G., 1992, Geologic map of the Dooley Mountain 7 ½’ quadrangle, Baker County, Oregon: U.S. Geological Survey Quadrangle Map GQ–1694, scale 1:24,000. [Also available at https://pubs.er.usgs.gov/publication/gq1694.]

Evans, J.G., 1995, Geologic map of the Brannan Gulch 7 ½’ Quadrangle, Baker County, Oregon: U.S. Geological Survey Geologic Quadrangle Map GQ–1744, scale 1:24,000. [Also available at https://pubs.er.usgs.gov/publication/gq1744.]

Evans, J.G., and Binger, G.B., 1997, Geologic map of the Westfall Butte 7 ½’ Quadrangle, Malheur County, Oregon: U.S. Geological Survey Open-File Report 97–481, 11-p. text, 1 sheet., scale 1:24,000. [Also available at https://pubs.er.usgs.gov/publication/ofr97481.]

Evans, J.G., and Binger, G.B., 1999, Geologic map of the Little Black Canyon quadrangle, Malheur County, Oregon: U.S. Geological Survey Open-File Report 98–493, 12-p. text, 1 sheet, scale 1:24,000. [Also available at https://pubs.er.usgs.gov/publication/ofr98493.]

Evarts, R.C., Conrey, R.M., Fleck, R.J., and Hagstrum, J.T., 2009, The Boring volcanic field of the Portland-Vancouver area, Oregon and Washington—Teconically anomalous forearc volcanism in an urban setting, *in* O’Connor, J.E., Dorsey, R.J, and Madin, I.P., eds., Volcanoes to vineyards—Geologic field trips through the dynamic landscape of the Pacific Northwest: Geological Society of America Field Guide 15, p. 253–270. [Also available at http://dx.doi.org/10.1130/2009.fld015(13).]

Ferns, M.L., 1989a, Geology and mineral resources map of the Graveyard Point quadrangle, Malheur County, Oregon, and Owyhee County, Idaho: Oregon Department of Geology and Mineral Industries Geological Map Series GMS–54, scale 1:24,000.

Ferns, M.L., 1989b, Geology and mineral resources map of the Owyhee Ridge quadrangle, Malheur County, Oregon: Oregon Department of Geology and Mineral Industries Geological Map Series GMS–53, scale 1:24,000.

Ferns, M.L., 1989c, Geology and mineral resources map of the Owyhee Dam quadrangle, Malheur County, Oregon: Oregon Department of Geology and Mineral Industries Geological Map Series GMS–56, scale 1:24,000.

Ferns, M.L., and Brooks, H.C., 1995, The Bourne and Green subterranes of the Baker terrane, northeastern Oregon–Implications for the evolution of the Blue Mountains island-arc system, *in* Vallier, T.L., and Brooks, H.C., eds., Geology of the Blue Mountains region of Oregon, Idaho, and Washington—Petrology and tectonic evolution of pre-tertiary rocks of the Blue Mountains region: U.S. Geological Survey Professional Paper 1438, p. 331–358. [Also available at https://pubs.er.usgs.gov/publication/pp1438.]

Ferns, M.L., Brooks, H.C., Evans, J.C., and Cummings., M.L., 1993a, Geologic map of the Vale 30 x 60 minute quadrangle, Malheur County, Oregon: Oregon Department of Geology and Mineral Industries Geological Map Series GMS–77, 12-p. text, 1 sheet, scale 1:100,000.

Ferns, M.L., and Cummings, M.L., 1992, Geology and mineral resources map of the Elbow quadrangle, Malheur County, Oregon: Oregon Department of Geology and Mineral Industries Geological Map Series GMS–62, scale 1:24,000.

Ferns, M.L., Evans, J.C., and Cummings, M.L., 1993b, Geologic map of the Mahogany Mountain 30' x 60' quadrangle, Malheur County, Oregon: Oregon Department of Geology and Mineral Industries Geological Map Series GMS–78, 12-p. text, 1 sheet, scale 1:100,000.

Ferns, M.L., and Madin, I.P., 1999, Geology of the Summerville quadrangle, Union County, Oregon: Oregon Department of Geology and Mineral Industries Geological Map Series GMS–111, 23-p. text, 1 sheet, scale 1:24,000.

Ferns, M.L., Madin, I.P., and Taubeneck, W.H., 2001, Reconnaissance geologic map of the La Grande 30′ x 60′ quadrangle, Baker, Grant, Umatilla, and Union Counties, Oregon: Oregon Department of Geology and Mineral Industries Reconnaissance Map Series RMS–1, 52-p. text, 1 sheet, scale 1:100,000.

Ferns, M.L., and McClaughry, J.D., 2013, Stratigraphy and volcanic evolution of the middle Miocene to Pliocene La Grande-Owyhee eruptive axis in eastern Oregon, *in* Reidel, S.P., Camp, V.E., Ross, M.E., Wolff, J.A., Martin, B.S., Tolan, T.L., and Wells, R.E., eds., The Columbia River flood basalt province: Geological Society of America Special Paper 497, p. 401–427. [Also available at http://dx.doi.org/10.1130/2013.2497(16).]

Ferns, M.L., and McConnell, V.S., 2005, Geoanalytical information layer for Oregon (GILO), release 1: Oregon Department of Geology and Mineral Industries Digital Data Series GILO–1, 1 CD.

Ferns, M.L., McConnell, V.S., Madin, I.P., and Johnson, J.J., 2010, Geology of the upper Grande Ronde basin, Union County, Oregon: Oregon Department of Geology and Mineral Bulletin B–107, 65-p. text, 1 sheet, scale 1:100,000, 1 CD.

Ferns, M.L., and O'Brien, J.P., 1992, Geology and mineral resources map of the Namorf quadrangle, Malheur County, Oregon: Oregon Department of Geology and Mineral Industries Geological Map Series GMS–74, scale 1:24,000.

Ferns, M.L., and Urbanczyk, K., 1990, Geology and mineral resources map of the Mitchell Butte quadrangle, Malheur County, Oregon: Oregon Department of Geology and Mineral Industries Geological Map Series GMS–61, scale 1:24,000.

Fiebelkorn, R.B., Walker G.W., MacLeod, N.S., McKee, E.H., and Smith, J.G., 1982, Index to K-Ar age determinations for the State of Oregon: U.S. Geological Survey Open-File Report 82–596, 40 p., 1 over-size sheet. [Also available at https://pubs.er.usgs.gov/publication/ofr82596.]

Ford, M.T., Grunder, A.I., and Duncan, R.A., 2013, Bimodal volcanism of the High Lava Plains and northwestern Basin and Range of Oregon–Distribution and tectonic implications of age-progressive rhyolites: American Geophysical Union Geochemistry, Geophysics, Geosystems, v. 14, no. 8, p. 2,836–2,857.

Fuller, R.E., 1931, The geomorphology and volcanic sequence of Steens Mountain in southeastern Oregon: University of Washington Publications in Geology, v. 3, no. 1, 40 p.

Gaylord, D.R., McClaughry, J.D., Felt, K.J., Ferns, M.L., Spall, B.N., and Cahoon, E., 2015, Stratigraphic and geochronologic confirmation of the middle Eocene Clarno Formation in NE Oregon [abs.]: Geological Society of America Abstracts with Programs, v. 47, no. 4, p. 56.

Geist, D., and Richards, M., 1993, Origin of the Columbia Plateau and Snake River plain—Deflection of the Yellowstone plume: Geology, v. 21, no. 9, p. 789–792. [Also available at http://dx.doi.org/10.1130/0091-7613(1993)021<0789:OOTCPA>2.3.CO;2.]

Gilbert, D., 1988, Geology and geochemistry of the Mahogany hot-springs gold prospect in the Owyhee region of southeastern Oregon: Seattle, Wash., University of Washington, M.S. thesis, 170 p.

Gilluly, J., 1937, Geology and mineral resources of the Baker quadrangle, Oregon: U.S. Geological Survey Bulletin 879, 119 p., 3 pls. [Also available at https://pubs.er.usgs.gov/publication/b879.]

Greene, R.C., 1973, Petrology of the welded tuff of Devine Canyon, southeastern Oregon: U.S. Geological Survey Professional Paper 797, 26 p. [Also available at https://pubs.er.usgs.gov/publication/pp797.]

Greene, R.C., Walker, G.W., and Corcoran, R.E., 1972, Geologic map of the Burns quadrangle, Oregon: U.S. Geological Survey Miscellaneous Geologic Investigations Map I–680, scale 1:250,000. [Also available at https://pubs.er.usgs.gov/publication/i680.]

Haddock, G.H., 1967, The Dinner Creek welded ash-flow tuff of the Malheur gorge area, Malheur County, Oregon: Eugene, Oreg., University of Oregon, Ph.D. dissertation, 11 p.

Hampton, E.R., and Brown, S.G., 1964, Geology and ground-water resources of the upper Grande Ronde River basin, Union County, Oregon: U.S. Geological Survey Water Supply Paper 1597, 99 p., 6 pls. [Also available at https://pubs.er.usgs.gov/publication/wsp1597.]

Hasten, Z.I., 2012, Mid-Miocene magmatism in the Owyhee Mountains, ID—Origin and petrogensis of volcanic rocks in the Silver City District: Manhattan, Kans., Kansas State University, M.S. thesis, 222 p.

Hess, E.N., 2014, Strontium, lead, and oxygen isotopic signatures of mid-Miocene silicic volcanism in eastern Oregon: Portland Oreg., Portland State University, M.S. thesis [Dissertations and Theses Paper 2079], 102 p., accessed at http://pdxscholar.library.pdx.edu/open_access_etds/2079.

Hooper, P.R., 2000, Chemical discrimination of Columbia River Basalt flows: American Geophysical Union Geochemistry, Geophysics, Geosystems, v. 1, no. 1, p. 1–14.

Hooper, P.R., Binger, G.B., and Lees, K.R., 2002, Ages of the Steens and Columbia River flood basalts and their relationship to extension-related calc-alkaline volcanism in eastern Oregon: Geological Society of America Bulletin, v. 114, no. 1, p. 43–50. [Also available at http://dx.doi.org/10.1130/0016-7606(2002)114<0043:AOTSAC>2.0.CO;2.]

Hooper, P.R., Camp, V.E., Reidel, S.P., and Ross, M.E., 2007, The origin of the Columbia River flood basalt province—Plume versus nonplume models, *in* Foulger, G.R., and Jurdy, D.M., eds., Plates, plumes, and planetary processes: Geological Society of America Special Paper 430, p. 635–668. [Also available at http://dx.doi.org/10.1130/2007.2430(30).]

Hooper, P.R., Gillespie, B.A., and Ross, M.E., 2011, The Eckler Mountain basalts and associated flows, Columbia River Basalt Group: Canadian Journal of Earth Sciences, v. 32, no. 4, p. 410–423, accessed at http://dx.doi.org/10.1139/e95-035.

Hooper, P.R., and Hawksworth, C.J., 1993, Isotopic and geochemical constraints on the origin and evolution of the Columbia River Basalt: Journal of Petrology, v. 34, no. 6, p. 1,203–1,246. [Also available at http://dx.doi.org/10.1093/petrology/34.6.1203.]

Hooper, P.R., Houseman, M.D., Beane, J.E., Caffrey, G.M., Engh, K.R., Scrivner, J.V., and Watkinson, A.J., 1995, Geology of the northern part of the Ironside Mountain inlier, northeastern Oregon, *in* Vallier, T.L., and Brooks, H.C., eds., Geology of the Blue Mountains region of Oregon, Idaho, and Washington: Petrology and tectonic evolution of pre-Tertiary rocks of the Blue Mountains region: U.S. Geological Survey Professional Paper 1438, p. 415–455. [Also available at https://pubs.er.usgs.gov/publication/pp1438.]

Hooper, P.R., and Swanson, D.A., 1990, The Columbia River Basalt Group and associated volcanic rocks of the Blue Mountains province, *in* Walker, G.W., ed., Geology of the Blue Mountains region of Oregon, Idaho, and Washington—Cenozoic geology of the Blue Mountains region: U.S. Geological Survey Professional Paper 1437, p. 63–99. [Also available at https://pubs.er.usgs.gov/publication/pp1437.]

Jarboe, N.A., Coe, R.S., Renne, P.R., and Glen, J.M.G., 2010, The age of the Steens reversal and the Columbia River Basalt Group: Chemical Geology, v. 274, nos. 3–4, p. 158–168, accessed at http://dx.doi.org/10.1016/j.chemgeo.2010.04.001.

Johnson, J.A., and Grunder, A.L., 2000. The making of intermediate composition magma in a bimodal suite—Duck Butte eruptive center, Oregon, USA: Journal of Volcanology and Geothermal Research, v. 95, nos. 1–4, p. 175–195, accessed at https://doi.org/10.1016/S0377-0273(99)00125-0.

Johnson, J.A., Hooper, P.R., Hawkesworth, C.J., and Binger, G.B., 1998, Geologic map of the Stemler Ridge quadrangle, Malheur County, southeastern Oregon: U.S. Geological Survey Open-File Report 98–105, 11-p. text, 1 over-size sheet, scale 1:24,000. [Also available at https://pubs.er.usgs.gov/publication/ofr98105.]

Johnson, K., and Schwartz, J.J., 2009, Overview of Jurassic-Cretaceous magmatism in the Blue Mountains province (NE Oregon & W. Idaho)—Insights from New Pb/U (SHRIMP-RG) age determinations [abs.]: Geological Society of America Abstracts with Programs, v. 41, no. 7, p. 182.

Jordan, B.T., Grunder, A.L., Duncan, R.A., and Deino, A.L., 2004, Geochronology of age-progressive volcanism of the Oregon High Lava Plains—Implications for the plume interpretation of Yellowstone: Journal of Geophysical Research, v. 109, no. B10, 10 p., accessed at http://dx.doi.org/10.1029/2003jB002776.

Kays, M.A., Ferns, M.L., and Brooks, H.C., 1987, Metamorphism of Triassic-Paleozoic belt rocks—A guide to field and petrologic relations in the oceanic mélange, Klamath and Blue Mountains, California and Oregon, in Ernst, W.G., ed., Metamorphism and crustal evolution of the western United States (Rubey Volume VII): Englewood, Cliffs, N.J., Prentice-Hall, p. 1,098–1,120.

Kimmel, P.G., 1982, Stratigraphy, age, and tectonic setting of the Miocene-Pliocene lacustrine sediments of the western Snake River Plain, Oregon and Idaho, in Bonnichsen, B., and Breckenridge, R.M., eds., Cenozoic geology of Idaho: Idaho Bureau of Mines and Geology Bulletin 26, p. 559–578.

Kittleman, L.R., Green, A.R., Haddock, G.H, Hagood, A.R., Johnson, A.M., McMurray, J.M., Russell, R.G., and Weeden, D.A., 1967, Geologic map of the Owyhee region, Malheur County, Oregon: University of Oregon Museum of Natural History Bulletin 8, scale 1:125,000.

Kittleman, L.R., Green, H.R., Hagood, A.R., Johnson, A.M., McMurray, J.M., Russell, R.G., and Weeden, D.A., 1965, Cenozoic stratigraphy of the Owyhee region, southeastern Oregon: University of Oregon Museum of Natural History Bulletin 1, 45 p.

Kuiper, K.F., Deino, A., Hilgen, F.J., Krijgsman, W., Renne, P.R., and Wijbrans, J.R., 2008, Synchronizing rock clocks of Earth history: Science, v. 320, no. 5875, p. 500–504, accessed at http://dx.doi.org/10.1126/science.1154339.

Kurz, G.A., Schmitz, M.D., and Northrup, C.J., 2008, Tracer isotope geochemistry and U-Pb zircon geochronology of intrusive rocks from the Wallowa and Olds Ferry arc terranes, Blue Mountains province, northeastern Oregon and west-central Idaho [abs.]: Geological Society of America Abstracts with Programs, v. 40, no. 1, p. 87.

La Maskin, T.A., Dorsey, R.J., and Vervoort, J.D., 2008, Tectonic controls on mudrock geochemistry, Mesozoic rocks of eastern Oregon and western Idaho, U.S.A.—Implications for Cordilleran tectonics: Journal of Sedimentary Research, v. 78, no. 12, p. 765–783, accessed at http://dx.doi.org/10:2110/jsr.2008.087.

Large, A.M., 2016, Silicic volcanism at the northern and western extent of the Columbia River Basalt rhyolite flare-up—Rhyolites of Buchanan volcanic complex and Dooley Mountain complex Oregon: Portland, Oreg., Portland State University, M.S. thesis, 175 p.

Le Bas, M.J., Le Maitre, R.W., Streckeisen, A., and Zanettin, B., 1986, A chemical classification of volcanic rocks based on the total alkali-silica diagram: Journal of Petrology, v. 27, no. 3, p. 745–750.

Leeman, W.P., 1982, Olivine tholeiitic basalts of the Snake River plain, *in* Bonnichsen, B., and Breckenridge, R.M., eds., Cenozoic geology of Idaho: Idaho Bureau of Mines and Geology Bulletin, 26, p. 181–191.

Lees, K.R., 1994, Magmatic and tectonic changes through time in the Neogene volcanic rocks of the Vale area, Oregon, northwestern U.S.A.: Milton Keynes, United Kingdom, The Open University, Ph.D. dissertation, 282 p.

Le Maitre, R.W., Bateman, P., Dudek, A., Keller, J., Lemeyre, J., Le Bas, M.J., Sabine, P.A., Schmid, R., Sorenson, H., Streckeisen, A., Wooley, A.R., and Zanettin, B., 1989, A classification of igneous rocks and glossary of terms: Oxford, United Kingdom, Blackwell Science Inc., 206 p.

Linneman, S.K., and Myers, J.D., 1990, Magmatic inclusions in the Holocene rhyolites of Newberry volcano, central Oregon: Journal of Volcanology and Geothermal Research, v. 95, no. B11, p. 17,677–17,691, accessed at http://dx.doi.org/10.1029/JB095iB11p17677.

MacLeod, N.S., Walker, G.W. and McKee, E.H., 1976, Geothermal significance of eastward increase in age of upper Cenozoic rhyolitic domes in southeastern Oregon, Proceedings of the Second United Nations Symposium on the Development and Use of Geothermal Resources, San Francisco, Calif.: v. 1, Washington, D.C., Government Printing Office, p. 465–476.

MacLeod, N.S., 1990a, Geology and mineral resources map of the Sheaville quadrangle, Malheur County, Oregon and Owyhee County, Idaho: Oregon Department of Geology and Mineral Industries Geological Map Series GMS–64, scale 1:24,000.

MacLeod, N.S., 1990b, Geology and mineral resources map of the Mahogany Gap quadrangle, Malheur County, Oregon and Owyhee County, Idaho: Oregon Department of Geology and Mineral Industries Geological Map Series GMS–65, scale 1:24,000.

Madin, I.P., 1998, Geologic map of the Tucker Flat quadrangle, Baker and Union counties, Oregon: Oregon Department of Geology and Mineral Industries, Geological Map Series GMS–110, 9-p. text, 1 sheet, scale 1:24,000.

Madin, I.P., and Ferns, M.L., 1997, Geologic map of the Malheur Butte quadrangle, Malheur County, Oregon: Oregon Department of Geology and Mineral Industries Open-File Report O–97–2, scale 1:24,000.

Malde, H.E., and Powers, H.A., 1962, Upper Cenozoic stratigraphy of the western Snake River Plain, Idaho: Geological Society of America Bulletin, v. 73, no. 10, p. 1,197–1,220.

Manley, C.R., and McIntosh, W.C., 2002, The Juniper Mountain volcanic center, Owyhee County, southwestern Idaho—Age relations and physical volcanology, *in* Bonnichsen, B., White, C.M., and McCurry, M., eds., Tectonic and magmatic evolution of the Snake River volcanic province: Idaho Geological Survey Bulletin 30, p. 205–227.

Mann, G.M., and Meyers, C.E., 1993, Late Cenozoic structures and correlations to seismicity along the Olympic-Wallowa lineament, northwest United States: Geological Society of America Bulletin, v. 105, no. 7, p. 853–871. [Also available at http://dx.doi.org/10.1130/0016-7606(1993)105<0853:LCSACT>2.3.CO;2.]

Marcy, P.I., 2014, Revisiting volcanology and composition of rhyolites and associated REE rich mafic clasts of the Three Fingers caldera, SE Oregon: Portland, Oreg., Portland State University, M.S. thesis [Dissertations and Theses Paper 1543], 200 p., accessed October 1, 2016, at http://pdxscholar.library.pdx.edu/open_access_etds/1543.

Marcy, P.I., Streck, M.J., and Ferns, M.L., 2013, Mid-Miocene silicic volcanism of the Three Fingers-Mahogany Mountain area, SE Oregon—Revisited [abs.]: American Geophysical Union Abstract, no. V23C–2487.

Markl, G., and White, C.M., 1999, Complex zoning between super-calcic pigeonite and augite from the Graveyard Point sill, Oregon—A record of the interplay between bulk and interstitial liquid fractionation: Contributions to Mineralogy and Petrology, v. 137, no. 1, p. 170–183.

Martin, B.S., Tolan, T.L., and Reidel, S.P., 2013, Revisions to the stratigraphy and distribution of the Frenchman Springs Member, Wanapum Basalt, *in* Reidel, S.P., Camp, V.E., Ross, M.E., Wolff, J.A., Martin, B.S., Tolan, T.L., and Wells, R.E., eds., The Columbia River flood basalt province: Geological Society of America Special Paper 497, p. 155–179. [Also available at http://dx.doi.org/10.1130/2013.2497(06).]

McClaughry, J.D., Ferns, M.L., and Gordon, C.L., 2009b, Field trip guide to the Neogene stratigraphy of the Lower Crooked basin and the ancestral Crooked River, Crook County, Oregon: Oregon Geology, v. 69, no. 1, p. 45–60, accessed at http://www.oregongeology.org/sub/quarpub/OrGeo.htm.

McClaughry, J.D., Ferns, M.L., Streck, M.J., Patridge, K.A., and Gordon, C.L., 2009a, Paleogene calderas of central and eastern Oregon—Eruptive sources of widespread tuffs in the John Day and Clarno Formations, *in* O'Connor, J.E., Dorsey, R.J., and Madin, I.P., eds., Volcanoes to vineyards—Geologic field trips through the dynamic landscape of the Pacific Northwest: Geological Society of America Field Guide 15, p. 407–434. [Also available at http://dx.doi.org/10.1130/2009.fld015(20).]

McClaughry, J.D., Wiley, T.J., Conrey, R.C., Jones, C.B., and Lite, K.E., 2012, Digital geologic map of the Hood River Valley, Hood River and Wasco Counties, Oregon: Oregon Department of Geology and Mineral Industries Open-File Report O–12–03, 142-p. text, 1 pl., scale 1:36,000, accessed at http://www.oregongeology.org/pubs/ofr/p-O-12-03.htm.

Merriam, J.C., 1901, A contribution to the geology of the John Day basin [Oregon]: University of California Publications in Geological Sciences, v. 2, no. 9, p. 269–314.

Miyashiro, A., 1974, Volcanic rock series in island arcs and active continental margins: American Journal of Science, v. 274, no. 4, p. 321–355. [Also available at http://dx.doi.org/10.2475/ajs.274.4.321.]

Nash, B.P., and Perkins, M.E., 2012, Neogene fallout tuffs from the Yellowstone hotspot in the Columbia Plateau region, Oregon, Washington and Idaho, USA: PLOS ONE, v. 7, no. 10, 13 p., accessed at http://dx.doi.org/10.1371/journal.pone.0044205.

O'Connor, J.E., and Burns, S.F., 2009, Cataclysms and controversy—Aspects of the geomorphology of the Columbia River, *in* O'Connor, J.E., Dorsey, R.J., and Madin, I.P., eds., Volcanoes to vineyards Geologic field trips through the dynamic landscape of the Pacific Northwest: Geological Society of America Field Guide 15, p. 237–251. [Also available at http://dx.doi.org/10.1130/2009.fld015(12).]

Othbert, K.L., O'Connor, J.E., and McDaniel, P.A., 1995, Field guide to the Quaternary geology of the Boise Valley and adjacent Snake River valley: Idaho Geological Survey Staff Report 51, 49 p.

Pardee, J.T., and Hewett, D.F., 1914, Geology and mineral resources of the Sumpter quadrangle, Oregon: Oregon Department of Geology and Mineral Industries, v. 1, no. 6, p. 7–128.

Pardee, J.T., Hewett, D.F., Rosenkranz, T.H., Katz, F.J., and Calkins, F.C., 1941, Preliminary geologic map of the Sumpter Quadrangle: Oregon Department of Geology and Mineral Industries Geologic Quadrangle Map QM–8, scale 1:96,000.

Pierce, K.L. and Morgan, L.A., 2009, Is the track of the Yellowstone hotspot driven by a deep mantle Plume? – Review of volcanism, faulting and uplift in light of new data: Journal of Volcanology and Geothermal Research, v. 118, nos. 1–3, p. 1–25, accessed at https://doi.org/10.1016/j.jvolgeores.2009.07.009.

Reidel, S.P., Camp, V.E., Tolan, T.L., Kauffmann, J.D., and Garwood, D.L., 2013b, Tectonic evolution of the Columbia River flood basalt province, *in* Reidel, S.P., Camp, V.E., Ross, M.E., Wolff, J.A., Martin, B.S., Tolan, T.L., and Wells, R.E., eds., The Columbia River flood basalt province: Geological Society of America Special Paper 497, p. 293–324. [Also available at http://dx.doi.org/10.1130/2013.2497(12).]

Reidel, S.P., Camp, V.E., Tolan, T.L., and Marin, B.S., 2013a, The Columbia River flood basalt province–Stratigraphy, areal extent, volume, and physical volcanology, *in* Reidel, S.P., Camp, V.E., Ross, M.E., Wolff, J.A., Martin, B.S., Tolan, T.L., and Wells, R.E., eds., the Columbia River flood basalt province: Geological Society of America Special paper 497, p. 1–43. [Also available at http://dx.doi.org/10.1130/2013.2497(01).]

Reidel, S.P., and Campbell, N.P., 1989, Structure of the Yakima fold belt, central Washington, *in* Joseph, N.L., Stofell, K.L., Evans, J.G., Kiilsgaard, T.H., Korosec, M.A., Logan, R.L., Miller, F.K., Phillips, W.M., Powell, R.E., Schasse, H.W., Schuster, J.E., Waggoner, S.Z., Walsh, T.J., and Whipple, J.W., eds., Geologic guidebook for Washington and adjacent areas: Washington Division of Geology and Earth Resources Information Circular 86, p. 275–303.

Reidel, S.P., Johnson, V.G., and Spane, F.A., 2002, Natural gas storage in basalt aquifers of the Columbia basin, Pacific Northwest USA; A guide to site characterization: Richland, Wash., Pacific Northwest National Laboratory, report no. PNNL–13962, 274 p.

Reidel, S.P., and Tolan, T.L., 2013, The Grande Ronde Basalt, Columbia River Basalt Group, *in* Reidel, S.P., Camp, V.E., Ross, M.E., Wolff, J.A., Martin, B.S., Tolan, T.L., and Wells, R.E., eds., The Columbia River flood basalt province: Geological Society of America Special Paper 497, p. 117–153. [Also available at http://dx.doi.org/10.1130/2013.2497(05).]

Reidel, S.P., Tolan, T.L, Hooper, P.R., Beeson, M.H., Fecht, K.R., Bentley, R.D., and Anderson, J.L., 1989, The Grande Ronde Basalt, Columbia River Basalt Group—Stratigraphic descriptions and correlations in Washington, Oregon, and Idaho, *in* Reidel, S.P., and Hooper, P.R., Volcanism and tectonism in the Columbia River flood-basalt province: Geological Society of America Special Paper 239, p. 21–53.

Robyn, T.L., 1979, Miocene volcanism in eastern Oregon—An example of calc-alkalic volcanism unrelated to subduction: Journal of Volcanology and Geothermal Research, v. 5, nos. 1–2, p. 149–161. [Also available at http://dx.doi.org/10.1016/0377-0273(79)90038-6.]

Russell, I., 1901, Geology and water-resources of Nez Perce County, Idaho—Part 1: U.S. Geological Survey Water-Supply Paper 53, 86 p. [Also available at https://pubs.er.usgs.gov/publication/wsp53.]

Rytuba, J.J., and Vander Meulen, D.B., 1991, Hot-spring precious-metal systems in the Lake Owyhee volcanic field, Oregon-Idaho, *in* Raines, G.L., Lisle, R.E,, Schafer, R.W., and Wilkinson, W.H., eds., Geology and ore deposits of the Great Basin—Symposium proceedings: Reno, Nev., Geological Society of Nevada, p. 1,085–1,096.

Rytuba, J.J., Vander Meulen, D.B., Barlock, V.E., Ferns, M.L., 1991, Hot spring gold deposits in the Lake Owyhee volcanic field, eastern Oregon, field trip 10 *of* Buffa, R.H., Coyner, A.R., eds., The geology and ore deposits of the Great Basin—Field trip guidebook compendium: Great Basin symposium on geology and ore deposits of the Great Basin, Reno, Nev., March 28–April 1, 1990, Reno, Nev., Geological Society of Nevada, p. 633–712.

Rytuba, J.J., Vander Meulen, D.B., and Minor, S.A., 1989, Geologic evolution of the Three Fingers caldera, Malheur County, Oregon [abs.]: Geological Society of America Abstracts with Programs, v. 21, no. 5, p. 138.

Rytuba, J.J., Vander Meulen, D.B., Plouff, D., Minor, S.A., 1985, Geology of the Mahogany Mountain caldera, Oregon [abs.]: Geological Society of America Abstracts with Programs, v. 17, no. 4, p. 263.

Schwartz, J.J., Johnson, K., Mueller, P., Valley, J., Strickland, A., and Wooden, J.L., 2014, Time scales and processes of Cordilleran batholith construction and high Sr/Y magmatic pulses—Evidence from the Bald Mountain batholith, northeastern Oregon: Geosphere, v. 10, no. 6, p. 1,456–1,481.

Schwartz, J.J., Snoke, A.W., Barnes, C.G., Gromet, I.P., and Johnson, K., 2010, Analysis of the Wallowa-Baker terrane boundary—Implications for tectonic accretion in the Blue Mountains province, northeastern Oregon: Geological Society of America Bulletin, v. 122, no. 3–4, p. 517–536. [Also available at http://dx.doi.org/10.1130/B26493.1.]

Seligman, A.N., Bindeman I.N., McClaughry, J., Stern R.A., and Fisher C., 2014, The earliest low and high δ18O caldera-forming eruptions of the Yellowstone plume–Implications for the 30–40 Ma Oregon calderas and speculations on plume-triggered delaminations: Frontiers in Earth Science, v. 2, no. 34, 9 p., accessed at http://dx.doi.org/10.3389/feart.2014.00034.

Sheppard., R.A., and Gude, A.I., 1986, Field trip guide to the Durkee zeolite deposit, Durkee, Oregon: Oregon Department of Geology and Mineral Industries, Oregon Geology, v. 48, no. 11, p. 127–129, 132.

Silberling, N.J., Jones, D.L., Blake, M.C., and Howell, D.G., 1984, Lithotectonic terrane map of the western conterminous United States: U.S. Geological Survey Miscellaneous Field Studies Map 1874–C, 20-p pamphlet, 1 sheet, scale 1:2,500,000. [Also available at https://pubs.er.usgs.gov/publication/mf1874C.]

Smith, G.O., 1901, Geology and water resources of a portion of Yakima County, Washington: U.S. Geological Survey Water-Supply Paper 55, 68 p. [Also available at https://pubs.er.usgs.gov/publication/wsp55.]

Steiner, A.R., 2015, Field geology and petrologic investigation of the Strawberry Volcanics, northeast Oregon: Portland, Oreg., Portland State University, Ph.D. dissertation [Dissertations and Theses Paper 2712], 213 p., accessed at http://pdxscholar.library.pdx.edu/open_access_etds/2712.

Steiner, A.R., and Streck, M.J., 2010, The "Strawberry volcanic field" of northeastern Oregon—Another Piece of the CRB Puzzle? [abs.]: American Geophysical Union Abstract, no. V23B–2407.

Steiner, A.R., and Streck, M.J., 2011, Strawberry rhyolites, Oregon–Northwestern extent of mid-Miocene flood basalt related rhyolites of the Pacific Northwest [abs.]: American Geophysical Union Abstract, no. T51H–2473.

Steiner, A.R., and Streck, M.J., 2013a, The Strawberry Volcanics—Generation of "orogenic" andesites from tholeiite within an intra-continental volcanic suite centered on the Columbia River flood basalt province, USA: Geological Society, London, Special Publications, v. 385, no. 1, 22 p.

Steiner, A.R., and Streck, M.J., 2013b, New insights to the mid-Miocene calc-alkaline lavas of the Strawberry Volcanics, NE Oregon, surrounded by the coeval tholeiitic Columbia River basalt province [abs.]: American Geophysical Union Abstract, no. V31A–2681.

Streck, M.J., 2014, Evaluation of crystal mush extraction models to explain crystal-poor rhyolites: Journal of Volcanology and Geothermal Research, v. 284, p. 74–94.

Streck, M.J., and Ferns, M.L., 2004, The Rattlesnake Tuff and other Miocene silicic volcanism in eastern Oregon, in Haller, K.M., and Wood, S.H., eds., Geological field trips in southern Idaho, eastern Oregon, and northern Nevada: U.S. Geological Survey Open-File Report 2004–1222, p. 4–19. [Also available at http://pubs.usgs.gov/of/2004/1222/.]

Streck, M.J, and Ferns, M.L., 2012, The Rhyolite flare-up of the Columbia River basalt province and its bearing on plume vs. non-plume models [abs.]: American Geophysical Union Abstract, no. DI53A–2372.

Streck, M.J., Ferns, M.L., and McIntosh, W., 2015, Large, persistent rhyolitic magma reservoirs above Columbia River Basalt storage sites—The Dinner Creek Tuff eruptive center, eastern Oregon: Geosphere, v. 11, no. 2, p. 226–235, accessed at http://dx.doi.org/10.1130/GES01086.1.

Streck, M.J., and Grunder, A.L., 1995, Crystallization and welding variations in a widespread ignimbrite sheet–The Rattlesnake Tuff, eastern Oregon, USA: Bulletin of Volcanology, v. 57, no. 3, p. 151–169.

Streck, M.J., and Grunder, A.L., 1997, Compositional gradients and gaps in high-silica rhyolites of the Rattlesnake Tuff, Oregon: Journal of Petrology, v. 38, no. 1, p. 133–163.

Streck, M.J., and Grunder, A.L., 1999, Enrichment of basalt and mixing of dacite in the rootzone of a large rhyolite chamber—Inclusions and pumices from the Rattlesnake Tuff, Oregon: Contributions to Mineralogy and Petrology, v. 136, no. 3, p. 193–212, accessed at http://dx.doi.org/10.1007/s004100050532.

Streck, M.J., and Grunder, A.L., 2008, Phenocryst-poor rhyolites of bimodal, tholeiitic provinces—The Rattlesnake Tuff and implications for mush extraction models: Bulletin of Volcanology, v. 70, no. 3, p. 385–401. [Also available at http://dx.doi.org/10.1007/s00445-007-0144-3.]

Streck, M.J., and Grunder, A.L., 2012, Temporal and crustal effects on differentiation of tholeiite to calcalkaline and ferro-trachytic suites, High Lava Plains, Oregon, USA: American Geophysical Union Geochemistry, Geophysics, Geosystems, v. 13, no. 11, 24 p. [Also available at http://dx.doi.org/10.1029/2012GC004237.]

Streck, M.J., McIntosh, W., and Ferns, M.L., 2016, Co-CRBG rhyolite volcanism reassessed [abs.]: Geological Society of America Abstracts with Programs, v. 48, no. 6.

Swanson, D.A., Anderson, J.L., Bentley, R.D., Byerly, G.R., Camo, V.E., Gardner, J.N., and Wright, T.L., 1979b, Reconnaissance geologic map of the CRBG in parts of eastern Washington and northern Idaho: U.S. Geological Survey Open-File Report 79–1363, 26-p. text., 12 pls., scale 1:250,000. [Also available at http://pubs.er.usgs.gov/publication/ofr791363.]

Swanson, D.A., Anderson, J.A., Camp, V.E., Hooper, P.R., Taubeneck, W.H., and Wright, T.L., 1981, Reconnaissance geologic map of the Columbia River Basalt Group, northern Oregon and western Idaho: U.S. Geological Survey Open-File Report 81–797, 20-p. text, 6 pls., scale 1:250,000. [Also available at http://pubs.er.usgs.gov/publication/ofr81797.]

Swanson, D.A., Wright, T.L, Hooper, P.R., and Bentley, R.D., 1979a, Revisions in stratigraphic nomenclature of the Columbia River Basalt Group: U.S. Geological Survey Bulletin 1457–G, 59 p., 1 pl. [Also available at https://pubs.er.usgs.gov/publication/b1457G.]

Taubeneck, W.H., 1970, Dikes of Columbia River Basalt in northeastern Oregon, western Idaho, and southeastern Washington, *in* Gilmour, E.H., and Straddling, D., eds., Proceedings of the Second Columbia River Basalt Symposium: Cheney, Wash., Eastern Washington State College, p. 73–96.

Taubeneck, W.H., 1980, Diatremes in Columbia River Basalt near the crest of the west escarpment of the Grande Ronde graben, northeast Oregon [abs.]: Geological Society of America Abstracts with Programs, v. 12, no. 3, p. 155.

Thayer, T.P., 1957, Some relations of later Tertiary volcanology and structure in eastern Oregon, v. 1 *of* Volcanology of the Cenozoic: 20th International Geological Congress, sec. 1, Mexico City, Mexico, 1956, sec. 1, p. 231–245.

Tolan, T.L., and Beeson, M.H., 1984, Intracanyon flows of the CRBG in the lower Columbia River gorge and their relationship to the Troutdale Formation: Geological Society of America Bulletin, v. 95, no. 4, p. 463–477.

Tolan, T.L., Martin, B.S., Reidel, S.P., Anderson, J.L., Lindsey, K.A., and Burt, W., 2009, An introduction to the stratigraphy, structural geology, and hydrogeology of the Columbia River flood-basalt province—A primer for the GSA Columbia River Basalt Group field trips, *in* O'Connor, J.E., Dorsey, R.J., and Madin, I.P., eds., Volcanoes to vineyards—Geologic field trips through the dynamic landscape of the Pacific Northwest: Geological Society of America Field Guide 15, p. 599–643. [Also available at http://dx.doi.org/10.1130/2009.fld015(28).]

Tolan, T.L., and Reidel, S.P., comps., 1989, Structure map of a portion the Columbia River flood-basalt province, *in* Reidel, S.P., and Hooper, P.R., eds., Volcanism and tectonism in the Columbia River flood-basalt province: Geological Society of America Special Paper 239, 1 sheet, scale 1:500,000.

U.S. Geological Survey, 2008, Geochemistry of rock samples from the National Geochemical Database: U.S. Geological Survey, Reston, VA.

Vander Meulen, D.B., 1989, Intracaldera tuffs and central-vent intrusion of the Mahogany Mountain caldera, eastern Oregon: U.S. Geological Survey Open-File Report 89–77, 69 p., 2 pls., map scale 1:72,750. [Also available at https://pubs.er.usgs.gov/publication/ofr8977.]

Vander Meulen, D.B., Rytuba, J.J., Grubensky, M.J., and Goeldner, C.A., 1987a, Geologic map of the Bannock Ridge quadrangle, Malheur County, Oregon: U.S. Geological Survey Miscellaneous Field Studies Map MF–1903, scale 1:24,000. [Also available at https://pubs.er.usgs.gov/publication/mf1903.]

Vander Meulen, D.B., Rytuba, J.J., Grubensky, M.J., Vercoutere, T.L., and Minor, S.A., 1987c, Geologic map of the Pelican Point quadrangle, Malheur County, Oregon: U.S. Geological Survey Miscellaneous Field Studies Map MF–1904, scale 1:24,000. [Also available at https://pubs.er.usgs.gov/publication/mf1904.]

Vander Meulen, D.B., Rytuba, J.J., Minor, S.A., Harwood, C.S., 1989, Preliminary geologic map of the Three Fingers Rock quadrangle, Malheur County, Oregon: U.S. Geological Survey Open-File Report 89–344, scale 1:24,000. [Also available at https://pubs.er.usgs.gov/publication/ofr89344.]

Vander Meulen, D.B., Rytuba, J.J., Vercoutere, T.L., and Minor, S.A., 1987b, Geologic map of the Rooster Comb quadrangle, Malheur County, Oregon: U.S. Geological Survey Miscellaneous Field Studies Map MF–1902, scale 1:24,000. [Also available at https://pubs.er.usgs.gov/publication/mf1902.]

Van Tassell, J., Ferns, M.L., and McConnell, V.S., 2000, Neogene sediment accumulation and subsidence rates, La Grande basin, northeast Oregon [abs.]: Geological Society of America Abstracts with Programs, v. 32, no. 6, p. 73–74.

Van Tassell, J., Ferns, M.L., McConnell, V.S., and Smith, G.R., 2001, The mid-Pliocene Imbler fish fossils, Grande Ronde Valley, Union County, Oregon, and the connection between Lake Idaho and the Columbia River: Oregon Department of Geology and Mineral Industries, Oregon Geology, v. 63, no. 3, p. 77–96.

Van Tassell, J., Ferns, M.L., McConnell, V.S., and Smith, G.R., 2002, Neogene history of the Grande Ronde Valley, NE Oregon [abs.]: Geological Society of America Abstracts with Programs, v. 34; no 5, p. 39.

Vogt, B.F., 1981, The stratigraphy and structure of the CRBG in the Bull Run Watershed, Multnomah and Clackamas Counties, Oregon: Portland, Oreg., Portland State University, M.S. thesis, 151 p.

Wacaster, S., Streck, M.J., Belkin, H.H., and Bodnar, R.J., 2011, Compositional zoning of the Devine Canyon tuff, Oregon [abs.]: American Geophysical Union Abstract, no. V21C–2517.

Waters, A.C., 1961, Stratigraphic and lithologic variations in the Columbia River Basalt: American Journal of Science, v. 259, no. 8, p. 583–611.

Watkins, N.D., and Baksi, A.K., 1974, Magnetostratigraphy and oroclinal folding of the Columbia River, Steens, and Owyhee basalts, Oregon, Washington, and Idaho: American Journal of Science, v. 274, no. 2, p. 148–189. [Also available at http://dx.doi.org/10.2475/ajs.274.2.148.]

Watters, T.R., 1989, Periodically spaced anticlines of the Columbia Plateau, *in* Reidel, S.P., and Hooper, P.R., eds., Volcanism and tectonism in the Columbia River flood-basalt province: Geological Society of America Special Paper 239, p. 283–292.

Webb, B.M., Streck, M.J., and Ferns, M.L., and McIntosh, W.C., 2015, Stratigraphy and geochemistry of a large, hotspot-related rhyolite of the Pacific Northwest—The Littlefield Rhyolite, eastern Oregon [abs.]: American Geophysical Union Abstract, no. V31E–3065.

Webb, B.M., Streck, M.J., McIntosh, W.C., and Ferns, M.L., 2016, Flow units of the Littlefield Rhyolite, eastern Oregon, constraining age and storage sites of Grande Ronde Basalt magmas [abs.]: Geological Society of America Abstracts with Programs, v. 48, no. 6.

Wells, R.E, Bukry, D., Friedman, R., Pyle, D., Duncan, R., Haeussler, P., and Wooden, J., 2014, Geologic history of Siletzia, a large igneous province in the Oregon and Washington Coast Range—Correlation to the geomagnetic polarity time scale and implications for a long-lived Yellowstone hotspot: Geosphere, v. 10, no. 4, p. 692–719, accessed at http://dx.doi.org/10.1130/GES01018.1.

Wells, R.E., Niem, A.R., Evarts, R.C., and Hagstrum, J.T., 2009, The Columbia River Basalt Group—From the gorge to the sea, *in* O'Connor, J.E., Dorsey, R.J., and Madin, I.P., eds., Volcanoes to vineyards—Geologic field trips through the dynamic landscape of the Pacific Northwest: Geological Society of America Field Guide 15, p. 737–774. [Also available at http://dx.doi.org/10.1130/2009.fld015(32).]

Wells, R.E., Simpson, R.W., Bentley, R.D., Beeson, M.H., Mangan, M.T., and Wright, T.L., 1989, Correlation of Miocene flows of the CRBG from the central Columbia River Plateau to the coast of Oregon and Washington, *in* Reidel, S.P., and Hooper, P.R., eds., Volcanism and tectonism in the Columbia River flood-basalt province: Geological Society of America Special Paper 239, p. 113–129.

White, C.M., 2007, The Graveyard Point intrusion—An example of extreme differentiation of Snake River Plain basalt in a shallow crustal pluton: Journal of Petrology, v. 48, no. 2, pp. 303–325.

Wolf, J.A., and Ramos, F.C., 2013, Source materials for the main phase of the Columbia River Basalt Group—Geochemical evidence and implications for magma storage and transport, *in* Reidel, S.P., Camp, V.E., Ross, M.E., Wolff, J.A., Martin, B.S., Tolan, T.L., and Wells, R.E., eds., the Columbia River flood basalt province: Geological Society of America Special paper 497, p. 273–291. [Also available at http://dx.doi.org/10.1130/2013.2497(11).]

Wolf, J.A., Ramos, F.C., Hart, G.I., Patterson, J.D., and Brandon, A.D., 2008, Columbia River flood basalts from a centralized crustal magmatic system, Nature Geoscience, v. 1, p. 177–180, accessed at http://dx.doi.org/10.1038/ngeo124.

Wood, J.D., 1976, The geology of the Castle Rock area, Grant, Harney and Malheur Counties, Oregon, Portland, Oreg., Portland State University, M.S. thesis [Dissertations and Theses Paper 2608], 132 p.

Wood, S.H., and Clemens, D.M., 2002, Geologic and tectonic history of the western Snake River Plain, Idaho and Oregon, *in* Bonnichsen B., White, C.M., and McCurry, M., eds., Tectonic and magmatic evolution of the Snake River volcanic province: Idaho Geological Survey Bulletin 30, p. 69–103.

Wright, E.W., Baisan, C., Streck, M.J., Wright, W.W., and Szejner, P., 2016, Dendrochronolgy and middle Miocene petrified oak—Modern counterparts and interpretation: Paleogeography, Paleoclimatology, Paleocology, v. 445, p. 38–49.

Menlo Park Publishing Service Center, California
Manuscript approved June 21, 2017
Edited by David Shields
Layout by Cory D. Hurd

Ferns and others—**Field-Trip Guide to Columbia River Basalts, Rhyolites, and Post-Plume Volcanism in Eastern Oregon**—Scientific Investigations Report 2017–5022–D

ISSN 2328-0328 (online)
https://doi.org/10.3133/sir20175022D